

Dissertation zur Erlangung des Doktorgrades  
der Fakultät für Chemie und Pharmazie  
der Ludwig-Maximilians-Universität München



**Unusual apoptotic signaling pathways in cancer cells  
induced by cephalostatin**

Anita Rudy

aus

Altötting

2007

## Erklärung

Diese Dissertation wurde im Sinne von § 13 Abs. 3 bzw. 4 der Promotionsordnung vom 29. Januar 1998 von Frau Prof. Dr. A. M. Vollmar betreut.

## Ehrenwörtliche Versicherung

Diese Dissertation wurde selbständig, ohne unerlaubte Hilfe erarbeitet.

München, am 22.02.2007

---

Anita Rudy

Dissertation eingereicht am:	22.02.2007
1. Gutachter:	Frau Prof. Dr. A. M. Vollmar
2. Gutachter:	Herr PD. Dr. C. Culmsee
Mündliche Prüfung am:	27.03.2007

---

# TABLE OF CONTENTS

<b>I</b>	<b>INTRODUCTION.....</b>	<b>1</b>
1	NATURAL PRODUCTS AS ANTICANCER AGENTS.....	1
2	THE CEPHALOSTATINS.....	2
3	AIM OF THE STUDY.....	5
4	PROGRAMMED CELL DEATH.....	6
5	APOPTOSIS SIGNAL TRANSDUCTION.....	8
5.1	CASPASES.....	9
5.1.1	CLASSIFICATION, STRUCTURE AND ACTIVATION.....	9
5.1.2	SUBSTRATES.....	11
5.1.3	REGULATION.....	12
5.2	EXTRINSIC PATHWAY.....	13
5.3	INTRINSIC PATHWAY.....	15
5.3.1	SMAC.....	17
5.3.2	APOPTOSIS REGULATION BY THE BCL-2 PROTEIN FAMILY.....	18
5.4	PIDDosome.....	19
5.5	APOPTOSIS DEREGLATION – TARGETS FOR DRUG DISCOVERY.....	20
<b>II</b>	<b>MATERIALS AND METHODS.....</b>	<b>22</b>
1	MATERIALS.....	22
1.1	CEPHALOSTATIN.....	22
1.2	REAGENTS.....	22
2	CELL CULTURE.....	23
2.1	CELL LINES.....	23
2.1.1	HUMAN LEUKEMIA JURKAT T CELL LINES.....	23
2.1.2	CARCINOMA CELL LINES.....	23
2.2	CULTIVATION.....	24
2.3	SEEDING FOR EXPERIMENTS.....	25
2.4	FREEZING AND THAWING.....	25
3	FLOW CYTOMETRY.....	26
3.1	NICOLETTI ASSAY.....	27
3.2	PHOSPHATIDYLSERINE TRANSLOCATION.....	29
4	MTT VIABILITY ASSAY.....	29
5	MICROSCOPY.....	30
5.1	LIGHT MICROSCOPY.....	30
5.2	FLUORESCENCE MICROSCOPY.....	30

---

5.3	CONFOCAL MICROSCOPY .....	31
6	CLONOGENIC ASSAY .....	31
7	WESTERN BLOT .....	32
7.1	SAMPLE PREPARATION .....	32
7.1.1	WHOLE CELL LYSATES.....	32
7.1.2	CYTOSOLIC AND MITOCHONDRIA CONTAINING FRACTIONS .....	33
7.2	PROTEIN QUANTIFICATION .....	34
7.3	SDS-PAGE .....	35
7.4	WESTERN BLOTTING AND DETECTION .....	36
7.5	STAINING OF GELS AND MEMBRANES .....	39
8	IMMUNOPRECIPITATION .....	39
9	siRNA .....	40
9.1	siRNAs TARGETING CASPASE-2, AIF AND RAIDD .....	41
9.2	SMAC siRNA .....	41
9.2.1	TRANSFORMATION OF DH5 <sub>α</sub> .....	42
9.2.2	PLASMID AMPLIFICATION AND PURIFICATION.....	42
9.3	TRANSFECTION OF JURKAT CELLS .....	43
10	STATISTICS .....	43
<b>III</b>	<b>RESULTS.....</b>	<b>44</b>
1	CYTOTOXICITY OF CEPHALOSTATIN 2, 10 AND 12 .....	44
1.1	CEPHALOSTATIN 2 IS THE MOST ACTIVE OF THE CEPHALOSTATINS .....	44
1.2	APOPTOSIS INDUCTION BY CEPHALOSTATIN 2, 10 AND 12.....	45
2	CEPHALOSTATIN 2 INDUCED APOPTOSIS IS NOT RESTRICTED TO JURKAT T CELLS.....	47
2.1	APOPTOSIS INDUCTION IN HELA CELLS.....	47
2.2	APOPTOSIS INDUCTION IN MCF-7 CELLS .....	48
2.3	CELL DEATH INDUCTION IN SK-MEL-5 CELLS .....	50
2.3.1	APOPTOSIS INDUCTION .....	50
2.3.2	CEPHALOSTATIN STRONGLY INHIBITS CLONAL TUMOR CELL GROWTH .....	52
3	CEPHALOSTATIN INDUCES CASPASE-DEPENDENT AND -INDEPENDENT CELL DEATH .....	53
3.1	CASPASE-DEPENDENT APOPTOSIS.....	53
3.2	CASPASE-INDEPENDENT APOPTOSIS .....	55
4	CELL DEATH INDUCTION IN SK-MEL-5 .....	56
4.1	STAT3 IS DEGRADED UPON CEPHALOSTATIN TREATMENT .....	56
4.2	CEPHALOSTATIN INDUCES CELL CYCLE ARREST AT G1 PHASE .....	57
4.3	SURVIVIN IS DEGRADED UPON CEPHALOSTATIN 2 TREATMENT.....	59

---

4.4	AIF IS NOT RESPONSIBLE FOR APOPTOSIS INDUCTION IN SK-MEL-5 CELLS .....	59
5	CEPHALOSTATIN INDUCES PREFERENTIAL SMAC RELEASE .....	61
5.1	SMAC BUT NOT CYTOCHROME C IS PREDOMINATELY RELEASED IN VARIOUS TUMOR CELLS UPON CEPHALOSTATIN TREATMENT. ....	61
6	MECHANISM OF CEPHALOSTATIN-INDUCED SMAC RELEASE .....	63
6.1	SMAC RELEASE IS NOT MEDIATED BY JNK OR CASPASE-2 .....	63
6.2	BAK DEFICIENCY DELAYS BUT CAN NOT PREVENT SMAC RELEASE .....	64
6.3	SMAC RELEASE IS PARTIALLY DEPENDENT ON CALPAIN .....	66
7	IMPACT OF SMAC ON CEPHALOSTATIN-INDUCED APOPTOSIS .....	67
7.1	XIAP OVEREXPRESSION CAN NOT PREVENT APOPTOSIS .....	67
7.2	SMAC SILENCING INHIBITS CEPHALOSTATIN-INDUCED APOPTOSIS .....	68
7.3	SMAC ENHANCES THE APOPTOTIC SIGNALING CASCADE .....	69
8	INVOLVEMENT OF CASPASE-2 IN CEPHALOSTATIN-INDUCED APOPTOSIS....	71
8.1	CASPASE-2 PARTICIPATES IN APOPTOSIS INDUCTION .....	71
8.2	CASPASE-2 IS ACTIVATED INDEPENDENT OF CASPASE-9 UPON CEPHALOSTATIN TREATMENT.....	73
9	CEPHALOSTATIN INDUCES THE FORMATION OF THE PIDDOSOME COMPLEX. ....	74
<b>IV</b>	<b>DISCUSSION .....</b>	<b>76</b>
1	COMPARISON OF CEPHALOSTATIN 2, 10 AND 12 .....	76
2	CELL TYPE INDEPENDENT APOPTOSIS INDUCTION.....	77
3	INVOLVEMENT OF CASPASES .....	77
4	CELL DEATH INDUCTION IN SK-MEL-5 CELLS.....	78
5	MECHANISM OF SMAC RELEASE.....	79
6	IMPACT OF SMAC ON APOPTOSIS .....	80
7	INVOLVEMENT OF CASPASE-2.....	81
<b>V</b>	<b>SUMMARY.....</b>	<b>83</b>
<b>VI</b>	<b>REFERENCES.....</b>	<b>85</b>
<b>VII</b>	<b>APPENDIX .....</b>	<b>95</b>
1	PUBLICATIONS .....	95
1.1	ABSTRACTS .....	95
1.2	ORIGINAL PUBLICATIONS .....	95

---

2	CURRICULUM VITAE .....	97
3	ACKNOWLEDGEMENTS.....	98

## INDEX OF FIGURES

Figure I.1 Fingerprint of cytotoxic profile of cephalostatin 1 and 2 evaluated by the NCI-60 screen (September 2005).....	3
Figure I.2 Chemical structure of cephalostatin 1, 2, 10 and 12 .....	4
Figure I.3 Overview of apoptotic and necrotic cell death.....	6
Figure I.4 Classification of caspases based on their prodomain structure or function .....	9
Figure I.5 Schematic representation of proteolytic caspase activation (modified from 31) ....	10
Figure I.6 Schematic representation of the inhibitor of apoptosis protein family (36).....	12
Figure I.7 The extrinsic apoptotic pathway.....	14
Figure I.8 The intrinsic apoptotic pathway.....	16
Figure I.9 Simplified illustration of removal of IAP-mediated caspase-inhibition by Smac .....	17
Figure I.10 Bcl-2 family members (modified from 40) .....	18
Figure I.11 The PIDDosome.....	19
Figure I.12 Consequences of persistent STAT3 activity. ....	21
Figure II.1 flow chamber of a flow cytometer (from 67).....	26
Figure II.2 Histogram of untreated PI-stained cells .....	28
Figure II.3 short interfering RNA (modified from 71). ....	40
Figure III.1 Cephalostatin 2 is the most active among the tested cephalostatins.....	44
Figure III.2 Apoptosis induced by cephalostatin 2, 10 and 12 is dose dependent .....	45
Figure III.3 Cephalostatin 2 induced apoptosis is dependent on time.....	46
Figure III.4 Cephalostatin induces apoptosis in HeLa cells.....	47
Figure III.5 Morphological alterations in cephalostatin-treated MCF-7 cells.....	48
Figure III.6 Cephalostatin induces apoptosis in MCF-7 $\pm$ caspase-3 cells .....	49
Figure III.7 Cephalostatin induces concentration dependent apoptosis in SK-Mel-5 cells.....	50
Figure III.8 Cephalostatin induces time dependent cell death in SK-Mel-5 cells.....	51
Figure III.9 Cephalostatin strongly inhibits clonogenic tumor growth .....	52
Figure III.10 Caspase-dependent apoptosis in Jurkat and HeLa cells .....	54
Figure III.11 Caspase-independent cell death in SK-OV-3 cells .....	55
Figure III.12 Cephalostatin induced cell death in SK-Mel-5 cells is caspase-independent ....	56
Figure III.13 Cephalostatin promotes STAT3 degradation .....	57
Figure III.14 Cephalostatin induces G1-phase arrest in SK-Mel-5 cells.....	58
Figure III.15 Cephalostatin promotes survivin downregulation.....	59
Figure III.16 AIF is not responsible for cephalostatin induced apoptosis in SK-Mel-5 cells ...	60
Figure III.17 Smac is selectively released in Jurkat T cells .....	61

Figure III.18 Smac is selectively released upon cephalostatin treatment regardless of cell type.....	62
Figure III.19 Cephalostatin induced Smac release is not dependent on JNK .....	63
Figure III.20 Cephalostatin induced Smac release is not dependent on caspase-2 .....	64
Figure III.21 Bak deficiency can not prevent Smac release and apoptosis induced by cephalostatin .....	65
Figure III.22 Cephalostatin induced Smac release is partially mediated by calpain.....	66
Figure III.23 XIAP overexpression does not prevent cephalostatin-induced cell death .....	67
Figure III.24 Smac siRNA inhibits cephalostatin-induced apoptosis .....	68
Figure III.25 Caspase-9 is essential for cephalostatin-induced cell death .....	69
Figure III.26 Smac silencing reduces activation of caspase-9, caspase-3 and caspase-2 but not caspase-4.....	70
Figure III.27 Cephalostatin activates caspase-2 .....	72
Figure III.28 Caspase-2 is activated independent of caspase-9. ....	73
Figure III.29 The PIDDosome is formed upon cephalostatin treatment. ....	75
Figure V.1 Summary of cephalostatin-induced cell death mechanisms .....	84

## INDEX OF TABLES

Table I.1 Anticancer agents derived from natural origin in development or clinical use (adapted from 2, 4, 5).....	2
Table I.2 Characteristics of different types of cell death (adapted from 23, 25, 26) .....	8
Table II.1: summary of used cell lines .....	24
Table II.2: Freezing medium.....	26
Table II.3 PAA-concentration in the separating gel .....	35
Table II.4 Primary antibodies.....	38
Table II.5 Secondary antibodies.....	38

## ABBREVIATIONS

AIF	Apoptosis inducing factor
ANOVA	Analysis of variance between groups
Apaf-1	Apoptotic protease-activating factor-1
APS	Ammonium persulfate
ASK1	Apoptosis signal-regulating kinase-1
ASK1-DN	ASK-1 dominant negative
ATP/dATP	Adenosine-5'-triphosphate/2'-desoxyadenosine-5'-triphosphate
Bcl	B-cell lymphoma
BH	Bcl-2 homology
BIR	Baculoviral IAP repeats
BSA	Bovine serum albumin
CAD	Caspase-activated DNase
CARD	Caspase recruitment domain
CED	Cell death abnormality
cIAP	Cellular inhibitor of apoptosis
DD	Death domain
DED	Death effector domain
DIABLO	Direct IAP binding protein with low pI
DISC	Death inducing signaling complex
DMSO	Dimethyl sulfoxide
DNA	Deoxyribonucleic acid
DR	Death receptor
DTT	Dithiothreitol
ECL	Enhanced chemoluminescence
EDTA	Ethylene diaminetetraacetic acid
EGTA	Ethylene glycol-bis(2-aminoethylether) tetraacetic acid
Endo G	Endonuclease G
ER	Endoplasmic reticulum
FACS	Fluorescence activated cell sorter
FADD	Fas-associated death domain
FasL	Fas ligand
FCS	Fetal calf serum
FCS	Forward scatter
FL	Fluorescence
GI	Growth inhibition
HEPES	N-(2-hydroxyethyl)piperazine-N'-(2-ethanesulfonic acid)
HFS	Hypotonic fluorochrome solution
HtrA2	High temperature requirement protein A2
IAP	Inhibitor of apoptosis protein
ICE	Interleukin-1 $\beta$ converting enzyme
IL	Interleukin

---

IMM	Inner mitochondrial membrane
JNK	c-Jun N-terminal kinase
kDa	kilo Dalton
LB	Lysogeny broth
MMP	Mitochondrial membrane permeabilization
mRNA	Messenger RNA
MTT	3-(4,5-dimethylthiazol-2-yl)-2,5-diphenyl tetrazolium bromide
NAIP	Neuronal apoptosis inhibitory protein
NCI	National cancer institute
nt	Nucleotide
OMM	Outer mitochondrial membrane
PAA	Polyacrylamide
PARP	Poly(ADP-ribose) polymerase
PBS	Phosphate buffered saline
PCD	Programmed cell death
PI	Propidium iodide
PIDD	p53 inducible protein with a death domain
PMSF	Phenylmethylsulphonylfluoride
PS	Phosphatidylserine
Q-VD-OPh	N-(2-Quinolyl)valyl-aspartyl-(2,6-difluorophenoxy)methyl ketone
RAIDD	RIP associated ICH-1/CED-3-homologous protein with DD
RNAi	RNA interference
RT	room temperature
SDS	Sodium dodecyl sulfate
SDS-PAGE	Sodium dodecyl sulfate polyacrylamide gel electrophoresis
SEM	Standard error mean
shRNA	Short hairpin RNA
siRNA	Short interfering RNA
Smac	Second mitochondria derived activator of caspases
SSC	Sideward scatter
STAT3	Signal transducer and activator of transcription 3
TBS-T	Tris buffered saline with tween
TEMED	N, N, N' N' tetramethylethylene diamine
TNF	Tumor necrosis factor
TNF-R1	TNF receptor 1
TRAIL	TNF-related apoptosis inducing ligand
UV	Ultraviolet
VDAC	Voltage dependent anion channel
WB	Western blot
XIAP	X-chromosome linked IAP
zVADfmk	N-benzyloxycarbonyl-Val-Ala-Asp(OMe)-fluoromethylketone
zVDVADfmk	N-benzyloxycarbonyl-Val-Asp-Val-Ala-Asp-fluoromethylketone



# I INTRODUCTION

## 1 NATURAL PRODUCTS AS ANTICANCER AGENTS

Since ancient times natural products have played a major role in the treatment of diseases. The American Indians used plant extracts from *Podophyllum peltatum* to effectively treat skin cancers. Podophyllotoxin is the main constituent of this plant's root and belongs to the group of anticancer agents known as podophyllins. Among this group etoposide is found, which is in regular use for the treatment of testicular teratoma and small-cell lung cancer (1).

Further discoveries based upon folk medicine were the substances vinblastine and vincristine, constituents of the plant *Vinca rosea*, which have significantly contributed to the successful treatment of cancer. These discoveries led to the beginning of a screening program for antitumor agents (see Table I.1) by the US National Cancer Institute (NCI) in 1960. Between 1960 and 1982 about 35,000 plant samples were tested, primarily against mouse leukemia cell lines. The most effective drug obtained from the screening was paclitaxel (Taxol), originally isolated from the bark of *Taxus brevifolia* (1,2).

In 1985, the NCI started a new program in which extracts from plants, animals and microorganisms (increasingly those of marine origin) were tested against a panel of 60 human cancer cell lines (1). The intention was to detect compounds that are active against solid tumors, which would have been missed in the original screen. And, in fact, almost 60% of drugs approved for cancer treatment today are of natural origin (3, 4).

The majority of chemotherapeutic drugs used in cancer therapy induce death in malignant cells through apoptosis or other kinds of programmed cell death. The inactivation of this cell death mechanism is a fundamental hallmark of cancer and leads to drug resistance. Therefore, compounds with unusual mechanisms of action are needed to circumvent chemoresistance. Natural compounds have the advantage of greater diversity than synthetic chemical libraries (5). Especially the chemical and biological diversity of the marine environment has not been acquired for a long time yet and provides great potential for the discovery of antitumor agents with novel molecular modes of action.

**Table I.1 Anticancer agents derived from natural origin in development or clinical use (adapted from 2, 4, 5)**

<b>Plant-derived anticancer agents</b>		
Compound	Source	Status
Etoposide	<i>Podophyllum peltatum</i>	Phase III/IV
Vinblastine, vincristine	<i>Vinca rosea</i>	Phase III/IV
Paclitaxel	<i>Taxus brevifolia, Taxus baccata</i>	Phase III/IV
<b>Microbe-derived anticancer agents</b>		
Compound	Source	Status
Bleomycin	<i>Streptomyces verticillus</i>	Phase III/IV
Daunomycin, doxorubicin	<i>Streptomyces sp</i>	Phase III/IV
Epothilone	<i>Sorangium cellulosum</i>	Phase III/IV
<b>Marine-organism-derived anticancer agents</b>		
Compound	Source	Status
Bryostatin 1	<i>Bugula neritina</i>	Phase I/II
Ecteinascidin-743	<i>Ecteinascidia turbinata</i>	Phase I/II
Spongistatin 1	<i>Hyrtios altum</i>	Preclinical

## 2 THE CEPHALOSTATINS

Until the mid 1960s, investigation of natural products with marine origin was essentially non-existent. Since then, about 10,000 new structures have been isolated from marine microorganisms, sponges and e.g. marine invertebrates (1).

A promising group of compounds with marine origin comprises the family of cephalostatins (6, 7, 8, 9, 10, 11, 12, 13, 14). The cephalostatins were isolated by Prof. G. R. Pettit from the South African marine tube worm *Cephalodiscus gilchristi* Ridewood (family Cephalodiscidae). Until today, 19 members of this family have been characterized, all of which show the same unique growth inhibitory profile (Figure I.1) in the NCI-60 cell line screen.

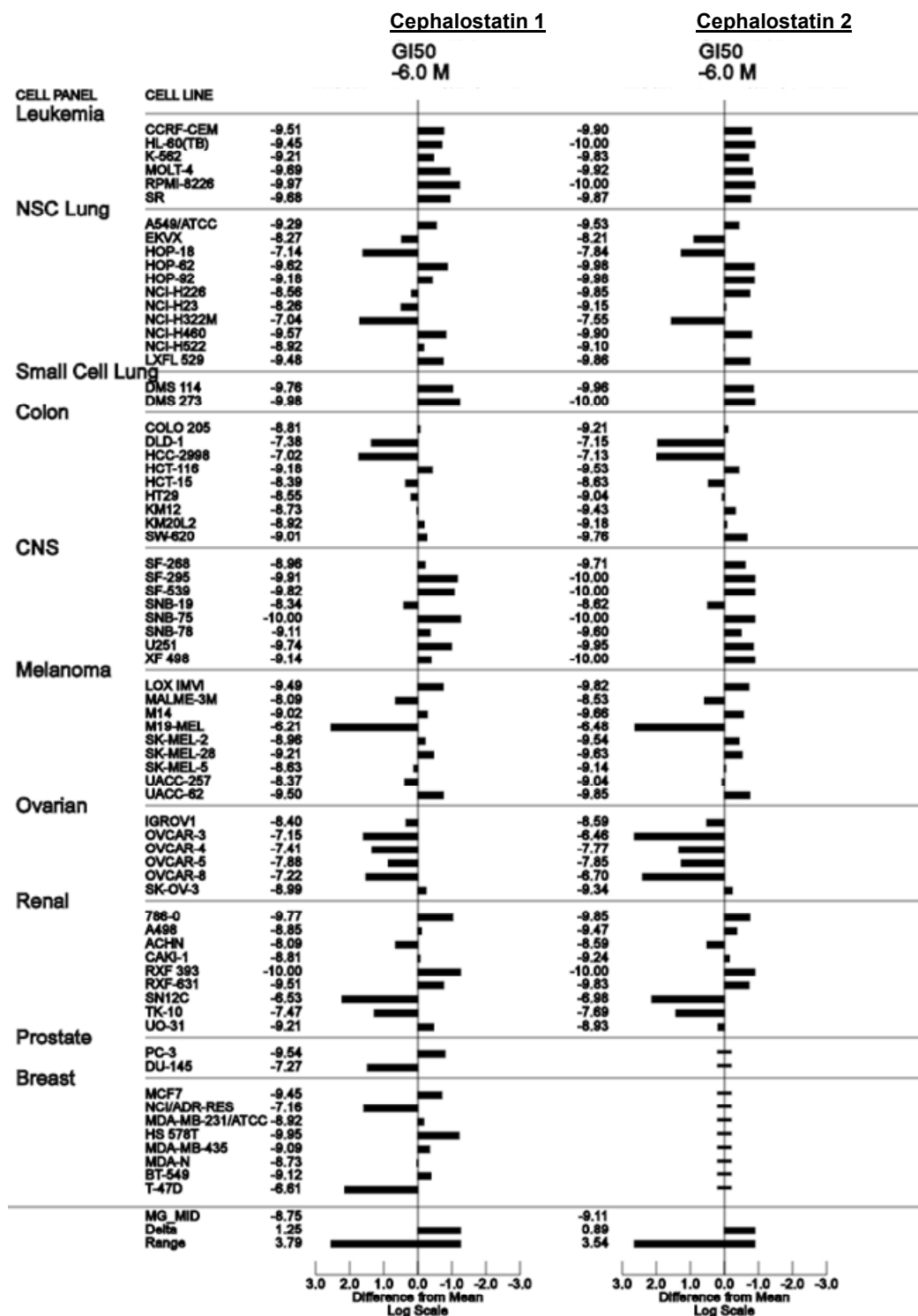


Figure I.1 Fingerprint of cytotoxic profile of cephalostatin 1 and 2 evaluated by the NCI-60 screen (September 2005).

The zero value represents the mean of all cell lines tested. The bars indicate the deviation of the mean data obtained from the individual cell line from the overall mean and marks the sensitivity of the cell lines for cephalostatin 1 or 2 (negative bars, less sensitive; positive bars, more sensitive) GI<sub>50</sub>: 50% growth inhibition in the 2 days cytotoxicity assay.

Surprisingly, the NCI compare analysis between cephalostatin and any other compound of the NCI standard agent database shows no apparent correlation (best correlation 0.5 with teniposide), suggesting that the cephalostatins might employ unique signaling pathways, differing from any other anticancer drug. First studies carried out by our group support this notion (15, 16, 17).

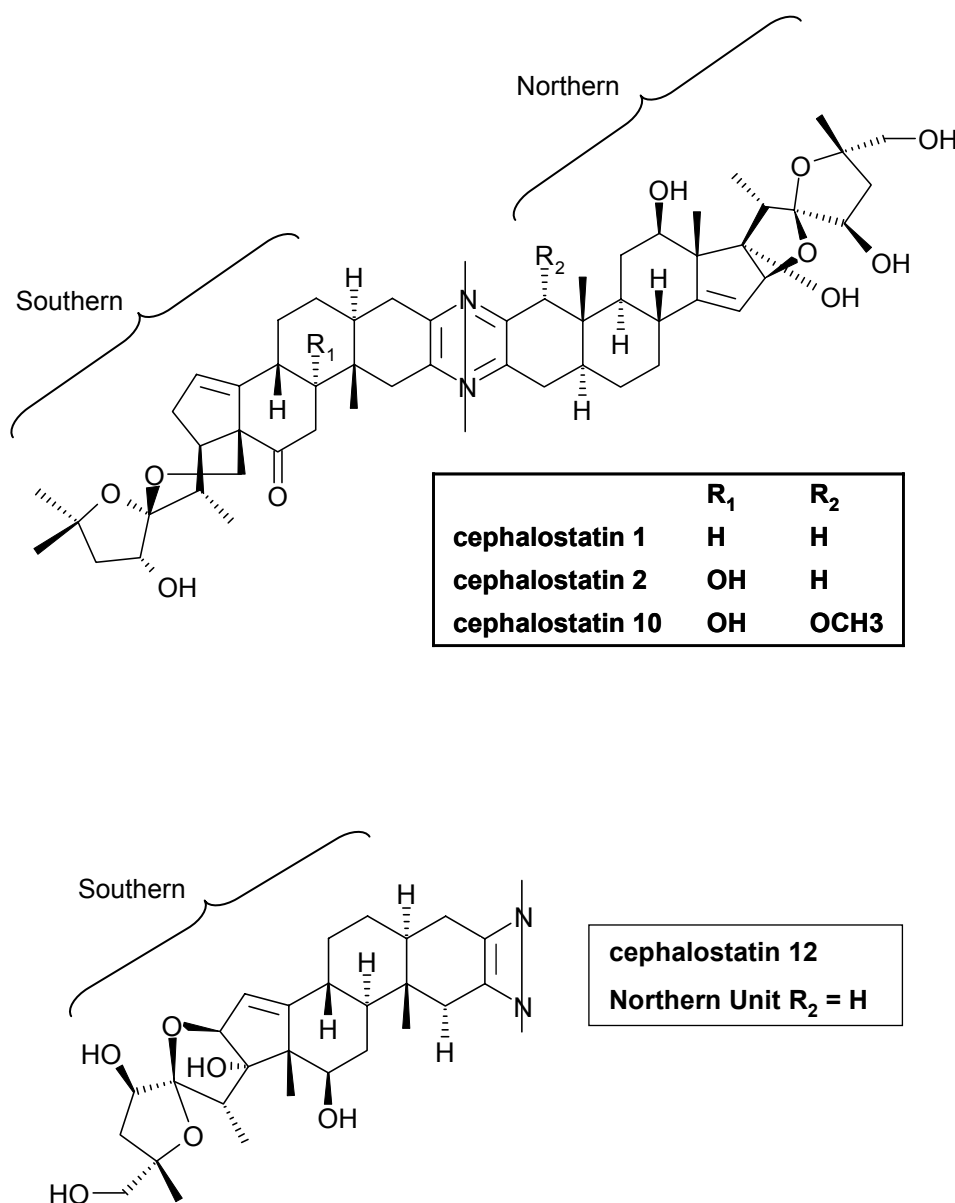


Figure I.2 Chemical structure of cephalostatin 1, 2, 10 and 12

Cephalostatin 1 and 2 are proven to be the most potent cephalostatins in the NCI-60 panel, with a GI<sub>50</sub> value of 1 nM (see Figure I.1). In addition to the *in vitro* screen,

cephalostatin 1 and 2 were successfully tested *in vivo* on several xenografts like leukemia and melanoma.

Although the cytotoxicity profile of the cephalostatins does not differ (see Figure I.1), their potency varies depending on the chemical composition (Figure I.2). Structure-activity studies on different cephalostatins revealed that the Northern part is the most shared unit among the cephalostatins and is also strongly associated with antitumor activity (18). Cephalostatin 10 shows dose dependencies comparable to cephalostatin 1 and 2 (6, 7, 10), whereas an increased level of hydroxylation in the Southern part results in decreased antitumor activity, as in the case of cephalostatin 12 (18).

### **3 AIM OF THE STUDY**

Cephalostatin has been intensively studied by our research group in the last years. The suggestion based on the NCI compare analysis that cephalostatin differs from other chemotherapeutic drugs known so far was confirmed by investigating the substance in Jurkat leukemia T cells. Cephalostatin-induced cell death is not dependent on the CD95/caspase-8 pathway and does not induce the formation of the apoptosome (15), although caspase-9 is an important initiator caspase for cephalostatin in Jurkat T cells (17). Further, the induction of endoplasmic reticulum stress could be shown for cephalostatin and that caspase-4 is an initiator caspase that partially contributes to caspase-9 activation (17).

The release of different mitochondrial proteins into cytosol is a hallmark of apoptosis. Cephalostatin was found to induce an early and predominant Smac release, whereas cytochrome c could not be detected in the cytosol (15). This fact deserves attention and asks for the release mechanism and the impact of Smac on cephalostatin-mediated apoptosis.

The aim of the present work was to further investigate the underlying mechanism and characteristics of cephalostatin induced cell death based on previous work of our group (15, 16, 17), with the following main topics:

1. Is cephalostatin-induced apoptosis restricted to Jurkat T cells?
2. How is the selective Smac release mediated by cephalostatin?
3. Does Smac release influence apoptosis induction by cephalostatin?

## 4 PROGRAMMED CELL DEATH

The balance between cell division and cell death is of utmost importance for the development and homeostasis of a multicellular organism. Deregulation of either process has pathologic consequences and can lead to disturbed embryogenesis, neurodegenerative diseases, autoimmunity and the development of cancer. Therefore, the balance between life and death is strictly controlled and damaged or unnecessary cells are eliminated by a process called programmed cell death (PCD) (19, 20).

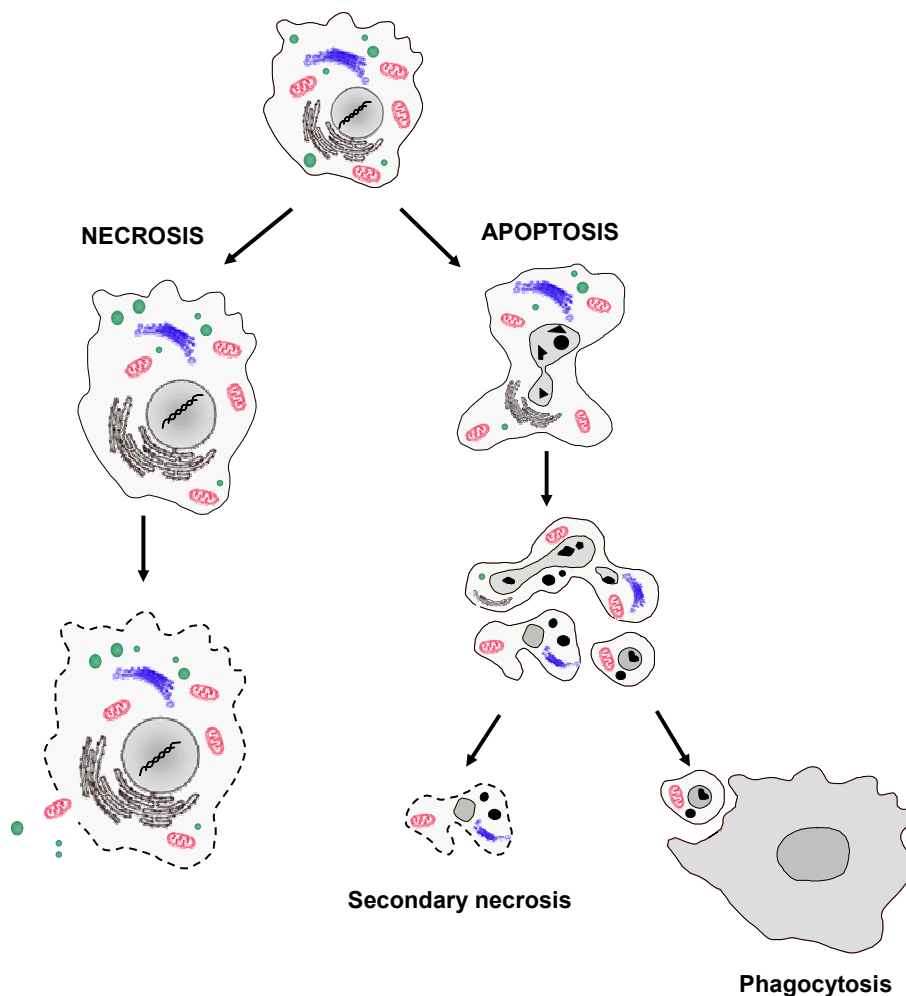


**Figure I.3 Overview of apoptotic and necrotic cell death**

Apoptosis is characterized by cell shrinkage, chromatin condensation and fragmentation of the cell in membrane enclosed apoptotic bodies. These are engulfed by macrophages (phagocytosis), thus preventing inflammation. In contrast, in necrosis the cell swells and the membrane ruptures. As a consequence cellular content is released into the surrounding tissue and inflammation is induced.

The classical ultrastructural studies of Kerr et al. (21) shed light on at least two distinct types of cell death, namely apoptosis and necrosis (Figure I.3). Apoptosis is the most common and best characterized form of PCD and was held synonymously for PCD over a long time. It is characterized by typical morphological changes such as cell shrinkage, chromatin condensation and cleavage by endonucleases and plasma membrane blebbing. Finally, the cell is fragmented into apoptotic bodies. These compact membrane-enclosed structures contain the cytosol and cell organelles. The “packaging” of the intracellular content prevents an inflammatory response, since the apoptotic bodies are engulfed by macrophages and thus removed from the tissue. An important step in this is the exposure of phosphatidylserine on the cell surface, which mediates the recognition of the apoptotic bodies by the macrophages. The morphological changes are a consequence of highly conserved, genetically controlled molecular and biochemical events, most notably mediated by caspases, a family of cysteine proteases activated in apoptosis (20).

Necrosis is – in contrast to apoptosis – an uncontrolled, passive form of death. It is usually the consequence of exposure e. g. to high concentrations of cytotoxic agents or of pathophysiological conditions, such as infection and ischemia. The swelling of the cell and rupture of the plasma membrane is a characteristic event in necrosis, resulting in the release of cellular content into the surrounding tissue and extensive inflammation. Typical attributes of apoptotic cell death like DNA fragmentation and formation of apoptotic bodies are absent in necrosis (20).

In recent years, it has become evident that the classic distinction of apoptosis and necrosis is a simplification of a highly complex system. Although caspase-mediated apoptosis is the underlying cell death program in many settings, it is unlikely that this mechanism is the only protection of an organism against unwanted and potentially harmful cells. Indeed, multiple alternative cell death pathways – even completely caspase independent ones – as well as crosstalk of PCD mechanisms are described. The various types of PCD share a common feature, namely that they are executed by active cellular processes (22, 23, 24). Since the characterization of signal transduction in alternative death styles is still in progress, one approach to classification is the nuclear morphology of the dying cell. Table I.2 gives an overview of characteristics related to different types of cell death, including morphological and biochemical features known so far.

Another approach is to classify caspase-independent cell death according to the cellular organelles involved. Thus, several models have been proposed to categorize PCD, but well defined terms are difficult to create and are probably artificial due to

the overlapping and commonly used signal transductions pathways between the different cell death mechanisms.

**Table 1.2 Characteristics of different types of cell death adapted from (23, 25, 26)**

Type of cell death	Morphological changes			Biochemical features
	Nucleus	Cell membrane	Cytoplasm	
<b>Apoptosis</b>	chromatin condensation, nuclear fragmentation, DNA laddering	blebbing	packaging into apoptotic bodies	caspase-dependent
<b>Autophagy</b>	partial chromatin condensation, DNA-fragmentation very late, if at all	blebbing	increased number of autophagic vesicles	caspase-independ., increased lysosomal activity
<b>Mitotic catastrophe</b>	multiple micronuclei, nuclear fragmentation	no consensus on the distinctive morphological appearance by now		caspase-independ. (at early stage)
<b>Necrosis</b>	clumping and random degradation of nuclear DNA	swelling, rupture	increased vacuolation, organelle degradation, mitochondrial swelling	no energy requirement

## 5 APOPTOSIS SIGNAL TRANSDUCTION

Apoptosis is a tightly regulated and highly conserved cell death program which requires the interaction of multiple factors. It can be triggered by various stimuli from outside (receptor mediated) or inside (intracellular stress) the cell. Upon such a signal caspases (cysteine-dependent aspartate-specific proteases) are activated in classical apoptosis, leading to cell death.

## 5.1 CASPASES

Although the first caspase, interleukin-1 $\beta$ -converting enzyme (ICE or caspase-1), was identified in humans, the critical involvement of caspases in apoptosis was discovered in the model organism *Caenorhabditis elegans*. There, the gene *ced-3* (cell death abnormality-3) was found to encode a cysteine protease, an essential component in developmental cell death that is closely related to the mammalian ICE. Since then, at least 14 distinct mammalian caspases have been identified, 12 of which are human. (27, 28)

### 5.1.1 CLASSIFICATION, STRUCTURE AND ACTIVATION

Caspases can be classified according to their structure, function and preferred substrates.

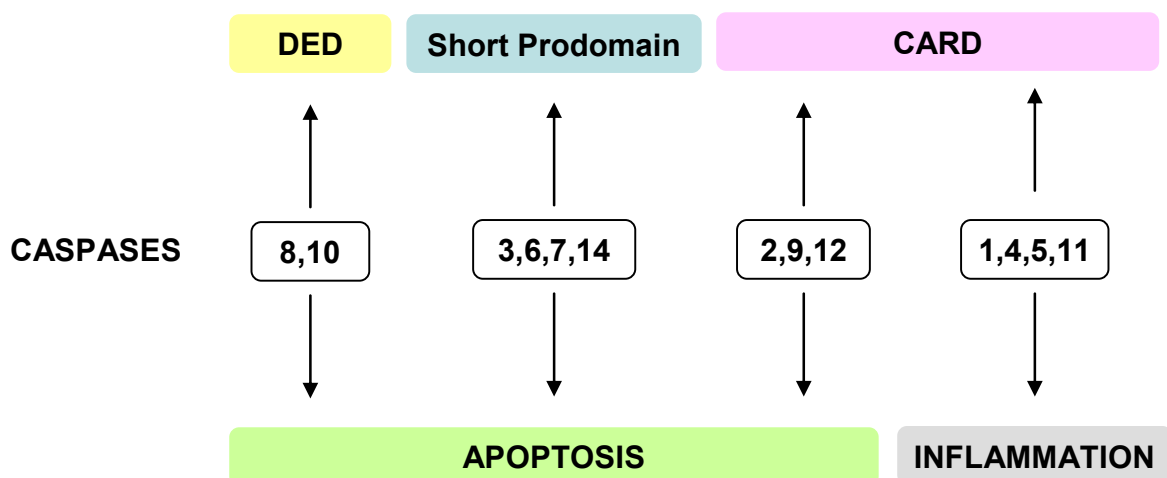


**Figure I.4 Classification of caspases based on their prodomain structure or function**

Caspases containing a long prodomain with a CARD (caspases 1, 2, 4, 5, 9, 11, 12) can be divided upon their function in inflammatory (caspases 1, 4, 5, 11) and apoptotic (caspases 2, 9, 12) caspases. Caspases-8 and 10 possess two DEDs in their long prodomain and belong to the apoptotic family members. Caspases 3, 6, 7 and 14 are apoptotic effector caspases with short prodomain.

If caspases are divided into groups by their structural characteristics, two main categories – caspases with long or short prodomain – are formed (Figure I.4).

Long prodomains comprise structural motifs in the death domain superfamily, including the caspase activation and recruitment domain (CARD) and the death effector domain (DED). Caspases with long prodomain (caspases 1, 2, 4, 5, 8, 9, 10, 11, 12) are enabled to interact with other proteins by these structures. This plays an important role in apoptotic signaling, since CARD and DED are the responsive elements for the recruitment of initiator caspases into death- or inflammation-inducing signaling complexes, where caspases are activated. Caspases 3, 6, 7 and 14 have short prodomains and are activated by other caspases upon proteolytic cleavage (27, 28,29).

Classification of caspases by their primary function leads to two groups comprised of inflammatory and apoptotic caspases, whereas the latter can be divided in initiator (caspases 2, 8, 9, 10, 12) and effector (caspases 3, 6, 7, 14) caspases (27).

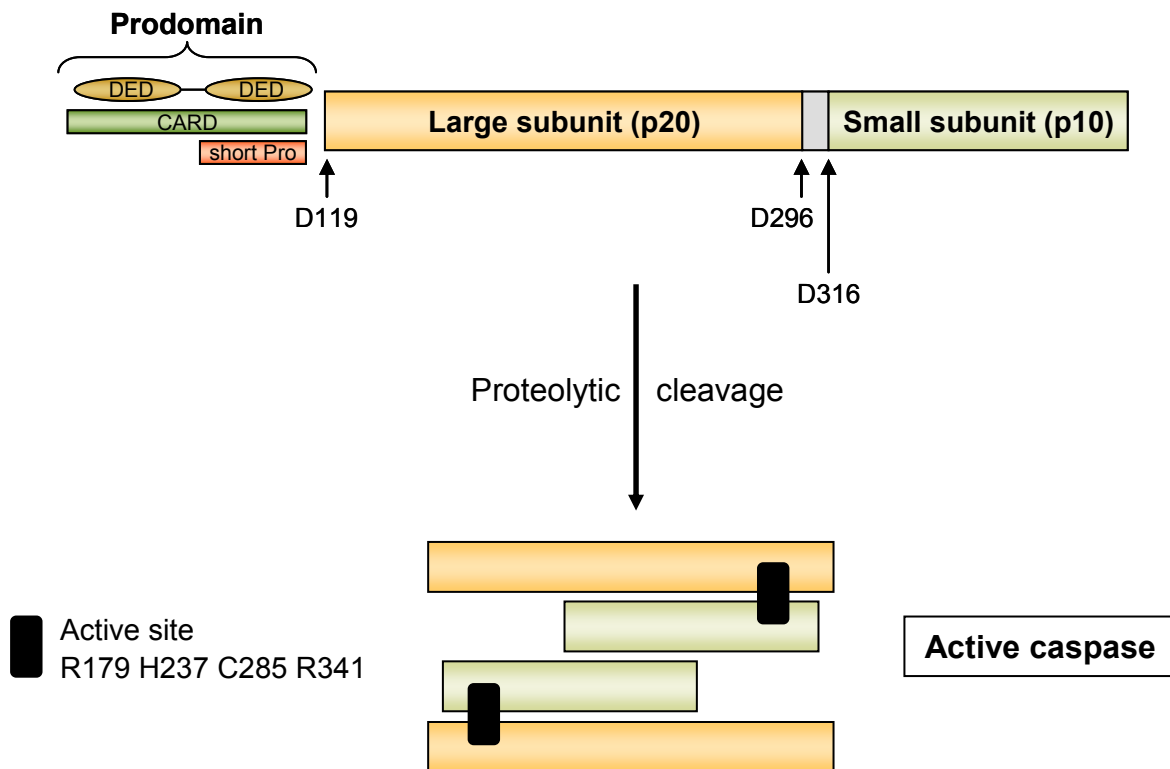


**Figure I.5 Schematic representation of proteolytic caspase activation (modified from 31)**

Activation proceeds by cleavage of the N-terminal domain at Asp119, Asp296 and Asp316 (all caspase-1 numbering convention) leading to a large (p20) and a small (p10) subunit. The activity and specificity determining residues (R179, H237, C285 and R341) are brought into the necessary structural arrangement for catalysis. Cys285 is the catalytic nucleophile. The active caspase is a tetramer of two heterodimers, each comprising a large and a small subunit and an active site.

All caspases are synthesized as catalytically inactive zymogens. The zymogens consist of the different N-terminal prodomains described above followed by a large subunit of approximately 20 kDa (p20) and a small subunit of 10 kDa (p10). The subunits are separated by a small linker sequence (30) (see Figure I.5).

To become catalytically active a procaspase must undergo conformational changes and usually has to be cleaved to produce its mature form. Mature caspases are formed by association of two monomers, with each monomer comprising the large (p20) and the small (p10) subunits. Each tetramer contains two active sites formed by residues of the large and small subunit (31, 32).

Effector caspases are activated by initiator caspases through removal of the N-terminal prodomain and the linker peptide within the protease domain by cleavage at specific internal Asp residues that separate the large and small subunits. As a consequence, a conformational change occurs and the catalytic activity of the effector caspase is enhanced (31). How initiator caspases are activated is not fully understood. Two models have been proposed, namely the induced proximity and the proximity-induced dimerization model, the latter stating that the initiator caspases are recruited to large protein complexes, brought into close proximity and get activated upon dimerization (32). At present, there are different complexes described like the death inducing signaling complex (DISC), the apoptosome and the PIDDosome.

### **5.1.2 SUBSTRATES**

Caspases recognize at least four (caspase-2 five) contiguous amino acids in their substrates P4-P3-P2-P1 and cleave after the C-terminal P1, which is usually an aspartate. The P3 position is a glutamine residue for all examined caspases, whereas the P4 position varies among different groups of caspases. Effector caspases cleave numerous proteins, including some that are responsible for structural integrity of the cell, as the DNA repair enzyme PARP (poly ADP-ribose polymerase), which is cleaved by caspase-3. Initiator caspases can activate effector caspases by proteolytic cleavage but have many other targets in the cell. For example, caspase-2 can cleave the protein golgin-160, which controls the integrity of the Golgi complex. A prominent caspase-8 substrate is the Bcl-2 family member Bid. After cleavage, Bid translocates to the mitochondria, thus promoting cytochrome c release (27). Overall, more than 280 caspase substrates are identified to date (33).

### 5.1.3 REGULATION

Because caspases play an important role in apoptosis initiation, their expression and activation state must be tightly regulated. Caspase regulation is achieved by transcriptional and posttranscriptional mechanisms. The conserved IAP (inhibitor of apoptosis) protein family can inhibit the enzymatic activity of caspases. Furthermore, caspase can be removed through proteasomal degradation promoted by IAPs. The IAP proteins were originally identified in the genome of baculovirus on the basis of their ability to suppress apoptosis in infected host cells. At least eight IAPs have been found in mammals (34, 35, 36) (see Figure I.6).

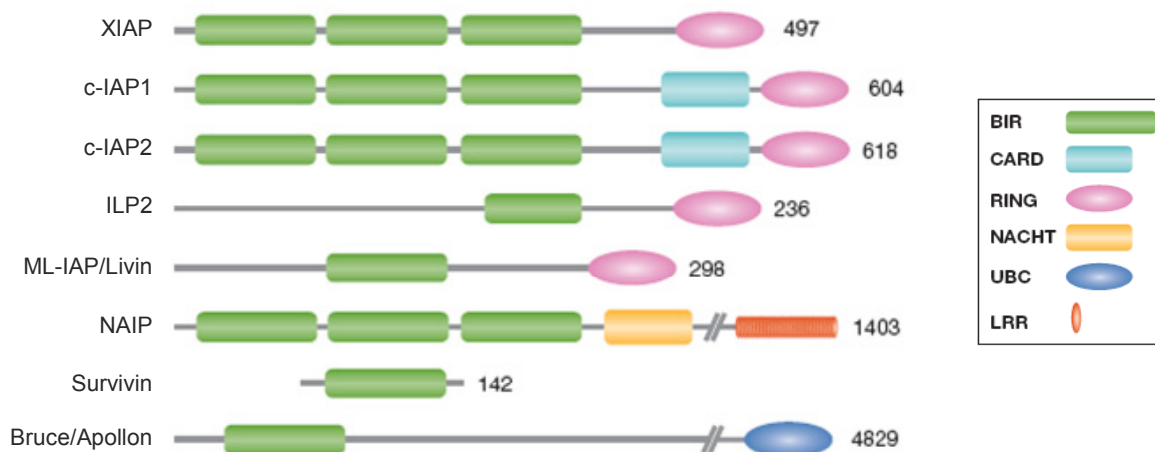


**Figure I.6 Schematic representation of the inhibitor of apoptosis protein family (36)**

IAPs have at least one baculoviral IAP repeat (BIR) domain. Additionally, most IAPs have other distinct functional domains such as the NACHT domain, the leucine-rich repeats (LRRs) and the RING (really interesting new gene) domain. The latter is an E3 ligase that presumably directs targets to the ubiquitin-proteasome degradation system. Bruce has an ubiquitin-conjugation (UBC) domain that is found in many ubiquitin-conjugating enzymes. (BIR, baculoviral IAP-repeat; cIAP, cellular IAP; IAP, inhibitor of apoptosis protein; ILP, IAP-like protein; ML-IAP, melanoma IAP; NAIP, neuronal apoptosis-inhibitory protein; NACHT, domain found in NAIP; XIAP, X-chromosome-linked IAP.)

The hallmark of IAPs is the baculoviral IAP repeat (BIR) domain, a ~80 amino acid zinc binding domain. XIAP, the most extensively studied IAP member contains three BIR domains with different functions: BIR3 potently inhibits the activity of processed caspase-9, whereas the linker region between BIR1 and BIR2 targets caspase-3 and -7. The IAP mediated inhibition of caspases is antagonized by a family of proteins

that contain an IAP-binding motif like the mitochondrial protein Smac/DIABLO (see chapter I5.3.1) and Omi/HtrA2. Except for survivin, all other IAPs contain other functional domains such as a RING domain, an E3 ligase that presumably directs targets to the ubiquitin proteasome degradation system (34, 35).

Survivin, the smallest member of the IAP family with a single BIR domain, is transcriptionally regulated by the oncogenic transcription factor STAT3 (37). The BIR domain of survivin is closely related to the BIR3 of XIAP and several studies showed that survivin is capable of binding caspases -3, -7 and -9 but this is still controversially discussed (38, 39). Besides its function in controlling apoptosis, the IAP member survivin seems to regulate the mitotic progression and the production of the survivin protein is upregulated in G2/M phase.

## 5.2 EXTRINSIC PATHWAY

There are two alternative pathways – the extrinsic and the intrinsic pathway - that initiate apoptosis depending on the origin of the death stimuli. The extrinsic pathway is mediated by death receptors on the cell surface and has a crucial role during development and for the immune system. The death receptors (DR) belong to the tumor necrosis factor (TNF) receptor superfamily, characterized by an extracellular ligand binding domain and an intracellular death domain. In mammals several death receptors are known as TNF-R1, TRAIL or CD95 (= Fas, APO-1), the latter being the most extensively studied. The TNF receptor superfamily includes the decoy receptors, which lack a functional death domain, thus building a negative regulation mechanism. (19, 40)

The extrinsic pathway (Figure I.7) is initiated upon binding of an extracellular ligand such as CD95L to its receptor (in this case CD95). After ligation, micro-aggregates are formed on the cell surface leading to the attraction of the intracellular adaptor protein FADD (Fas-associated death domain protein) via the death domains. FADD, in turn recruits the inactive caspase-8 or -10 zymogens through interaction with their death effector domain (DED) to the so called DISC (death inducing signaling complex). At the DISC the initiator caspases get active, which is in type I cells sufficient to initiate apoptosis directly via the induction of downstream effector caspases like caspase-3 and -7. (19)

In type II cells the amount of active caspase-8 is not enough, so an amplification of the apoptotic signal via the mitochondria takes place. This crosstalk is mediated by

the cleavage of Bid into truncated Bid (tBid) by active caspase-8. Subsequently tBid translocates to the mitochondria and induces the release of apoptotic proteins like cytochrome c (41).

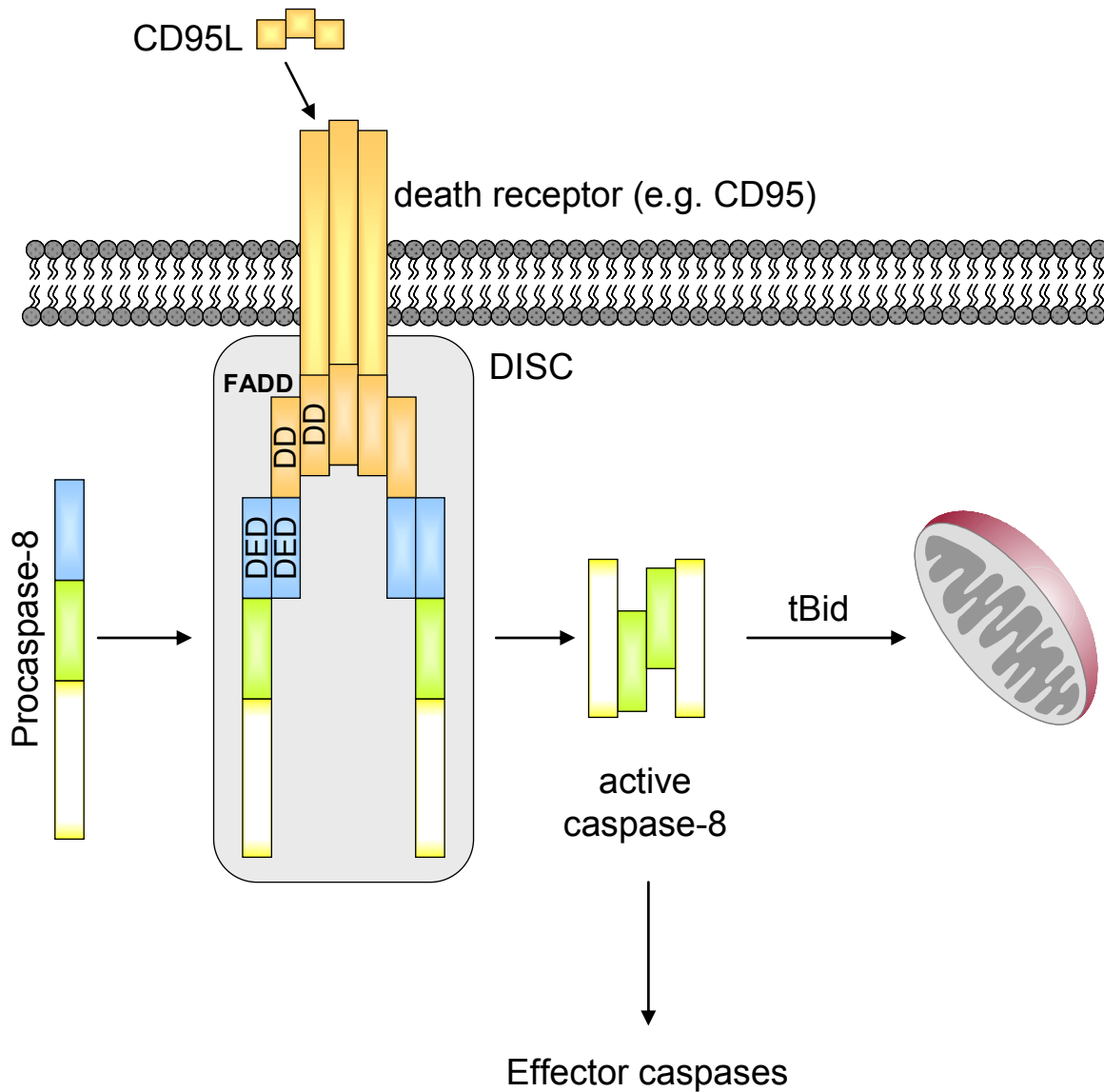


**Figure I.7 The extrinsic apoptotic pathway**

On binding of CD95 ligand to its receptor CD95, trimerization takes place and FADD is recruited to the cytosolic domain via interaction with the death domain (DD). Caspase-8 binds to the complex thus forming the death inducing signaling complex (DISC), where it is activated. An amplification of the apoptotic signal is possible upon caspase-8 mediated cleavage of Bid, which translocates to mitochondria.

### 5.3 INTRINSIC PATHWAY

Mitochondria, the main energy producers of the cell, are essential for maintaining cellular life and play a major role in the apoptotic process at the same time. Besides amplifying the extrinsic apoptotic pathway, mitochondria are the central organelles involved in the propagation of death signals originating from inside the cell. Such signals can be for example DNA-damage, oxidative stress or signals induced by chemotherapeutic drugs. The central event of intrinsic apoptosis induction is the mitochondrial membrane permeabilization (MMP) of the outer (OMM) and the inner (IMM) mitochondrial membrane. MMP causes the dissipation of the mitochondrial membrane potential ( $\Delta\psi_m$ ), which is required for mitochondrial functions as ion transport or energy conservation. When outer membrane integrity is lost proapoptotic proteins from the mitochondrial inter-membrane space are released into cytosol and either activate caspases or act in a caspase-independent manner leading to cell death. Cytochrome c, Smac/Diablo (second mitochondria derived activator of caspases / direct IAP binding protein with low pI), Omi/HtrA2 (high temperature requirement protein A2), AIF (apoptosis inducing factor) and EndoG (endonuclease G) belong to these apoptotic factors (42, 43).

AIF translocates from mitochondria into the nucleus and causes caspase-independent cell death. It induces chromatin condensation and high molecular weight DNA fragmentation. AIF is a flavoprotein with dual roles in life and death since besides its role in apoptosis its participation in the formation of the respiratory complex I was shown. EndoG also translocates to the nucleus and mediates internucleosomal DNA-fragmentation (44).

Cytochrome c is involved in electron transport and induces upon apoptotic stimuli the energy-dependent (ATP/dATP) formation of the apoptosome (Figure 1.8). This oligomeric complex consists of the protein Apaf-1 (apoptotic protease activating factor 1) whose conformation is changed after binding to cytochrome c, ATP/dATP and procaspase-9. In the apoptosome complex caspase-9 is activated and initiates the caspase cascade, finally leading to cell death (19, 45).

For the prevention of accidental caspase activation there is a negative regulatory mechanism by the inhibitors of apoptosis proteins (IAPs) (see 1.5.1.3). These in turn are inactivated by Smac (see 1.5.3.1) and Omi/HtrA2. Omi is a serine protease that has been reported to cleave cIAPs and to participate in caspase-independent apoptosis (40, 46, 47, 48).

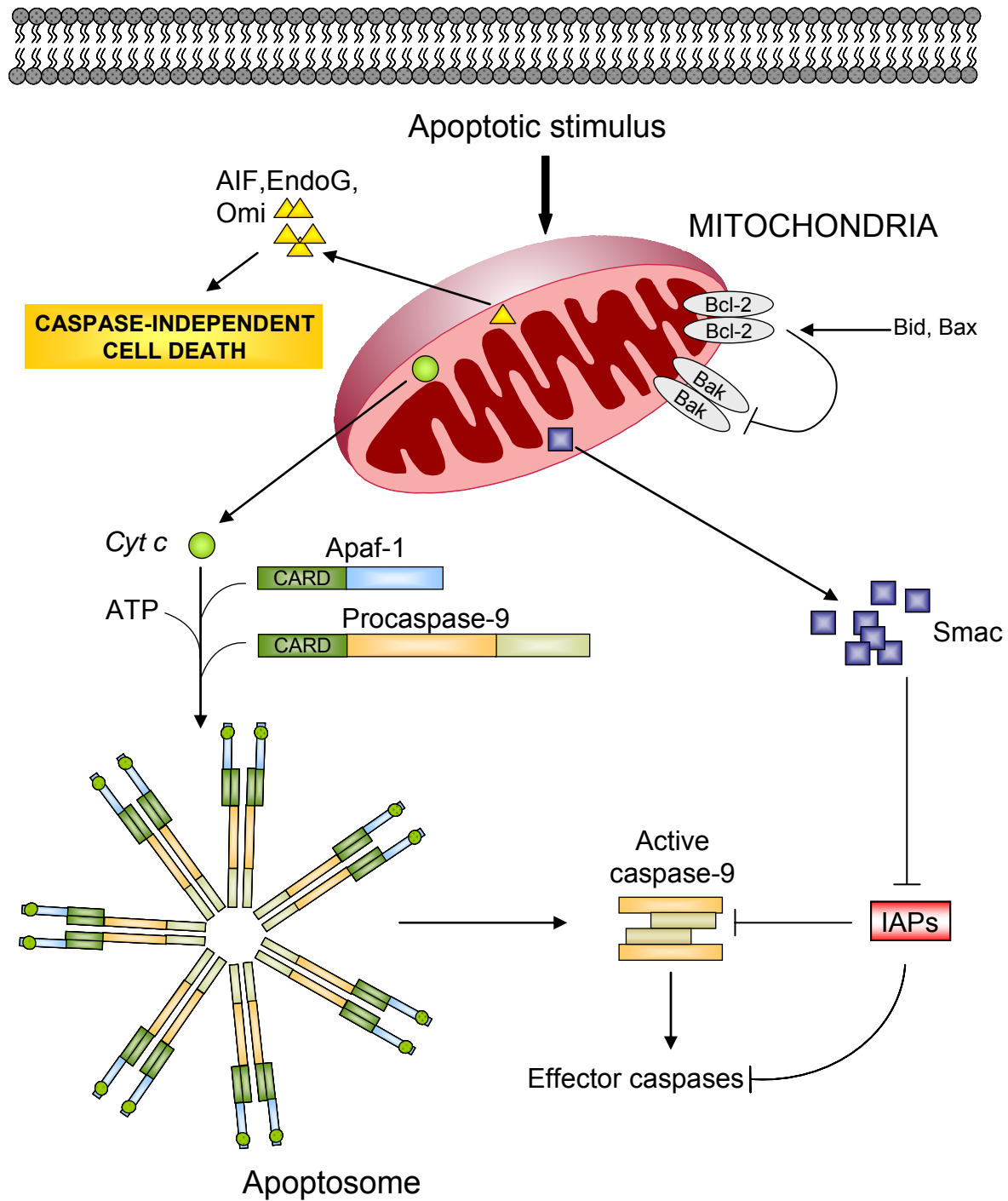


**Figure I.8 The intrinsic apoptotic pathway**

Mitochondria are the central organelles in the intrinsic apoptosis pathway. Upon many different stimuli like chemotherapeutic drugs, the mitochondria membrane is permeabilized and proapoptotic proteins are released into cytosol. A complex is formed consisting of cytochrome c, Apaf-1 and procaspase-9, where this caspase is activated and initiates the activation of effector caspases. Smac abolishes the negative regulation on caspases by IAP. AIF, Omi and EndoG are supposed to induce caspase-independent cell death. Bcl-2 family proteins (e.g. Bax, Bid) regulate the intrinsic pathway.

### 5.3.1 SMAC

Smac is the best known antagonist of the IAP family and reactivates processed initiator as well as effector caspases through distinct mechanisms, although both require physical interaction with IAPs. Smac is a constitutively expressed protein located in inter-membrane space. Its N-terminal 55 residues encode a mitochondria-targeting sequence, which is proteolytically removed to generate the 23 kDa mature Smac on entry into the mitochondria. This cleavage results in the exposure of four hydrophobic amino acids (Ala-Val-Pro-Ile), the tetrapeptide IAP binding motif at the N-terminus (30).

Caspase-9 contains a similar internal IAP binding tetrapeptide motif (Ala-Thr-Pro-Phe), which is exposed after activation (proteolytic cleavage). This leads to the recruitment of XIAP to active caspase-9, thus inhibiting the caspase. Smac binds via its IAP binding motif to a highly conserved surface groove on the BIR3 domain of XIAP and competitively displaces the bound caspase-9, thus reactivating it (Figure I.9).

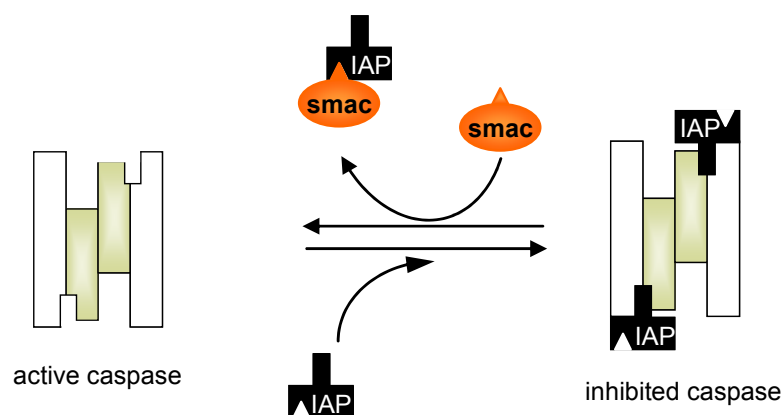


**Figure I.9 Simplified illustration of removal of IAP-mediated caspase-inhibition by Smac**

Smac can bind various IAPs through its N-terminal tetrapeptide binding motif. In case of initiator caspase-9, which has a similar IAP binding motif, active caspase-9 is displaced competitively with Smac from XIAP. The inhibition of effector caspases by XIAP is abolished by steric reasons after binding of Smac to BIR2 of IAPs.

Smac plays a less immediate role in removing the IAP-mediated inhibition of effector caspases, since the binding site of the IAP binding motif of Smac maps to BIR2 and BIR3, but the IAP fragment responsible for inhibiting caspase-3 and -7 is the linker between the BIR1 and BIR2 domain of XIAP. Although the mechanism is not fully



anion channel). Upon a death stimulus Bak and Bax undergo a conformational change, oligomerize and induce the formation of a pore in the OMM through which e.g. cytochrome c and Smac are released. Another model proposes that Bax targets one or more components of the permeability transition in the IMM (40, 52).

Group III, also known as BH3-only proteins, has many members whose common feature is the presence of a single BH3 domain. These proteins fulfill their proapoptotic function either by activating proapoptotic proteins like Bax or by inhibiting antiapoptotic Bcl-2 proteins. Bid for example is thought to induce the conformational change in Bax/Bak, which leads to insertion in the OMM.

## 5.4 PIDDosome

Recruitment to large macromolecular complexes is a critical step in activating initiator caspases. This is well established for caspase-8, which is recruited to the death inducing signaling complex (extrinsic pathway, see I.5.2) and for caspase-9, which is activated in the apoptosome (intrinsic pathway, see I.5.3) complex. Besides these two complexes the inflammasome is known with the inflammatory initiator caspases -1 and -5 as constituents (53).

Caspase-2 is one of the most conserved caspases and shares the commonness of the initiator caspases named above: it contains a CARD, the responsible structural element for recruitment to the described protein complexes.

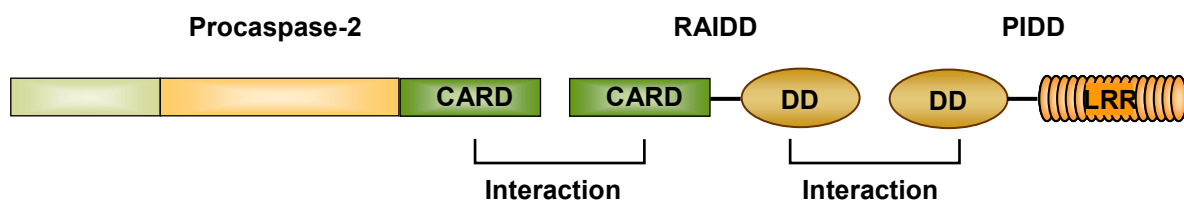


**Figure I.11 The PIDDosome**

Caspase-2 can be activated via the PIDDosome. This complex consists of procaspase-2, the adaptor protein RAIDD and the p53-inducible protein with a death domain (PIDD). Procaspase-2 and RAIDD can interact via their caspase-recruitment domain (CARD). RAIDD interacts with PIDD via a death domain (DD). PIDD also contains LRR (leucine rich repeats), a protein interaction motif found in various proteins with diverse function.

Indeed, a complex for the activation of caspase-2 was recently described as well. The so called PIDDosome (Figure I.11) is a large protein complex with a molecular weight in excess of 670 kDa. It consists of the adaptor protein RAIDD (RIP-associated ICH1/CED3-homologous protein with a death domain) and PIDD (p53-induced protein with a death domain). RAIDD contains a CARD through which it can bind caspase-2 and a DD that allows interaction with PIDD (54, 55, 56).

Besides the death domain PIDD contains N-terminal leucine-rich repeats (LRRs), protein interaction motifs probably for recognizing signals of unknown nature (53, 56, 57).

Activation of the PIDDosome is described to sensitize cells to genotoxic stress, but in addition to DNA-damage cell lysis under hypotonic conditions initiates the assembly (56).

At present, it is unclear whether additional factors are involved in the assembly of the PIDDosome.

### **5.5 APOPTOSIS DEREGLATION – TARGETS FOR DRUG DISCOVERY**

Deregulation of apoptosis can disrupt the balance between proliferation and cell death and can lead to diseases as cancer. In many cancers, proapoptotic proteins have inactivating mutations or are deleted or the expression of antiapoptotic proteins is upregulated. Cancers that possess alterations in proteins involved in the extrinsic or intrinsic cell death signaling are often resistant to chemotherapy. The metastatic melanoma for instance still has poor prognosis with response rates ranging from 10 to 25% and a mean survival of 8 month for single dacarbazine treatment. Neither combination of dacarbazine with other drugs nor immunotherapy could effectively improve the therapy outcome. Therefore, new strategies to restore programmed cell death are needed and might be effective against many cancers. One promising approach is the investigation of the altered signal network in cancer growth regulation in order to act with specificity at molecular level. At present, agonistic antibodies against TRAIL receptors or antisense oligonucleotides targeting the antiapoptotic protein Bcl-2 are in clinical trials. Inhibitors of the antiapoptotic IAP family are under preclinical examination (58, 59, 60).

In this respect STAT3 (signal transducer and activator of transcription) is – among many others – a very interesting therapeutic target, since it joins numerous

oncogenic signaling pathways and is constitutively activated at 50 – 90% frequency in diverse human cancers, whereas it is tightly controlled and transiently activated in non-transformed cells (61). Persistent STAT3 activity leads to profound changes in gene expression patterns altering cell survival and proliferation, angiogenesis and metastasis and immune evasion (61).

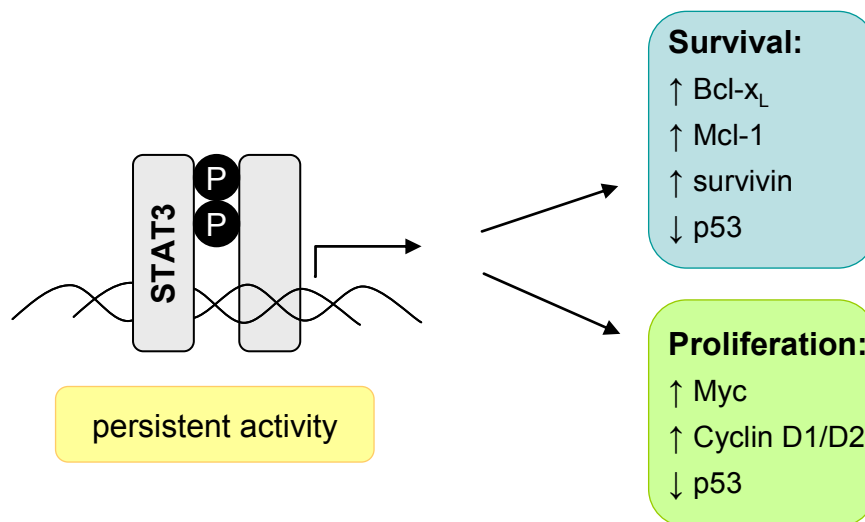


**Figure I.12 Consequences of persistent STAT3 activity**

Constitutive activity of STAT3 leads to alterations in the regulation of cell survival and proliferation. ↑ = upregulation; ↓ = downregulation.

The first anti-apoptotic factor found to be regulated by STAT3 was Bcl-x<sub>L</sub>, but since then many other proteins, e.g. survivin or cyclin D1, that are crucial for tumor cell proliferation and survival have been found to be controlled by this transcription factor (Figure I.12). First studies have shown that interruption of survivin activity via phosphorylation mutants or inhibition of protein synthesis via antisense oligonucleotides leads to caspase-dependent and caspase-independent PCD (62, 63, 64).

Survivin is ubiquitously expressed during development but is absent in most adult tissues. In contrast, it is highly expressed in cancer cells and associated with decreased patient survival, making survivin as well as STAT3 attractive diagnostic and therapeutic targets (64).

## II MATERIALS AND METHODS

### 1 MATERIALS

#### 1.1 CEPHALOSTATIN

Cephalostatin 2, cephalostatin 10 and cephalostatin 12 were isolated as described in (6, 11, 10). The substances were kindly provided by Prof. G. R. Pettit (Cancer Research Institute, Arizona State University, Tempe, USA). The 10 mM stock solutions prepared in DMSO were stored at -20°C.

#### 1.2 REAGENTS

<b>Reagent</b>	<b>Company</b>	<b>Reagent</b>	<b>Company</b>
Complete	Roche, Mannheim, Germany	Polyacrylamide	Roth GmbH, Karlsruhe, Germany
DMEM	PAN Biotech, Aidenbach, Germany	Propidium iodide	Sigma, Taufkirchen, Germany
DMSO	Roth GmbH, Karlsruhe, Germany	Puromycin	PAA Laboratories, Cölbe, Germany
Etoposide	Calbiochem, Schwalbach, Germany	Q-VD-OPh	Calbiochem, Schwalbach, Germany
FCS gold	PAN Biotech, Aidenbach, Germany	RPMI 1640	PAN Biotech, Aidenbach, Germany
G418 sulfate	PAA Laboratories, Cölbe, Germany	SP600125	Calbiochem, Schwalbach, Germany
Hoechst 33342	Sigma, Taufkirchen, Germany	Staurosporine	Calbiochem, Schwalbach, Germany
McCoy's 5a	PAN Biotech, Aidenbach, Germany	Thapsigargin	Sigma, Taufkirchen, Germany
Mitotracker Red	Molecular Probes, Karlsruhe, Germany	zVAD-fmk	Calbiochem, Schwalbach, Germany
MTT	Sigma, Taufkirchen, Germany	zVDVAD	MBL, Woburn, USA
Paclitaxel	Sigma, Taufkirchen, Germany		

## **2 CELL CULTURE**

### **2.1 CELL LINES**

#### **2.1.1 HUMAN LEUKEMIA JURKAT T CELL LINES**

All human leukemia Jurkat T cell lines were cultivated in RPMI 1640 containing 2 mM L-glutamine supplemented with 10% fetal calf serum (FCS) and 1% pyruvate.

Caspase-9-deficient and -reconstituted Jurkat T cells (65) and Bak-deficient and reconstituted Jurkat T cells (courtesy of Prof. Dr. K. Schulze-Osthoff, Düsseldorf, Germany) were cultured in the medium described above containing heat-inactivated FCS.

Jurkat cells stably overexpressing XIAP were provided by Dr. C. Duckett (University of Michigan). These cells were cultivated in the medium described for Jurkat T cells in the presence of 1 µg/ml puromycin every fifth passage.

#### **2.1.2 CARCINOMA CELL LINES**

The human cervix carcinoma cell line HeLa was obtained from the German Collection of Microorganisms and Cell Cultures (DSMZ, Braunschweig, Germany). The human melanoma cell line SK-Mel-5 was obtained from the American Type Culture Collection (ATCC, Manassas, USA). HeLa and SK-Mel-5 cells were cultivated in DMEM containing 2 mM L-glutamine supplemented with 10% fetal calf serum and 1% pyruvate. The human ovarian cancer cell line SK-OV-3 was obtained from ATCC and cultivated in McCoy's 5a supplemented with 10% fetal calf serum. MCF-7 cells and caspase-3 reconstituted MCF-7 cells were kindly provided by Prof. Dr. K. Schulze-Osthoff. MCF-7 stably transfected with either Smac-YFP or cytochrome c-GFP (66) were provided by Prof. Dr. J.H.M. Prehn. All MCF-7 cells were grown in RPMI 1640 containing 2 mM L-glutamine supplemented with 10% heat-inactivated fetal calf serum. See Table II.1 for a summary of the used cell lines.

**Table II.1: summary of used cell lines**

<b>Jurkat T cell clones</b>	<b>Carcinoma cell lines</b>
Wild type J16	HeLa
Caspase-9-deficient cells	SK-Mel-5
Caspase-9-reconstituted cells	SK-OV-3
XIAP-overexpressing Jurkat cells	MCF-7 +/- Caspase-3
Bak-deficient cells	MCF-7 smac-YFP
Bak-reconstituted cells	MCF-7 cytochrome c-GFP

## 2.2 CULTIVATION

All cell lines were cultured at 37°C and 5% CO<sub>2</sub> in humidified atmosphere. Cell density and viability was determined by staining with trypan blue using a VI-CELL™ cell viability analyzer (Beckman Coulter, Krefeld, Germany).

The Jurkat subclones were split three times a week and diluted with prewarmed medium to 1 x 10<sup>5</sup> cells/ml respectively 7 x 10<sup>4</sup> cells/ml before weekends. Cell density never exceeded 1 x 10<sup>6</sup> cells/ml in order to maintain genetic stability. For the same reason cells were not used for experiments any longer after reaching passage 20.

HeLa, SK-Mel-5, SK-OV-3 and MCF-7 cells were grown as monolayer and split when reaching 80 - 90% confluence. Briefly, cells were washed with prewarmed PBS (see below) and detached with 3 ml Trypsin/EDTA (see below) / 75 cm<sup>2</sup> flask. After detaching, Trypsin/EDTA was inactivated by adding 7 ml medium and cells were centrifuged (180 x g, 10 min, RT). Cells were resuspended in fresh medium and 1 - 3 x 10<sup>6</sup> cells were transferred to 75 cm<sup>2</sup> cell culture flasks.

### **PBS (pH 7.4)**

NaCl	7.2 g
Na <sub>2</sub> HPO <sub>4</sub>	1.48 g
KH <sub>2</sub> PO <sub>4</sub>	0.43 g
<hr/>	
H <sub>2</sub> O ad 1,000 ml	

### **Trypsin/EDTA (T/E)**

Trypsin	0.50 g
EDTA	0.20 g
<hr/>	
PBS ad 1,000 ml	

## 2.3 SEEDING FOR EXPERIMENTS

Jurkat leukemia T cells were seeded approximately 16 h before experiments at a density of  $0.5 \times 10^6$  cells/ml. Alternatively, cells were seeded 2-3 h before stimulation, with higher density ( $0.7 \times 10^6$  cells/ml). Cells were centrifuged ( $180 \times g$ , 10 min, RT), resuspended in prewarmed medium and cell density was determined by VI-CELL™ cell viability analyzer. Cells were diluted with medium to the desired concentration and seeded in 24-well tissue culture plates for all experiments except MTT viability assay (96-well plates, see II .4) and clonal survival assay (6-well plates, see II .6).

Carcinoma cell lines were detached and centrifuged as described in II.2.1.2. Cell concentration was adjusted to  $0.2\text{-}0.3 \times 10^6$  cells/ml and seeded in 12- or 24-well plates the day before the experiment. Before stimulating the cells medium was removed and replaced by fresh medium.

## 2.4 FREEZING AND THAWING

In order to preserve a sufficient stock of each cell line, long term storage took place in liquid nitrogen. Therefore, cells in low passages were frozen in special medium (Table II.2: Freezing medium), containing DMSO for avoiding cell rupture.

Cells were centrifuged ( $180 \times g$ , 10 min,  $4^\circ\text{C}$ ) and resuspended in ice-cold freezing medium at a concentration of  $2\text{-}3 \times 10^6$  cells/ml. 1.5 ml cell suspension was transferred into each cryovial and frozen at  $-20^\circ\text{C}$  over night. Afterwards, vials were stored at  $-80^\circ\text{C}$  for permanent usage or transferred into liquid nitrogen after two days for long term storage.

Cells were defrosted by gently dissolving in 10 ml prewarmed medium. Subsequent, cells were centrifuged ( $180 \times g$ , 10 min, RT) to remove DMSO and dead cells. After resuspension in fresh medium, cells were left to grow for at least five days before any experiments.

Table II.2: Freezing medium

	HeLa	Jurkat	MCF-7	SK-Mel-5	SK-OV-3
RPMI 1640	-	70%	70%	-	-
DMEM	80%	-	-	80%	-
McCoy's 5a	-	-	-	-	85%
FCS gold	10%	20%	20%	10%	10%
DMSO	10%	10%	10%	10%	5%

### 3 FLOW CYTOMETRY

Flow cytometry is a technology that allows the measurement of multiple physical characteristics of single particles at the same time. These particles, usually cells, are suspended in a stream of fluid and pass through a beam of light. The list of measurable parameters includes properties like a particle's relative size, relative granularity or internal complexity and relative fluorescence intensity. Among other things, this method is suitable for measuring cell cycle, apoptosis, viability, protein expression and localization, cell surface antigens and enzymatic activity.

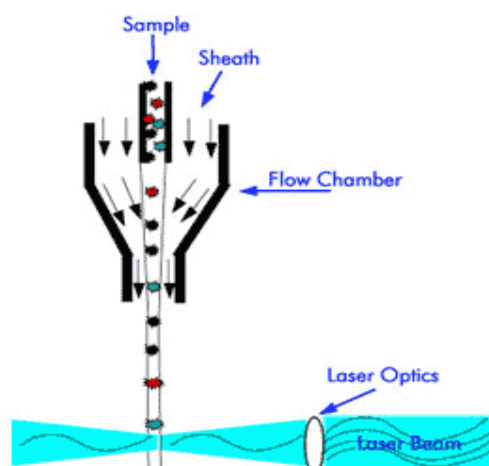


Figure II.1 flow chamber of a flow cytometer (from 67)

The fluid stream transporting the cells should be positioned in the center of the laser beam to yield optimal illumination and the cells or particles should move through the laser beam one by one. For this reason the sample is injected into a stream of sheath fluid within the flow chamber, where the sheath fluid accelerates the particles and restricts them to the center of the sample core (see Figure II.1). This process is called hydrodynamic focusing.

When particles pass the laser beam, the light is scattered and simultaneously, if the particles have been stained with fluorescence dyes able to absorb the laser light, fluorescence occurs. The scattered and fluorescent light is collected by lenses and forwarded to the appropriate detectors.

Morphological parameters like the relative size and granularity of a cell influences the light scattering. In line with the laser beam the forward scatter (=FSC) proportional to cell size is measured. Light scattered perpendicular to the laser is called sideward scatter (SSC) and is characteristic for the internal complexity. Fluorescence was measured by using the appropriate filters for the respective fluorochromes (e.g. FL2 for detection of propidium iodide). All measurements were performed on a FACSCalibur (Becton Dickinson, Heidelberg, Germany), equipped with a 488 nm argon laser. Sheath fluid is composed as seen below (FACS buffer).

#### **FACS buffer (pH 7.37)**

NaCl	8.12 g
KH <sub>2</sub> PO <sub>4</sub>	0.26 g
Na <sub>2</sub> HPO <sub>4</sub>	2.35 g
KCl	0.28 g
Na <sub>2</sub> EDTA	0.36 g
LiCl	0.43 g
Na-azide	0.20 g

H<sub>2</sub>O ad 1,000 ml

### **3.1 NICOLETTI ASSAY**

A simple and rapid method for quantification of apoptosis is the measurement of DNA fragmentation, a characteristic event caused by the activation of endonucleases. According to the method of Nicoletti et al. (68) cells are permeabilized in a hypotonic buffer (HFS buffer, hypotonic fluorochrome solution),

which contains propidium iodide for staining the DNA. The resulting red fluorescence is measured by flow cytometry. Figure II.2 shows a characteristic histogram of untreated control cells after staining with propidium iodide. Fluorescence intensity is proportional to DNA content resulting in a peak containing  $2n$  DNA content ( $G_0/G_1$ ), whereas cells in  $G_2/M$  phase emit higher fluorescence due to  $4n$  DNA content. Upon eluting the low molecular weight fragments of apoptotic cells by the hypotonic buffer less dye is taken up and the resulting hypodiploid region left to the  $G_0/G_1$  peak is considered apoptotic (sub  $G_1$ ).

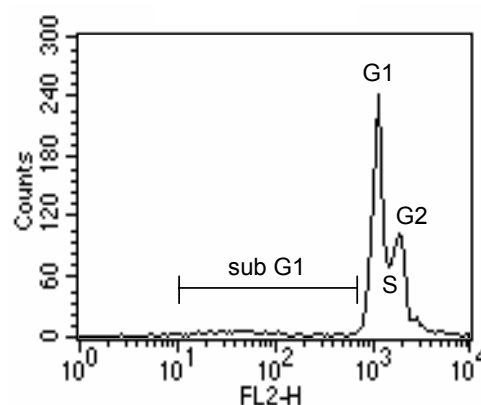


**Figure II.2 Histogram of untreated PI-stained cells**

Jurkat cells were permeabilized and stained with propidium iodide (PI). A typical histogram of untreated cells is shown with different peaks representing cell cycle distribution. The region left to the  $G_1$  peak is considered apoptotic (sub  $G_1$ ).

**Protocol:** Jurkat cells and adherent cell lines were seeded as described in chapter II.2.3 and either left untreated or stimulated with the required substances. After different incubation times cells were harvested by centrifugation ( $600 \times g$ , 10 min,  $4^\circ\text{C}$ ) and washed once with cold PBS. Cells were incubated in  $250 \mu\text{l}$  (Jurkat cells) or  $500 \mu\text{l}$  (adherent cell lines) HFS buffer (see below) overnight at  $4^\circ\text{C}$  and analyzed by flow cytometry. The percentage of sub  $G_1$  region was determined as a parameter of apoptotic cells.

#### **HFS buffer**

Sodium citrate	0.1% (w/v)
Triton X-100	0.1% (v/v)

PBS ad 1,000 ml

Shortly before use, add  $50 \mu\text{g/ml}$  propidium iodide.

### 3.2 PHOSPHATIDYLSERINE TRANSLOCATION

An early event in apoptosis is the loss of cell membrane asymmetry. In healthy cells, the phospholipid phosphatidylserine (PS) is located on the cytoplasmic side of the membrane. Upon apoptotic stimuli it translocates to the outer leaflet of the cell membrane. The annexin V assay makes use of this exposure of PS for the detection of cells in early or immediate apoptosis, even before events like DNA fragmentation can be measured. Annexin V is a small  $\text{Ca}^{2+}$  dependent protein with a high and selective affinity for PS. It can be tagged with FITC without compromising its binding properties to PS thus enabling the marked cells to be analyzed by flow cytometry. An additional staining with PI opens the opportunity to distinguish between live cells (Annexin V negative, PI negative), apoptotic cells (Annexin V positive, PI negative) and necrotic cells (Annexin V positive, PI positive).

Protocol: Phosphatidylserine translocation was analyzed by the Annexin V-FITC Detection Kit (BenderMed Systems, Vienna, Austria) according to the manufacturer's instructions. Briefly, cells were either left untreated or stimulated with the required substances for different periods of time and collected by centrifugation (600 x g, 4°C, 10 min). They were washed once with cold PBS, resuspended in 1x binding buffer and incubated with Annexin V-FITC solution for 15 min at room temperature. After another centrifugation step (600 x g, 4°C, 10 min), the pellet was resuspended and PI solution was added. The probes were immediately analyzed by FACS. Only Annexin V positive and PI negative cells were considered apoptotic.

## 4 MTT VIABILITY ASSAY

The mitochondrial respiratory activity is a parameter for cell viability. Though, a method for cytotoxicity determination of a substance is to measure this activity by the MTT assay. This colorimetric assay uses the tetrazolium salt MTT (3-(4,5-dimethylthiazol-2-yl)-2,5-diphenyl tetrazolium bromide). It is based on the reduction of MTT by enzymes of the mitochondrial electron transport assembly, leading to the formation of a blue formazan derivative. The reduction is

proportional to the activity of the assembly and thus to the vitality of the cells. The absorption of the formazans can be measured at 550 nm in a spectrophotometer.

Protocol: Cells were seeded at a concentration of  $7 \times 10^5$  (Jurkat cells) or  $0.15 \times 10^5$  (SK-Mel-5) cells/ml in a 96-well plate (100  $\mu$ l per well) the day before stimulation. After stimulation 10  $\mu$ l of MTT solution (stock solution: 5 mg/ml in PBS, sterile filtered and kept in aliquots at  $-20^\circ\text{C}$ ) was added to each well and incubated at  $37^\circ\text{C}$  for 60 minutes. Afterwards, cells were lysed by adding 190  $\mu$ l DMSO to each well and shaking the plates in the dark for another hour. Finally, the absorption of the solubilized formazan crystals was measured at 550 nm in an ELISA plate reader (SLT spectra, SLT Labinstruments, Crailsheim, Germany).

## **5 MICROSCOPY**

### **5.1 LIGHT MICROSCOPY**

The characteristic morphological changes of apoptosis as well as other forms of programmed cell death, such as shrinking, swelling or formation of apoptotic bodies can be easily detected by light microscopy.

Cells were left untreated or stimulated with the required substances for different periods of time. Cells were viewed with a Zeiss Axiovert 25 microscope (Zeiss, Oberkochen, Germany) at 40 x magnification and images were obtained with a connected reflex camera.

### **5.2 FLUORESCENCE MICROSCOPY**

A characteristic feature of an apoptotic cell is condensation of DNA followed by its fragmentation. Vital staining of DNA with Hoechst 33342 allows visualization of DNA changes in a fluorescence microscope. The dye is cell permeable and intercalates in the DNA due to its planar structure. Healthy cells emit only weak blue fluorescence since the DNA is distributed evenly in the nucleus. The nucleus of apoptotic cells is smaller in size and due to the condensed DNA shows a strong blue signal.

Protocol: Cells were either left untreated or stimulated with cephalostatin for various periods of time. 10  $\mu$ l of Hoechst solution (0.1 mg/ml in H<sub>2</sub>O) were added to each well and the plate was incubated at 37°C for approximately 5 min. Subsequently, pictures were taken with a Zeiss Axiovert 25 microscope (Zeiss, Jena, Germany) and connected camera.

### 5.3 CONFOCAL MICROSCOPY

In a conventional light microscope all object points are illuminated parallel, whereas the organism in a confocal LSM is irradiated in a point wise manner. The out of focus information is eliminated by a pinhole, allowing high-quality images with a maximum resolution. Confocal imaging enables three-dimensional studies of thick specimens and colocalization of signals from different fluorochromes.

Protocol: for the visualization of Smac and cytochrome c release a LSM 510 Meta (Zeiss, Oberkochen, Germany) was used. MCF-7 cells stably expressing either cytochrome c-GFP or Smac-YFP (66) were seeded on glass coverslips in 24-well plates and grown overnight. Cells were stimulated with 1  $\mu$ M cephalostatin or 2  $\mu$ M staurosporine. 1 hour prior to the end of stimulation cells were stained with 100 nM Red 580 (Molecular Probes, Karlsruhe, Germany). Cells were washed 3 times with PBS and fixed with 3% paraformaldehyde in PBS for 15 min at room temperature and washed again three times with PBS. Glass coverslips were then covered with a droplet of fluorescent mounting medium and mounted on a microscope slide.

## 6 CLONOGIC ASSAY

Clonogenic assay or colony formation assay is an *in vitro* long term cell survival assay to determine the effectiveness of cytotoxic agents. It is based on the ability of a single cell to grow into a colony. The assay essentially tests every cell in the population for its ability to undergo “unlimited” division.

Protocol: SK-Mel-5 cells were seeded as described in II.2.3 and treated with 50 nM cephalostatin or 50 nM taxol for 2 hours. Afterwards cells were detached and washed with PBS to remove eventually remaining substances. Cell count was

determined and  $1 \times 10^4$  SK-Mel-5 cells were seeded in 6-well plates. Cells were left to grow for 8 days and colonies were stained with crystal violet. Since SK-Mel-5 cells don't possess the ability to form colonies, but grow as loosely spreaded network, instead of counting the colonies crystal violet was solved and absorption at 550 nm was measured. Untreated control cells were set 100% viability.

## 7 WESTERN BLOT

Western blot is a method to detect specific proteins present in a given sample, for example a cell lysate. Denaturated proteins are first separated by mass using gel electrophoresis and then transferred onto a membrane. Afterwards proteins can be visualized by immunodetection using a specific antibody.

### 7.1 SAMPLE PREPARATION

#### 7.1.1 WHOLE CELL LYSATES

##### General lysis buffer

Tris-HCl, pH 7.5	30 mM
NaCl	150 mM
EDTA	2 mM
Triton X-100	1%
Complete™	

##### Sample buffer (5x)

3.125 M Tris-HCl, pH 6.8	100 $\mu$ l
Glycerol	500 $\mu$ l
SDS 20%	250 $\mu$ l
DTT 16%	125 $\mu$ l
Pyronin Y 5%	5 $\mu$ l

H<sub>2</sub>O ad 1 ml

##### Lysis buffer for phosphorylated proteins

Tris-HCl, pH 7.5	20 mM
NaCl	137 mM
Na <sub>4</sub> P <sub>2</sub> O <sub>7</sub>	2 mM
EDTA	2 mM
C <sub>3</sub> H <sub>7</sub> Na <sub>2</sub> O <sub>6</sub> P (Na glycerolphosphate)	20 mM
NaF	10 mM
Na <sub>3</sub> VO <sub>4</sub>	2 mM
PMSF	1 mM
Triton X-100	1%
Glycerol	10%
Complete™	

**Protocol:** Jurkat cells or adherent cell lines were seeded (see II.2.3) and left untreated or stimulated with cephalostatin 2 or the respective positive controls. After incubation cells were harvested by centrifugation (1500 rpm, 10 min, 4°C) and washed once with cold PBS. The adherent cell lines had to be detached by Trypsin/EDTA and were also centrifuged and washed. Pellets were resuspended in the appropriate lysis buffer (100 µl for three wells) and incubated on ice for 30 min or stored at -20°C. Subsequently, lysates were centrifuged at 10,000 x g, 4°C for 10 min. Supernatants were transferred to new tubes and protein concentration was determined by the Bradford method as described in IV.7.2. Lysates were diluted 1:5 with 5 x sample buffer and boiled at 95°C for 5 min. Afterwards, samples were stored at -20°C or used immediately for western blot analysis. PMSF, Na<sub>3</sub>VO<sub>4</sub> and Complete™ were added to the lysis buffers immediately before use.

### 7.1.2 CYTOSOLIC AND MITOCHONDRIA CONTAINING FRACTIONS

In apoptosis, molecules like cytochrome c and Smac normally localized in the intermembrane space of mitochondria are released into the cytosol. There they are part of activation complexes for caspases or they translocate into the nucleus where they participate in DNA fragmentation (Endonuclease G, AIF). For analyzing the release of these factors, the cytosol has to be separated from the mitochondria. This is accomplished by a permeabilization buffer containing a low concentration of digitonin which forms complexes with cholesterol in the cell membrane. Thus, small pores develop through which the cytosol is eluted into the iso-osmotic buffer while organelles are retained inside the cell. The protocol was carried out as described previously (15).

#### **Permeabilization buffer (pH 7.2)**

Mannitol	210 mM
Sucrose	70 mM
Hepes pH 7.2	10 mM
EGTA	0.2 mM
Succinate	5 mM
BSA	0.15% (w/v)
Digitonin	60 µg/ml

Protocol: Cells were seeded and stimulated as for whole cell lysate preparation. Three wells for each probe were pooled and centrifuged at 360 x g, 4°C for 10 min. The supernatant was discarded thoroughly. After washing the cells with cold PBS, the pellets were resuspended carefully in 100 µl permeabilization buffer and incubated on ice for 20 min. The cytosolic fraction was obtained by centrifugation of the cell suspension at 360 x g (4°C, 10 min) and the supernatant was cleared of any remaining cell fragments at 13,000 x g (4°C, 10 min). The pellet of the first centrifugation after permeabilization containing the mitochondria, the other organelles and the membranes was resuspended in 0.1% Triton-X 100 in PBS (100 µl) and lysed for 15 min on ice. The supernatant of a subsequent centrifugation step (13,000 x g, 4°C, 10 min) constitutes the mitochondria-enriched fraction. Protein determination was carried out with the Bradford method. The probes were diluted with 5x sample buffer and boiled at 95°C for 5 min. Afterwards, they were separated immediately by SDS-PAGE or stored at -20°C.

## 7.2 PROTEIN QUANTIFICATION

The protein content in samples was quantified by the Bradford (69) method. This method is based upon the binding of the dye Coomassie Brilliant Blue G-250 to hydrophobic parts of proteins. After binding to proteins, the absorption maximum of this dye shifts from 465 to 595 nm and absorbance is measured at 595 nm.

Protocol: 10 µl of a calibration curve containing increasing concentrations of BSA in H<sub>2</sub>O (0 up to 25 mg/ml BSA) and 10 µl of 1:10 in H<sub>2</sub>O diluted cell lysates were incubated with 190 µl of Bradford solution (Bio-Rad, Munich, Germany, diluted 1:5 in H<sub>2</sub>O) in 96-well plates for 5-10 min and absorbance of samples at 592 nm was measured in a microplate absorbance reader (Sunrise™, Tecan, Crailsheim, Germany). Before electrophoresis, the required volumes of 1x sample buffer were added to the protein solutions in order to achieve the same protein concentration in all samples.

### 7.3 SDS-PAGE

Equal amounts of the above described protein samples are separated by discontinuous denaturing SDS-PAGE according to Laemmli (70). The anionic detergent sodium dodecyl sulphate (SDS) is used to solubilize the proteins upon binding to hydrophobic parts. Thereby protein secondary and tertiary structures are destroyed. Further unfolding is achieved by the reducing agent dithiothreitol (DTT), which cleaves disulfide bonds. Proteins get highly negative charged by SDS and are though drawn towards the anode in an electric field. Therefore, the proteins are separated solely by their size in the polyacrylamide gel. This discontinuous electrophoresis system consists out of two layers: the stacking gel, where the proteins are concentrated and the separating gel, where the proteins are separated.

<b>Stacking gel</b>		<b>Separating gel (10%)</b>	
PAA solution 30%	1.7 ml	PAA solution 30%	5 ml
1.25M Tris-HCl, pH 6.8	1 ml	1.5M Tris-HCl, pH 8.8	3.75 ml
SDS 10%	100 $\mu$ l	SDS 10%	150 $\mu$ l
H <sub>2</sub> O	7.0 ml	H <sub>2</sub> O	6.1 ml
TEMED	20 $\mu$ l	TEMED	15 $\mu$ l
APS (10%)	100 $\mu$ l	APS (10%)	75 $\mu$ l

#### **Electrophoresis buffer**

Tris Base	3 g
Glycine	14.4 g
SDS	1 g
H <sub>2</sub> O ad 1,000 ml	

Table II.3 PAA-concentration in the separating gel

<b>Protein</b>	<b>Acrylamide concentration</b>
PARP, PIDD	7,5 %
caspase-9, AIF, STAT3	10 %
caspase-2, caspase-4, caspase-3	12 %
Smac, cytochrome c, RAIDD, survivin	15 %

Depending on the molecular weight of the investigated proteins the polyacrylamide (PAA) (Rotiphorese™ Gel 30, Roth, Karlsruhe, Germany) concentration was adjusted to yield an optimal separation (see Table II.3 PAA-concentration in the separating gel). To determine the molecular weight, samples are compared with prestained broad range molecular weight markers (precision All Blue®, Bio-Rad, Munich, Germany; MBI-Fermentas, Germany).

Electrophoresis was performed using a vertical Mini Protean III system (Bio-Rad, Munich, Germany) connected to a power supply (Biometra, Göttingen, Germany). Electrophoresis was run at 100 V for 21 min for stacking of proteins and at 200 V for 35-40 min for the separation of proteins.

## 7.4 WESTERN BLOTTING AND DETECTION

Subsequent to electrophoresis, proteins are transferred from the gel onto blotting membranes, which are incubated with specific antibodies. Afterwards proteins were visualized by chemiluminescence.

Tank blot technique was used to carry out western blot analysis. Nitrocellulose membranes (Hybond™-ECL™, Amersham Biosciences, Freiburg, Germany) were activated by soaking in freshly prepared 1x blotting buffer for at least 15 minutes. Afterwards, transfer sandwiches were assembled as follows:

### **sandwich holder cathode side**

---

wetted pad  
soaked blotting paper  
gel  
membrane  
soaked blotting paper  
wetted pad

---

### **sandwich holder anode side**

Sandwiches were inserted in a transfer device (Mini Trans-Blot®, Bio-Rad, Munich, Germany), the electrophoresis chamber was filled up with 1 x buffer and transfer was performed at 4 °C at 100 V for 90 min or at 23 V overnight, with magnetic stirring.

<b>Blotting buffer (5x) stock solution</b>		<b>Blotting buffer (1x)</b>	
Tris Base	15.2 g	5x blotting buffer	200 ml
Glycine	72.9 g	Methanol	200 ml
H <sub>2</sub> O ad 1,000 ml		H <sub>2</sub> O ad 1,000 ml	

After transfer, membranes were blocked in 5% non-fat dry milk in Tris-buffered saline with Tween (TBS-T) for 1 h at room temperature. After a short washing in TBS-T, membranes were incubated in the respective primary antibody solutions (Table II.4 Primary antibodies) overnight at 4°C or for 2 h at RT with gently shaking.

After 3 x 10 minutes washing steps in TBS-T, membranes were incubated with secondary antibodies (see Table II.5) conjugated to horseradish peroxidase for 1 h at room temperature or overnight at 4°C. After washing the membrane as described above, proteins of interest were visualized using the ECL Plus™ Western Blotting detection reagent (Amersham Biosciences, Freiburg, Germany). Membranes were exposed to X-ray film for the appropriate time periods and subsequently developed in a tabletop film processor (Curix 60, Agfa, Cologne, Germany).

<b>TBS-T (pH 8.0)</b>	
Tris base	3 g
NaCl	11.1 g
Tween 20	1 ml
H <sub>2</sub> O ad 1,000 ml	

**Table II.4 Primary antibodies**

<b>primary antibody</b>	<b>isotype</b>	<b>dilution</b>	<b>company</b>
AIF	rabbit IgG	1:1,000	Chemicon, Hofheim, Germany
caspase-2	mouse IgG <sub>1</sub>	1:1,000	BD Biosciences, Heidelberg, Germany
caspase-3	mouse IgG <sub>2a</sub>	1:1,000	BD Biosciences, Heidelberg, Germany
caspase-4	mouse IgG <sub>1</sub>	1:1,000	MBL, Woburn, USA
caspase-9	rabbit IgG	1:1,000	Cell Signaling, Frankfurt, Germany
cytochrome c	mouse IgG <sub>1</sub>	1:1,000	Cell Signaling, Frankfurt, Germany
PARP	mouse IgG <sub>1</sub>	1:100	Calbiochem, Bad Soden, Germany
PIDD	rabbit IgG	1:1,000	Alexis
RAIDD	mouse IgG <sub>1</sub>	1:1,000	MBL, Woburn, USA
Smac	rabbit IgG	1:500	Biozol, Eching, Germany
STAT3	rabbit IgG	1:1,000	Cell signaling, Frankfurt, Germany
pStat3 Ser 727	rabbit IgG	1:1,000	Cell signaling, Frankfurt, Germany
pStat3 Tyr 705	mouse IgG <sub>1</sub>	1:1,000	Cell signaling, Frankfurt, Germany
survivin	rabbit IgG	1:1,000	Cell signaling, Frankfurt, Germany

**Table II.5 Secondary antibodies**

<b>secondary antibody</b>	<b>dilution</b>	<b>company</b>
goat anti mouse IgG <sub>1</sub> : HRP	1:1,000	Biozol, Eching, Germany
goat anti rabbit :HRP	1:10,000	Dianova, Hamburg, Germany
goat anti mouse IgG <sub>2A</sub> :HRP	1:1,000	Biozol, Eching, Germany

## 7.5 STAINING OF GELS AND MEMBRANES

Equal protein loading and blotting of samples was checked by staining of gels with Coomassie Brilliant blue as well as staining of membranes after Western blot experiments with Ponceau S. In contrast to Coomassie staining, Ponceau S stain is reversible.

After tank blot procedure gels were shaken and stained with Coomassie blue solution for 10 min at room temperature. Next gels were washed several times in destaining solution until the proteins appeared as blue bands and could be distinguished against the background.

### Coomassie staining solution

Coomassie Blue	3 g
Glacial acetic acid	100 ml
Ethanol	450 ml

H<sub>2</sub>O ad 1,000 ml

### Destaining solution

Glacial acetic acid	100 ml
Ethanol	300 ml

H<sub>2</sub>O ad 1,000 ml

Membranes were stained in Ponceau staining solution (0.2% Ponceau S in 5% acetic acid) for 5 minutes. Afterwards, membranes were washed in H<sub>2</sub>O until the background disappeared. To remove the Ponceau staining completely, membrane was washed in TBS-T.

## 8 IMMUNOPRECIPITATION

Immunoprecipitation is a method used for the enrichment of the proteins of interest. Therefore a specific antibody is incubated with a cell lysate to form the antigen-antibody complex. This complex can be precipitated e.g. by addition of Protein G or Protein A, which has high affinity to the Fc-part of immunoglobulins. After dissociating and denaturizing the proteins by boiling, the precipitate can be investigated by Western blot analysis.

Protocol: Jurkat cells were seeded as described in II.2.3 and stimulated for 1 h with 50 nM cephalostatin 2, 2  $\mu$ M etoposide or 3  $\mu$ M thapsigargin. Afterwards, cells

were lysed in general lysis buffer and the amount of protein was determined. Simultaneously, 50  $\mu$ l Protein A Sepharose Beads (Sigma) for each sample were centrifuged, washed and resuspended in lysis buffer. 2.5  $\mu$ l of the respective antibody was added per 50  $\mu$ l Protein A solution and gently inverted at 4°C for approximately 3 h. After that, the Protein A-antibody solution was centrifuged (3,000 x g, 2 minutes, 4°C) and carefully washed three times with lysis buffer. 300 – 400  $\mu$ g protein were filled up to a final volume of 250  $\mu$ l with lysis buffer and added to the bead solution. In order to allow the immune complexes to form, the samples were gently shaken over night at 4°C by end over end rocking. In the next step the precipitates were harvested by centrifugation and 40  $\mu$ l of the supernatant were kept as binding control. The remaining pellet was carefully washed three times with 500  $\mu$ l lysis buffer. After completely removing the last wash solution, sample was mixed with 2-mercaptoethanol containing Laemmli sample buffer, boiled at 95°C for 5 minutes and analyzed by Western blot.

## 9 siRNA

RNA interference (RNAi) is a widespread phenomenon found in fungi, plants and animals.

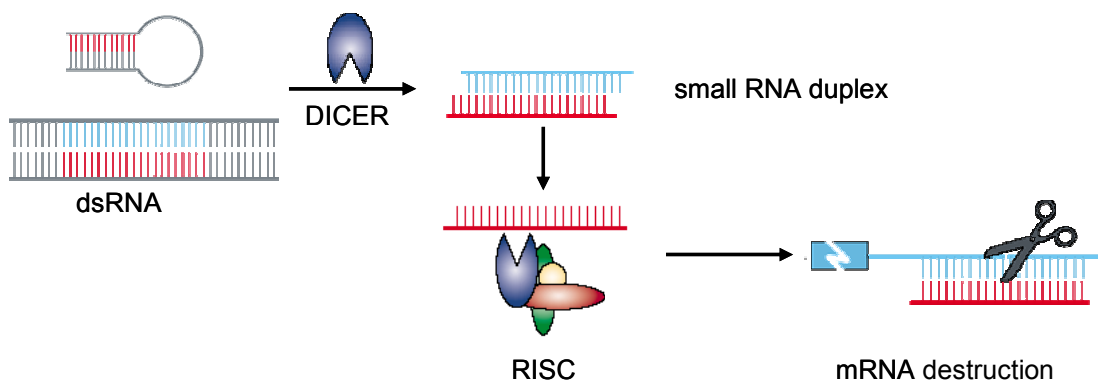


**Figure II.3 short interfering RNA (modified from 71)**

RNA interference is an ancient defense mechanism against foreign double stranded (ds) RNA. 21-23 nucleotides long small interfering (si) RNAs are cleaved by DICER out of long dsRNAs. These siRNAs (small RNA duplex) can be chemically synthesized for laboratory use. The antisense strand is guided to the RNA induced silencing complex (RISC), where the corresponding mRNA strand is bound and degraded, leading to gene silencing.

It concerns about double stranded (ds) RNAs that trigger specific gene silencing. Long dsRNA molecules are converted by an enzyme called DICER into smaller (21-23 nt) RNAs. The antisense short RNAs (siRNA) are incorporated into a RNA induced silencing complex (RISC). The RISC binds the target mRNA and silences gene expression by cleaving it (Figure II.3). Since DICER can cleave hairpin RNAs, DNA vectors that contain such RNA substrates are commonly used. Another possibility is to introduce post-DICER cleavage products (siRNAs) to initiate RNAi. In the present work both systems are used. DNA vectors were applied for silencing Smac and short interfering (si) RNA for caspase-2, AIF and RAIDD.

## 9.1 siRNAs TARGETING CASPASE-2, AIF AND RAIDD

Sense and antisense siRNA oligonucleotides corresponding to nucleotides 94-114 of caspase-2 (5'-aaacagctgttgaggcgaa-3') (72), nucleotides 6-27 of RAIDD (5'-ggccagagacaaacaagtactc-3') (56), AIF nucleotides ggaaatagggaaagatccdTdT, (73) and oligonucleotides corresponding to a nonsense sequence were purchased from Biomers.net GmbH (Ulm, Germany). The single stranded siRNA oligonucleotides were dissolved to 100 µM stock solutions in RNase free water. They were annealed to create the 20 µM double-stranded siRNAs as follows: 15 µl of sense and 15 µl of antisense siRNA were combined with 30 µl RNase free H<sub>2</sub>O and 15 µl annealing buffer (Ambion). This solution was incubated at 90°C for 1 minute and was left to cool down until temperature reached 37°C. Afterwards the double stranded siRNA was incubated for further 5 minutes at room temperature and stored at -20°C.

## 9.2 SMAC siRNA

The plasmids bearing siRNAs against Smac, a nonsense sequence and the vector alone were kindly provided by Dr. S. Fulda (University Hospital Ulm, Germany). Two siRNAs against Smac were used:

pSUPER.retro129

(5'-gatccccgaagcgggtgttctcagaattcaagagattctgagaacaccgcttcttttggaaa-3')

and pSUPER.retro1188

(5'-gatcccccctgtccagttgtacgattcaagagaatcgtacaaactggacaggtttttggaaa-3').

For propagation, the plasmids were transformed into DH5 $\alpha$  and a glycerol stock was raised (see chapter II9.2.1).

### 9.2.1 TRANSFORMATION OF DH5 $\alpha$

*E.coli* strain DH5 $\alpha$  was transformed as follows: 1  $\mu$ g of each plasmid was incubated with 100  $\mu$ l of bacteria on ice for 30 min, followed by 30 seconds at 42°C. Afterwards bacteria were placed back on ice for 1-2 min. 900  $\mu$ l of room temperature lysogeny broth (LB) medium (Gibco/Invitrogen, Karlsruhe, Germany) were added to each tube and bacteria were incubated in a water bath at 37°C for 90 min. 50  $\mu$ l of bacteria suspension were spread onto ampicillin (Calbiochem, Schwalbach, Germany)-agar plates. Plates were incubated at 37°C overnight.

#### **LB agar**

Lennox L Broth Base	20 g
Agar	15 g
Ampicillin (100 mg/ml)	1 ml

H<sub>2</sub>O ad 1,000 ml

#### **LB medium**

Lennox L Broth Base	20 g
Ampicillin (100 mg/ml)	1 ml

H<sub>2</sub>O ad 1,000 ml

Ampicillin was added to LB medium freshly before use.

### 9.2.2 PLASMID AMPLIFICATION AND PURIFICATION

Colonies were picked from the agar plates and inoculated in 2-3 ml of LB medium containing ampicillin. Bacteria were grown in a thermoshaker (Thermoshake THO 500, Gerhardt, Königswinter, Germany) over night at 37°C. Afterwards, a part of the bacteria culture was used to isolate the plasmids with a QIAprep® Miniprep kit (QIAGEN, Hilden, Germany) according to the manufacturer's instruction and dissolved in nuclease-free H<sub>2</sub>O. Presence of plasmids was confirmed by running probes in 1 % agarose gels. Subsequent, bacteria cultures were expanded and plasmid isolation was done by a QIAprep® Maxiprep kit. Received plasmids were dissolved in nuclease-free H<sub>2</sub>O and stored at -20°C.

To preserve the bacteria cultures glycerol stocks were prepared by mixing 775  $\mu$ l of an overnight bacteria culture with 225  $\mu$ l of 80% glycerol and frozen at  $-80^{\circ}\text{C}$ .

### **9.3 TRANSFECTION OF JURKAT CELLS**

Jurkat cells were transfected by electroporation with the Nucleofector™ II device (Amaxa, Cologne, Germany) according to the manufacturer's protocol.  $4 \times 10^6$  Jurkat T cells in exponential growing phase were transfected with 2  $\mu$ g of pSUPER.retro129 and 2  $\mu$ g of pSUPER.retro1188 in a 1:1 mixture of the siRNA constructs. Antibiotic selection with 2  $\mu$ g/ml puromycin was started the day after transfection. After another 24 h antibiotic was removed. Cells were seeded and stimulated on day 4 after nucleofection. Efficiency of RNA interference was checked by Western Blot analysis using antibodies against Smac/DIABLO. Cells transfected with siRNAs targeting AIF, caspase-2 and RAIDD were used 24 hours after transfection.

## **10 STATISTICS**

All experiments were performed at least three times. Results are expressed as mean value  $\pm$  SEM. Statistical analysis was performed with GraphPad Prism™ version 3.03 using one-way ANOVA with Bonferroni or Dunnett multiple comparison post-test or unpaired two-tailed Student's T test. P values  $< 0.05$  were considered significant.

## III RESULTS

### 1 CYTOTOXICITY OF CEPHALOSTATIN 2, 10 AND 12

#### 1.1 CEPHALOSTATIN 2 IS THE MOST ACTIVE OF THE CEPHALOSTATINS

In order to investigate the cytotoxic effects of cephalostatin (CPH) 2, 10, and 12 the MTT assay was used. Jurkat T cells were incubated with increasing concentrations of the different CPHs for 24 hours. Dose response curves (Figure III.1) were created and  $IC_{50}$  values were calculated. The  $IC_{50}$  value for cephalostatin 2 is 1 nM, for cephalostatin 10 is 9.7 nM and the  $IC_{50}$  value for cephalostatin 12 is 560 nM, clearly pointing to the highest cytotoxic activity for cephalostatin 2.

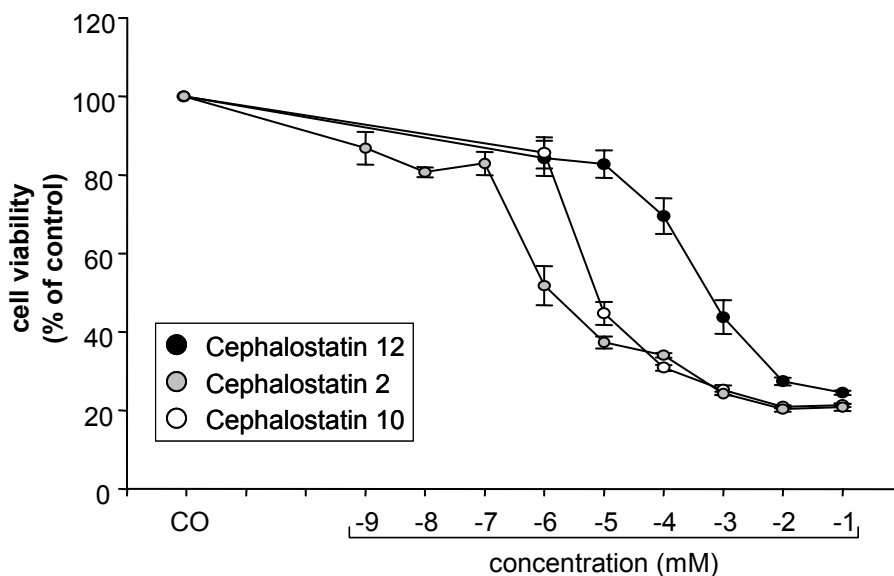


**Figure III.1 Cephalostatin 2 is the most active among the tested cephalostatins**

Jurkat T cells were left either untreated (CO) or stimulated with increasing concentrations of CPH 2, 10 or 12 for 24 hours. Impairment of cell viability was analyzed by MTT assay as described in "Materials and Methods". Represented are the mean  $\pm$  SEM of at least three independent experiments.

## 1.2 APOPTOSIS INDUCTION BY CEPHALOSTATIN 2, 10 AND 12

In order to examine whether the observed cytotoxicity is due to programmed cell death, a classical feature of apoptosis, the DNA-fragmentation, was measured by staining with propidium iodide according to the Nicoletti method. As expected from the  $IC_{50}$  values cephalostatin 2 was the strongest inducer of apoptosis in Jurkat T cells. Apoptosis is already significantly induced at a concentration of 5 nM (see Figure III.2) whereas a significant onset of DNA-fragmentation for CPH 10 starts at 500 nM and for CPH 12 at 1  $\mu$ M.

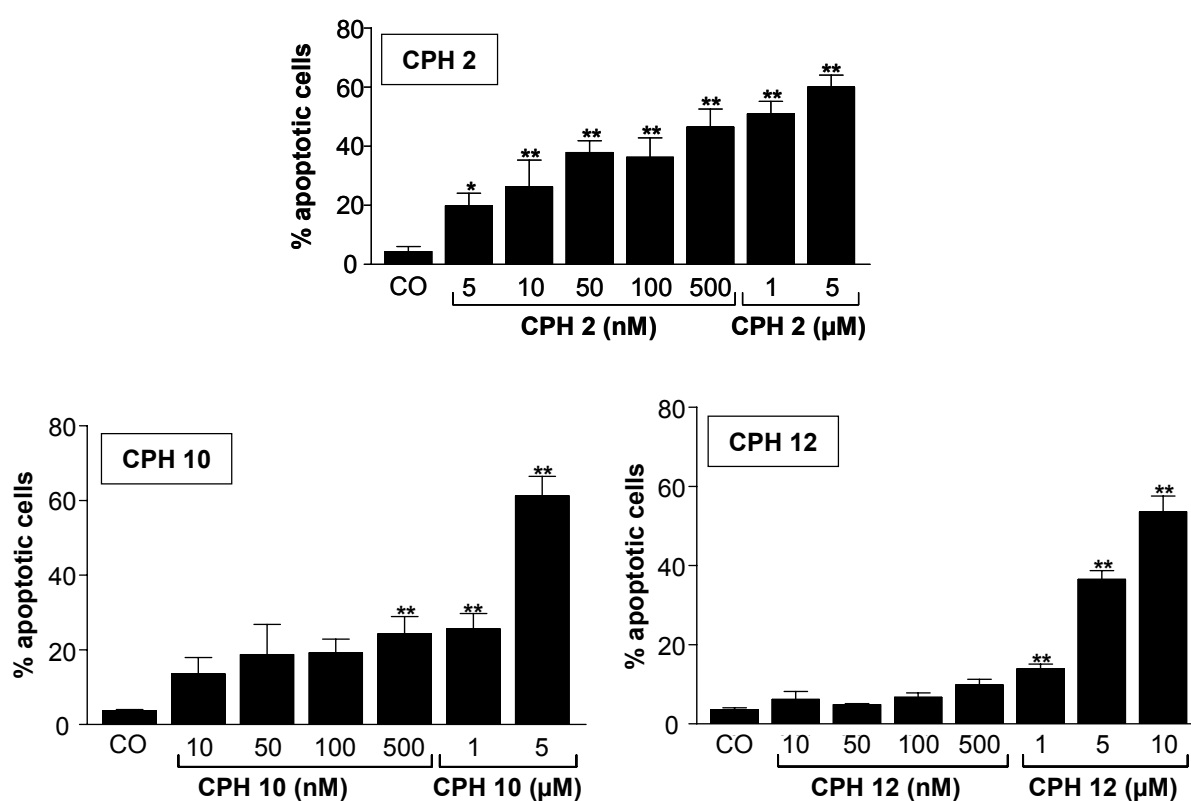


**Figure III.2 Apoptosis induced by cephalostatin 2, 10 and 12 is dose dependent**

Cells were left untreated (CO) or treated with cephalostatin 2, 10 or 12 (CPH 2, CPH 10, and CPH 12) in increasing concentrations for 24 hours. Apoptotic cells were quantified by flow cytometry as described in "Materials and Methods". All experiments were carried out three times. Bars, the mean  $\pm$  SE of three independent experiments performed in triplicate. (\*,  $P < 0.05$ ; \*\*,  $P < 0.01$  ANOVA/Dunnett).

Since cephalostatin 2 is the most potent inducer of apoptosis, it was used for all further experiments. For all investigations in Jurkat T cells 50 nM CPH 2 was applied, which induces about 40% DNA-fragmentation after 24 h of treatment (Figure III.2). Furthermore, the response of Jurkat cells to CPH 2 preceded dependent on time (Figure III.3), reaching a significant level after 24 h of treatment.

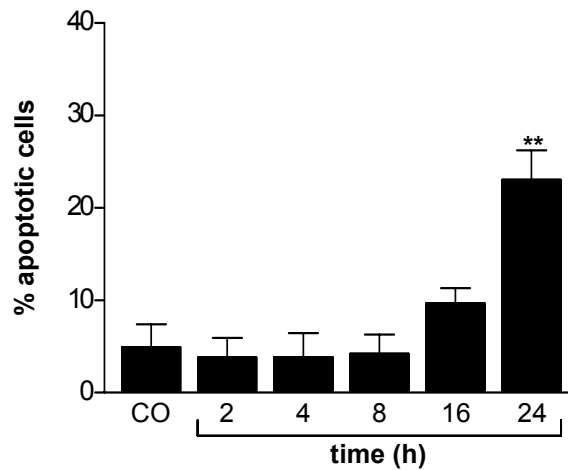


**Figure III.3 Cephalostatin 2 induced apoptosis is dependent on time**

Cells were left untreated (CO) or treated with 50 nM cephalostatin 2 for the indicated times. Apoptotic cells were quantified by flow cytometry as described in "Materials and Methods". All experiments were carried out three times. Bars, the mean  $\pm$  SE of three independent experiments performed in triplicate. (\*\*,  $P < 0.01$  ANOVA/Dunnett).

## 2 CEPHALOSTATIN 2 INDUCED APOPTOSIS IS NOT RESTRICTED TO JURKAT T CELLS

### 2.1 APOPTOSIS INDUCTION IN HELA CELLS

To investigate whether apoptosis mediated by cephalostatin 2 is restricted to Jurkat T cells the impact of the substance on different carcinoma cell lines was determined. The first cell line, established in 1951 from human tissue, is the cervix carcinoma cell line HeLa, which is now one of the most common cell lines worldwide. HeLa cells were treated with cephalostatin for different time periods and DNA-fragmentation was measured by the Nicoletti method. Figure III.4 shows that cephalostatin induces time dependently cell death, reaching significance after treatment for 40 hours.

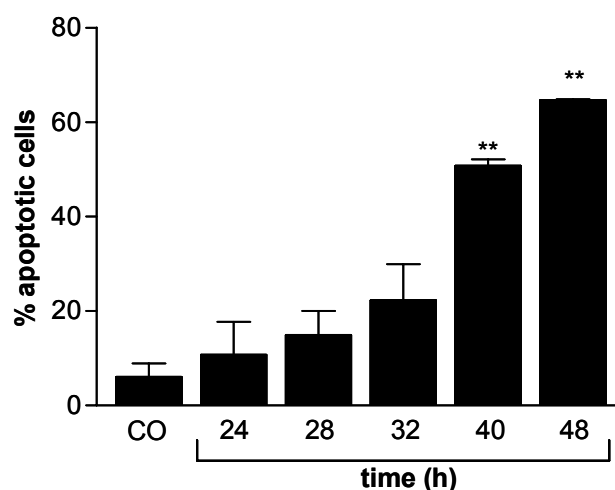


**Figure III.4 Cephalostatin induces apoptosis in HeLa cells**

HeLa cells were left untreated (CO) or treated with 50 nM cephalostatin 2 for the indicated times. Apoptotic cells were quantified by flow cytometry as described in "Materials and Methods". All experiments were carried out two times. Bars, the mean  $\pm$  SE of two independent experiments performed in triplicate. (\*\*,  $P < 0.01$  ANOVA/Dunnett).

## 2.2 APOPTOSIS INDUCTION IN MCF-7 CELLS

Next, the breast adenocarcinoma cell line MCF-7, which is deficient for caspase-3 due to a deletion mutation (74), and the caspase-3 reconstituted cell line were tested for apoptosis induction by cephalostatin. As described in I.4, apoptotic cells detach and undergo morphological changes like cell shrinkage and the formation of apoptotic bodies.

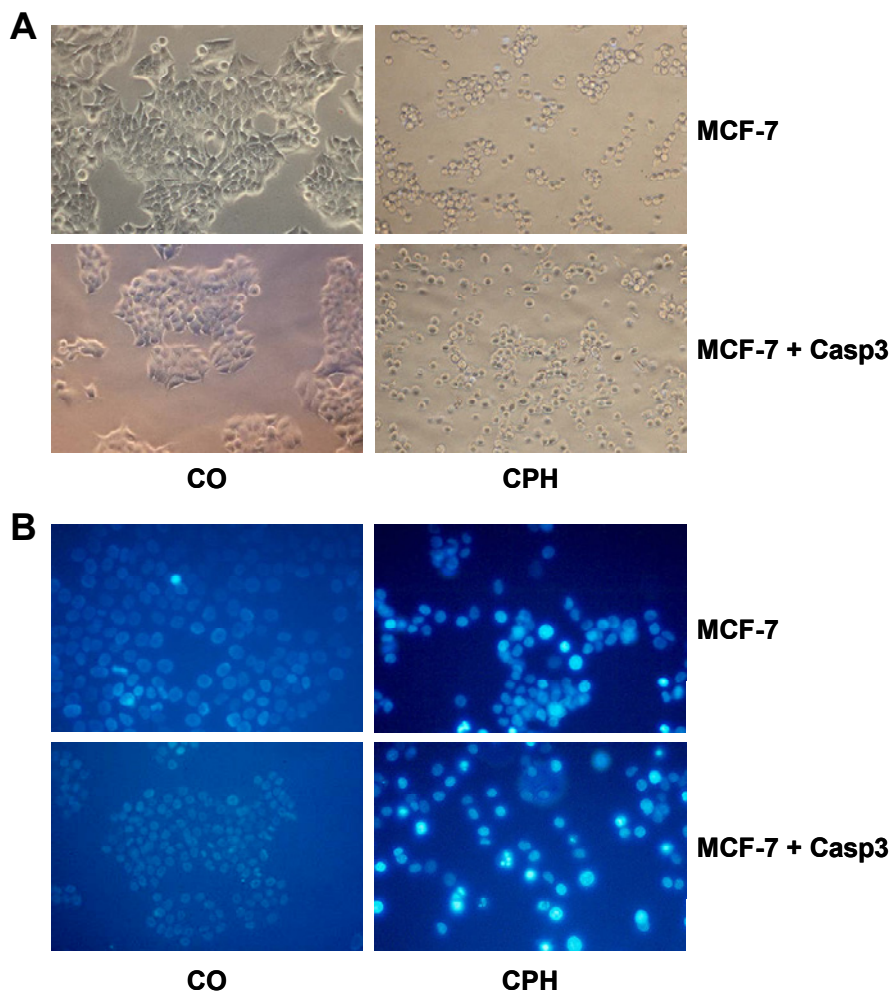


**Figure III.5 Morphological alterations in cephalostatin-treated MCF-7 cells**

A) Light microscopic pictures of MCF-7  $\pm$  caspase-3 cells. MCF-7 (upper panel) and caspase-3 reconstituted (lower panel) cells were left untreated (CO) or treated with 1  $\mu$ M cephalostatin 2 (CPH). After 24 h treatment pictures were taken. B) Fluorescence microscopy pictures of MCF-7  $\pm$  caspase-3 cells. MCF-7 (upper panel) and caspase-3 reconstituted (lower panel) cells were left untreated (CO) or treated with 1  $\mu$ M cephalostatin 2 (CPH) for 24 h. Nuclei were stained with Hoechst 33342 and analyzed by fluorescence microscopy.

Treatment with cephalostatin 2 induces the detachment of MCF-7 cells with or without caspase-3 and initiates strong cell shrinkage after 24 hours (Figure III.5 A).

Besides changes in size and shape of the whole cell, the nucleus of an apoptotic cell is subject of numerous biochemical processes as well. EndoG and other enzymes condense the chromatin and finally the DNA is fragmented by endonucleases like CAD (caspase-activated DNase). Upon staining 24 h cephalostatin 2 treated cells with the vital dye Hoechst 33342 condensation of the DNA can clearly be observed (Figure III.5). Untreated cells show faint blue staining, whereas treated cells show intensive blue colour indicating chromatin condensation. If stimulation with cephalostatin is extended from 24 to 48 h also DNA-fragmentation can be measured by PI-staining (Figure III.6). Interestingly, cephalostatin mediated cell death is not amplified by reconstitution of caspase-3.

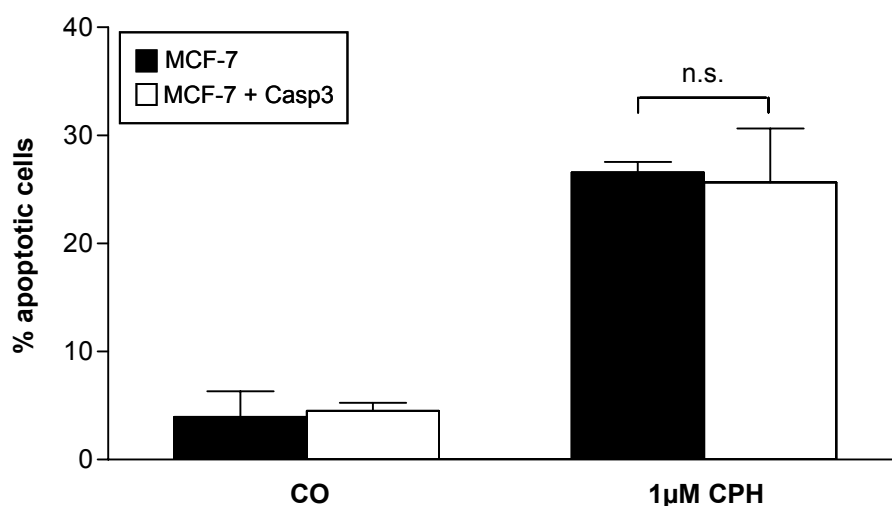


**Figure III.6 Cephalostatin induces apoptosis in MCF-7  $\pm$  caspase-3 cells**

Cells were left untreated (CO) or treated with 1  $\mu$ M cephalostatin 2 (CPH) for 48 h. Apoptotic cells were quantified by flow cytometry as described in "Materials and Methods". All experiments were carried out two times. Bars, the mean  $\pm$  SE of two independent experiments performed in triplicates. ( $P < 0.05$  ANOVA/Dunnett, n.s. not significant).

## 2.3 CELL DEATH INDUCTION IN SK-MEL-5 CELLS

### 2.3.1 APOPTOSIS INDUCTION

Metastatic melanoma is a very aggressive form of skin cancer, which is resistant to most forms of therapy, including systemic therapy and immunotherapy. The combination of chemotherapy and e.g. interleukin-2 has failed in clinical trials, implying resistance mechanisms in melanoma, which are highly complex (61). For this reason the melanoma cell line SK-Mel-5 was employed to test the activity of cephalostatin. As shown in Figure III.7 cephalostatin 2 induces dose dependent DNA-fragmentation after 48 h of treatment, becoming significant at a concentration of 100 nM. For further experiments cephalostatin was used in a concentration of 1  $\mu$ M. Taxol also induces apoptosis and was used as positive control.

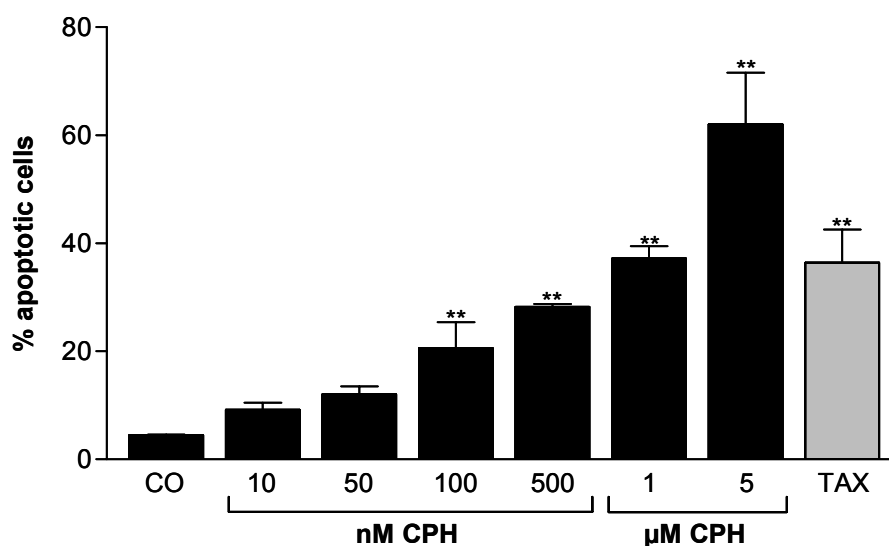


**Figure III.7 Cephalostatin induces concentration dependent apoptosis in SK-Mel-5 cells**

Cells were left untreated (CO), treated with increasing concentrations of cephalostatin 2 (CPH) or with 50 nM taxol (TAX) for 48 h. Apoptotic cells were quantified by flow cytometry as described in “Materials and Methods”. All experiments were carried out at least two times. Bars, the mean  $\pm$  SE of at least two independent experiments performed in triplicates. (\*\*,  $P < 0.01$  ANOVA/Dunnett).

As for Jurkat and HeLa cells cephalostatin 2 induced apoptosis proceeds with time as shown by MTT (Figure III.8 upper panel) and Nicoletti test (Figure III.8 lower panel), but cephalostatin has to be applied for a longer time and in a 20-fold higher concentration to get comparable apoptosis levels than in Jurkat or HeLa cells. This

sustains the fact, that melanoma belong to the more chemoresistant tumors. Since cell viability of SK-Mel-5 is still about 50% after 3 days of treatment a long term assay was performed in order to investigate if the remaining viable cells retain their ability to grow.

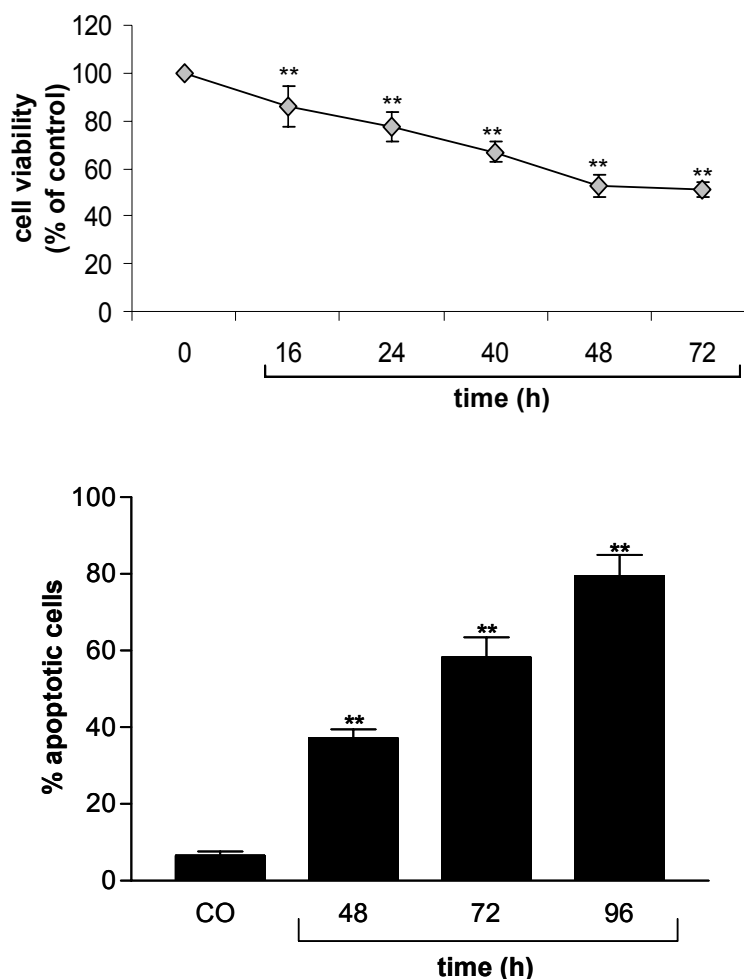


**Figure III.8 Cephalostatin induces time dependent cell death in SK-Mel-5 cells**

Upper panel: SK-Mel-5 cells were left either untreated (CO) or stimulated with 1  $\mu$ M cephalostatin 2 for 16 up to 72 hours. Impairment of cell viability was analyzed by MTT assay as described in "Materials and Methods". Represented are the mean  $\pm$  SEM of three independent experiments (\*\*,  $P < 0.01$  ANOVA/Dunnett). Lower panel: SK-Mel-5 cells were left either untreated (CO) or stimulated with 1  $\mu$ M cephalostatin 2 for 48 up to 96 hours. DNA-fragmentation was analyzed by the Nicoletti method as described in "Materials and Methods". Represented are the mean  $\pm$  SEM of three independent experiments (\*\*,  $P < 0.01$  ANOVA/Dunnett).

### 2.3.2 CEPHALOSTATIN STRONGLY INHIBITS CLONAL TUMOR CELL GROWTH

As long term assay the clonogenic or colony formation assay was performed. It is an *in vitro* cell survival assay to determine the effectiveness of cytotoxic agents. It essentially tests every cell in the population for its ability to undergo unlimited division. The difference to short term tests like the measurement of DNA-fragmentation is that cells are not evaluated after e. g. a short period of 24 h but instead are left to grow for one week. Thus it can be ascertained whether the percentage of cells that do not show DNA-fragmentation in the Nicoletti assay or are still viable in MTT assay die later or are able to grow and form new colonies, a clear sign of chemoresistance. Beyond that, cells are treated for just 2 hours with cephalostatin, a mode which is closer related to *in vivo* conditions in chemotherapy.

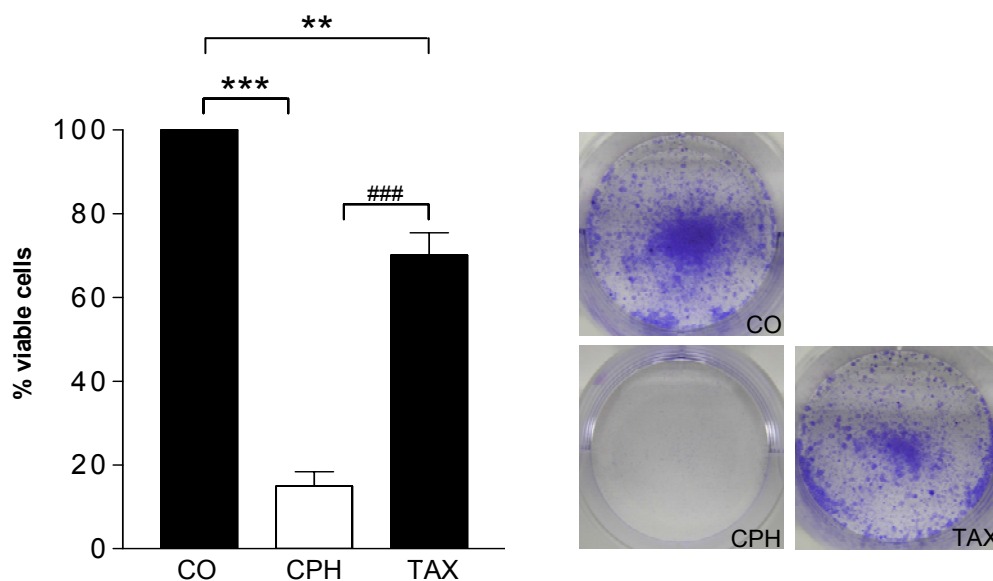


**Figure III.9 Cephalostatin strongly inhibits clonogenic tumor growth**

Left panel: SK-Mel-5 cells were seeded as described in “Materials and Methods” and left untreated (CO) or stimulated with 50 nM cephalostatin-2 (CPH) or 50 nM taxol (TAX) for 2 hours. Subsequent, cells were detached, washed with PBS and seeded again in a concentration of 10,000 cells/well. Cells were left to grow for one week and stained with crystal violet. Intracellular crystal violet was solved and absorption at 550 nm was measured. Absorption of untreated cells was set 100% viability. Represented are the mean  $\pm$  SEM of three independent experiments (\*\*,  $P < 0.01$ ; \*\*\*, ###  $P < 0.001$  unpaired two-tailed t test). Right panel: Before solving intracellular crystal violet pictures were taken. One representative picture out of three independent experiments performed in triplicates is shown.

Normally, colonies can be counted after staining with crystal violet, but since SK-Mel-5 cells do not form colonies but grow as a loosely spread network, pictures were taken and after solving the dye, absorption was measured and the percentage of viable cells was calculated by setting untreated cells 100% viable. Cephalostatin-treatment results in strong inhibition of clonogenic tumor growth as shown in Figure III.9. Most importantly, taxol which is also able to induce apoptosis measured by DNA-fragmentation (see Figure III.7) to a comparable extent has an explicit lower capacity of inhibiting the growth of SK-Mel-5 melanoma cells than cephalostatin. This clearly points to the potential of cephalostatin to fight chemoresistance.

### **3 CEPHALOSTATIN INDUCES CASPASE-DEPENDENT AND -INDEPENDENT CELL DEATH**

#### **3.1 CASPASE-DEPENDENT APOPTOSIS**

Caspases are the major executioners of classical apoptotic morphology induced by varying stimuli. But there is growing evidence that apoptotic cell death can also be mediated by other factors like cathepsins, calpains or AIF (41, 75, 76).

Cephalostatin is known to mediate apoptosis via caspases in Jurkat T cells (15). Figure III.10 A shows that apoptosis in Jurkat cells can be inhibited by use of the broad range caspase inhibitor zVADfmk (25  $\mu$ M).

In order to prove that this is not a cell type specific phenomenon additional cell lines were investigated. HeLa cells were preincubated for 1 h with the PANcaspase inhibitor zVADfmk (25  $\mu$ M) and apoptosis was measured by FACS analysis. As expected, Figure III.10 B show that caspase inhibition prevents cephalostatin-2 induced DNA-fragmentation in HeLa cells, indicating that the signaling pathway relies on caspases in these cells. The same observation is made for etoposide, a classical caspases-dependent inducer of apoptosis.

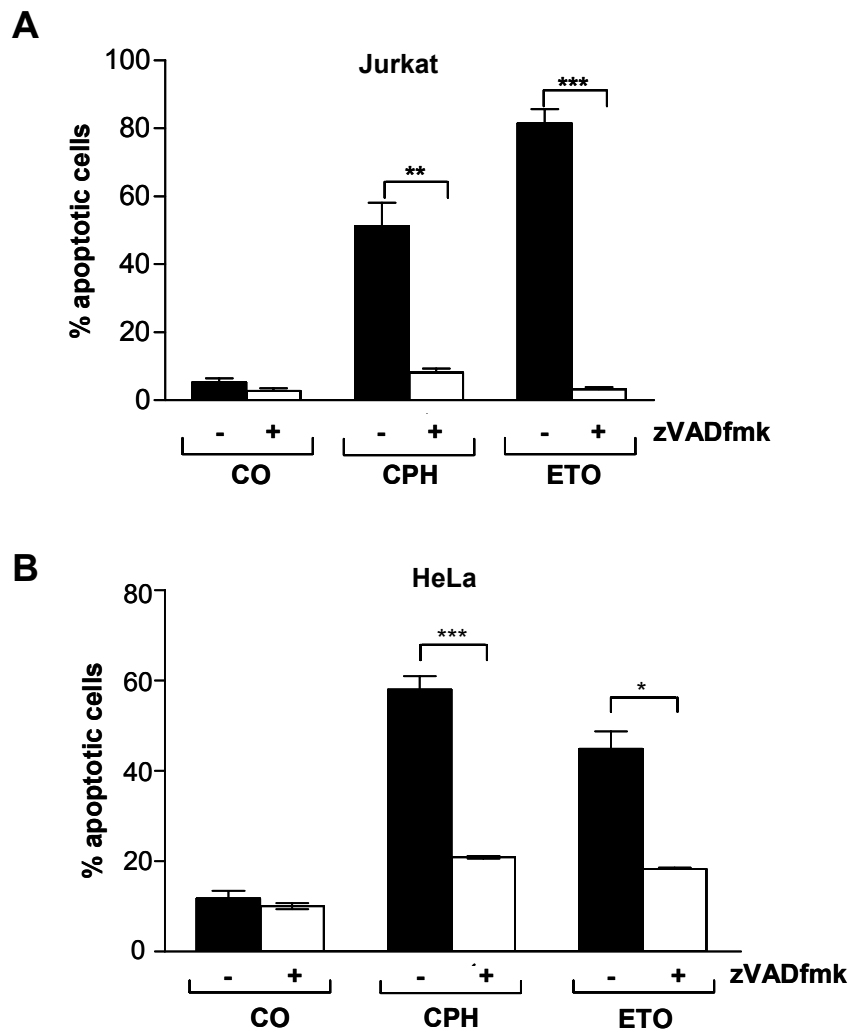


**Figure III.10 Caspase-dependent apoptosis in Jurkat and HeLa cells**

A) **Jurkat** cells were left untreated (CO) or treated with 50 nM cephalostatin 2 or 2  $\mu$ M etoposide (ETO) for 24 h. Cells were preincubated with 25  $\mu$ M PANcaspase inhibitor zVADfmk for 1 h. Apoptotic cells were quantified by flow cytometry as described in "Materials and Methods". All experiments were carried out two times. Bars, the mean  $\pm$  SE of two independent experiments performed in triplicate. (\*\*,  $P < 0.01$ ; \*\*\*,  $P < 0.001$  unpaired two-tailed t test). B) **HeLa** cells were left untreated (CO) or treated with 50 nM cephalostatin 2 or 10  $\mu$ M etoposide (ETO) for 40 h. Cells were preincubated with 25  $\mu$ M PANcaspase inhibitor zVADfmk for 1 h. Apoptotic cells were quantified by flow cytometry as described in "Materials and Methods". All experiments were carried out three times. Bars, the mean  $\pm$  SE of three independent experiments performed in triplicate (\*,  $P < 0.05$ ; \*\*\*,  $P < 0.001$  unpaired two-tailed t test).

### 3.2 CASPASE-INDEPENDENT APOPTOSIS

As another model the ovarian cancer cell line SK-OV-3 was employed. Cephalostatin is able to induce apoptosis in these cells, but surprisingly a different result concerning caspase dependence is obtained (Figure III.11).

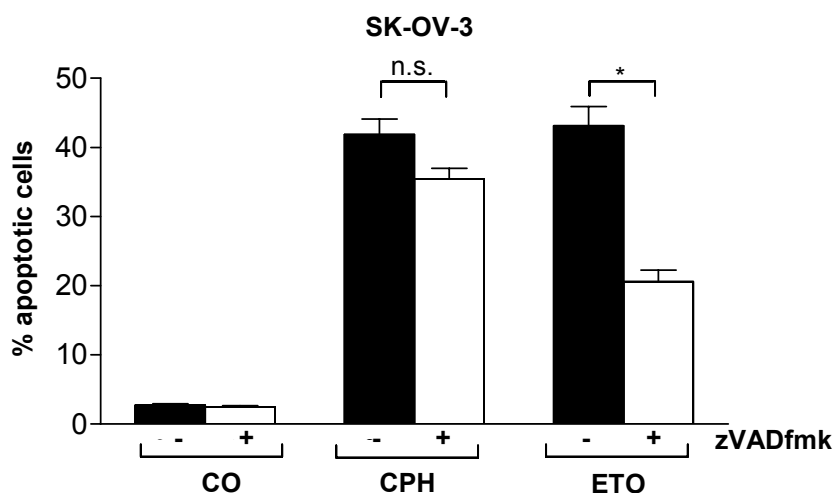


**Figure III.11 Caspase-independent cell death in SK-OV-3 cells**

**SK-OV-3** cells were left untreated (CO) or treated with 1  $\mu$ M cephalostatin 2 (CPH) or 50  $\mu$ M etoposide (ETO) for 48 h. Cells were preincubated with 25  $\mu$ M PANcaspase inhibitor zVADfmk for 1 h. Apoptotic cells were quantified by flow cytometry as described in "Materials and Methods". All experiments were carried out two times. Bars, the mean  $\pm$  SE of two independent experiments performed in triplicate. (n.s. not significant; \*  $P < 0.05$  unpaired two-tailed t test).

Although a slight decrease in cephalostatin-caused DNA-fragmentation is observed, this inhibition by zVADfmk is – contrary to etoposide – not significant. This is evidence to suggest, that – dependent on cell type – there exists a caspase-independent besides the caspase-dependent mechanism by which cephalostatin induces cell death.

This observation was further confirmed by caspase-inhibitory experiments in the SK-Mel-5 cell line. The application of zVADfmk could not block apoptosis induction as well. To exclude that this caspase inhibitor is not able to prevent caspase activity another cell permeable, irreversible broad-spectrum caspase inhibitor QVD-OPh (N-(2-Quinolyl)valyl-aspartyl-(2,6-difluorophenoxy)methyl ketone) was used.

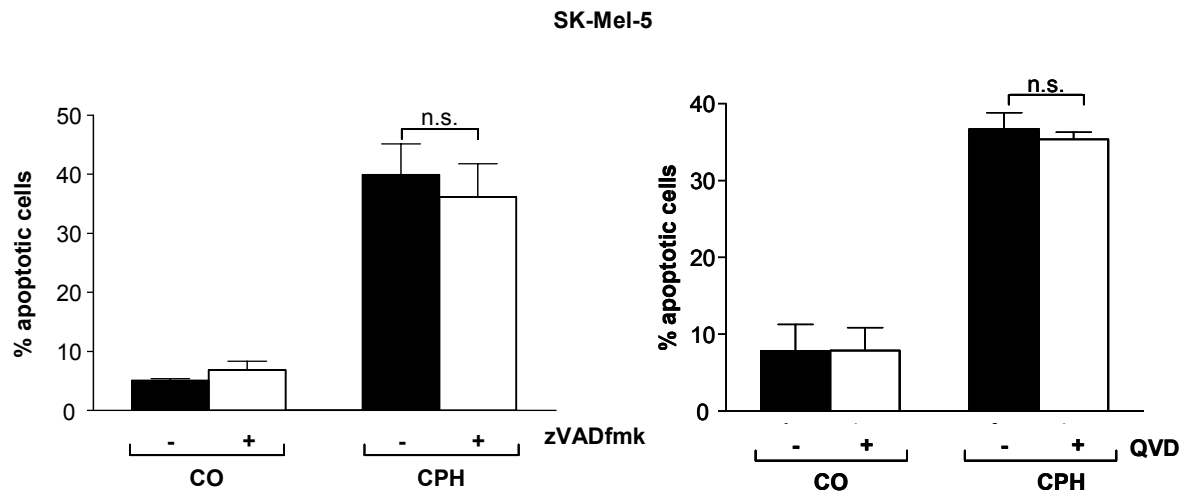


**Figure III.12 Cephalostatin induced cell death in SK-Mel-5 cells is caspase-independent**

SK-Mel-5 cells were left untreated (CO) or treated with 1  $\mu$ M cephalostatin 2 (CPH) for 48 h. Cells were preincubated with 25  $\mu$ M PANcaspase inhibitor zVADfmk (left panel) or 500 nM QVD-OPh (right panel) for 1 h. Apoptotic cells were quantified by flow cytometry as described in “Materials and Methods”. All experiments were carried out three times. Bars, the mean  $\pm$  SE of three independent experiments performed in triplicate. (n.s. not significant; \*  $P < 0.05$  unpaired two-tailed t test).

Again, no inhibition of cephalostatin 2 induced cell death could be achieved, confirming the concomitance of caspase-dependent and independent pathways for cephalostatin contingent on the used cell type.

## 4 CELL DEATH INDUCTION IN SK-MEL-5

### 4.1 STAT3 IS DEGRADED UPON CEPHALOSTATIN TREATMENT

STAT3 (Signal transducer and activator of transcription 3) is an important molecule mediating tumor-cell proliferation and survival, tumor angiogenesis and invasion. Activation of STAT3 involves phosphorylation on tyrosine 705 (dimerization, nuclear translocation and DNA binding) and serine 727 (transcriptional activity). In normal cells activation of STAT3 is rapid and transient, whereas it is proved constitutively active in a growing number of human cancer cell lines. Thus STAT3 has emerged as an important target for cancer therapy (37). As shown by clonal survival assay proliferation of SK-Mel-5 cells is strongly

inhibited upon cephalostatin treatment. Therefore we were interested if STAT3 as a central tumor survival signaling molecule is affected by cephalostatin. SK-Mel-5 cells were treated with 1  $\mu$ M cephalostatin 2 for 24 up to 48 h. As shown in Figure III.13 cephalostatin promotes STAT3 inhibition not only by preventing the phosphorylation on tyrosine 705 but also by degrading the serine 727 phosphorylated form and the total protein.

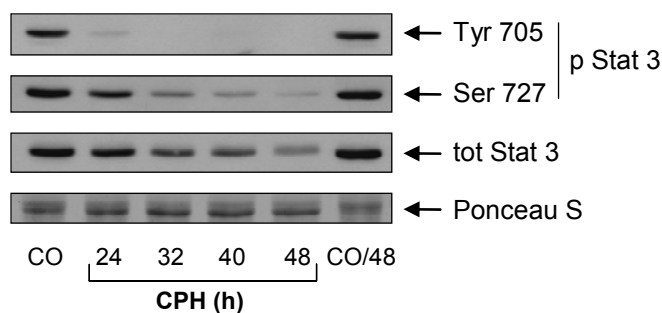


**Figure III.13 Cephalostatin promotes STAT3 degradation**

SK-Mel-5 cells were either left untreated (CO harvested together with the 24 and 32 h treated samples, CO/48 harvested together with the 40 and 48 h treated samples) or treated with cephalostatin 2 (CPH; 1  $\mu$ M) for the indicated times. Total STAT3 level and phosphorylation of STAT3 on Tyr 705 and Ser 727 was analyzed by Western blot. Equal protein loading was controlled by staining membranes with Ponceau S (a representative section of the stained membrane is shown). All experiments were carried out two times.

## 4.2 CEPHALOSTATIN INDUCES CELL CYCLE ARREST AT G1 PHASE

The oncogenic transcription factor STAT3 upregulates many tumorigenic genes, of which Bcl-x<sub>L</sub> was discovered first. Since then many other proteins that are crucially involved in tumor cell proliferation and survival have been found to be under the control of STAT3, including Mcl-1, survivin and cyclin D1 (37).

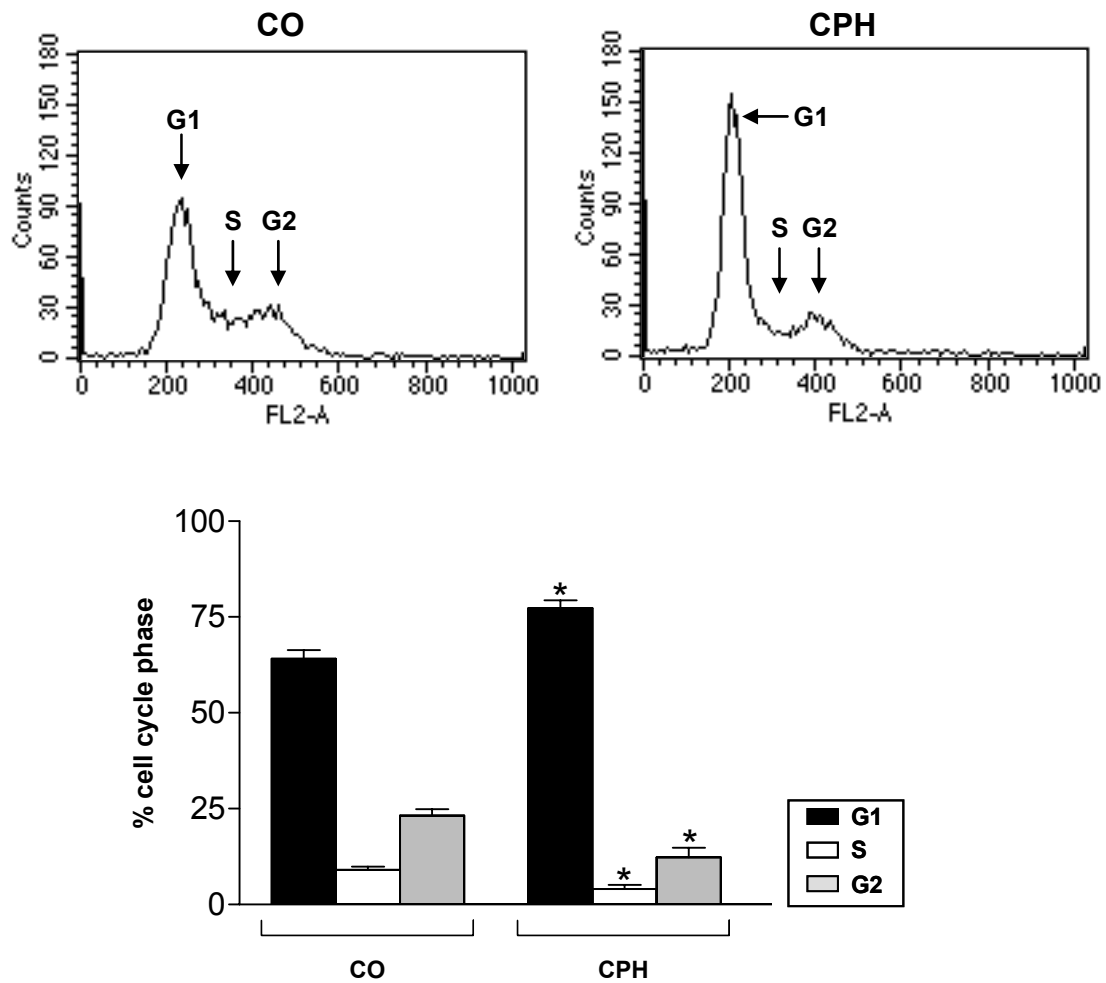


**Figure III.14 Cephalostatin induces G<sub>1</sub>-phase arrest in SK-Mel-5 cells**

Upper panel: SK-Mel-5 cells were either left untreated (CO) or treated with cephalostatin 2 (CPH; 1  $\mu$ M) for 24 h. Cells were harvested and stained with PI as for the Nicoletti method described in "Materials and Methods". Cell cycle distribution was quantified by flow cytometry. A representative histogram out of three independent experiments is shown. Lower panel: SK-Mel-5 cells were either left untreated (CO) or treated with cephalostatin 2 (CPH; 1  $\mu$ M) for 24 h. Cells were harvested and stained with PI as for the Nicoletti method described in "Materials and Methods" Cell cycle distribution was quantified by flow cytometry. All experiments were carried out three times. Bars, the mean  $\pm$  SE of three independent experiments performed in triplicates. (\*,  $P < 0.05$  unpaired two-tailed t test)

Since cyclin D1 promotes cell cycle transition from G<sub>1</sub> to S-Phase we investigated the influence of cephalostatin on cell cycle distribution of SK-Mel-5 cells.

Indeed, the percentage of cells in G<sub>1</sub> phase increases significantly whereas fewer cells are found in S and G<sub>2</sub>/M Phase upon cephalostatin treatment for 24 hours (Figure III.14).

### 4.3 SURVIVIN IS DEGRADED UPON CEPHALOSTATIN 2 TREATMENT

Survivin, another STAT3 regulated protein, which belongs to the IAP family, inhibits apoptosis and thus we were interested if survivin is influenced by cephalostatin. As shown in Figure III.15 survivin is completely degraded upon cephalostatin treatment.

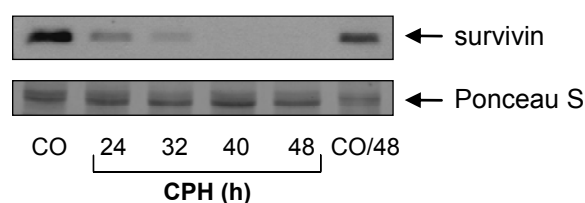


**Figure III.15 Cephalostatin promotes survivin downregulation**

SK-Mel-5 cells were either left untreated (CO harvested together with the 24 and 32 h treated samples, CO/48 harvested together with the 40 and 48 h treated samples) or treated with cephalostatin 2 (CPH; 1  $\mu$ M) for the indicated times. Survivin level was analyzed by Western blot. Equal protein loading was controlled by staining membranes with Ponceau S (a representative section of the stained membrane is shown). All experiments were carried out three times.

### 4.4 AIF IS NOT RESPONSIBLE FOR APOPTOSIS INDUCTION IN SK-MEL-5 CELLS

As a consequence of survivin downregulation the release of mitochondrial proteins and caspase-dependent as well as caspase-independent apoptosis is observed (62, 63). AIF is one of the factors known to induce caspase-independent DNA-fragmentation (77). Since cephalostatin-induced apoptosis is not dependent on caspases in SK-Mel-5 cells, we were interested if AIF mediates cell death in this case. Therefore, we applied siRNA technique in order to investigate the effect of AIF on cephalostatin mediated apoptosis. As shown in Figure III.16 (lower panel) cells were effectively transfected with siRNA targeting AIF. As control a nonsense siRNA was used. Cells were treated with cephalostatin 2 for 48 h and DNA-fragmentation was determined by FACS analysis. No difference in apoptosis induction could be detected between cells transfected with AIF siRNA and nonsense siRNA upon cephalostatin treatment. In order to avoid that the lack of AIF induces caspase-dependent apoptosis as a compensatory mechanism, we

used the broad-spectrum caspase inhibitor Q-VD-OPh. But this also could not prevent cell death, suggesting a caspase as well as AIF independent mechanism of apoptosis for cephalostatin in the SK-Mel-5 cell line.

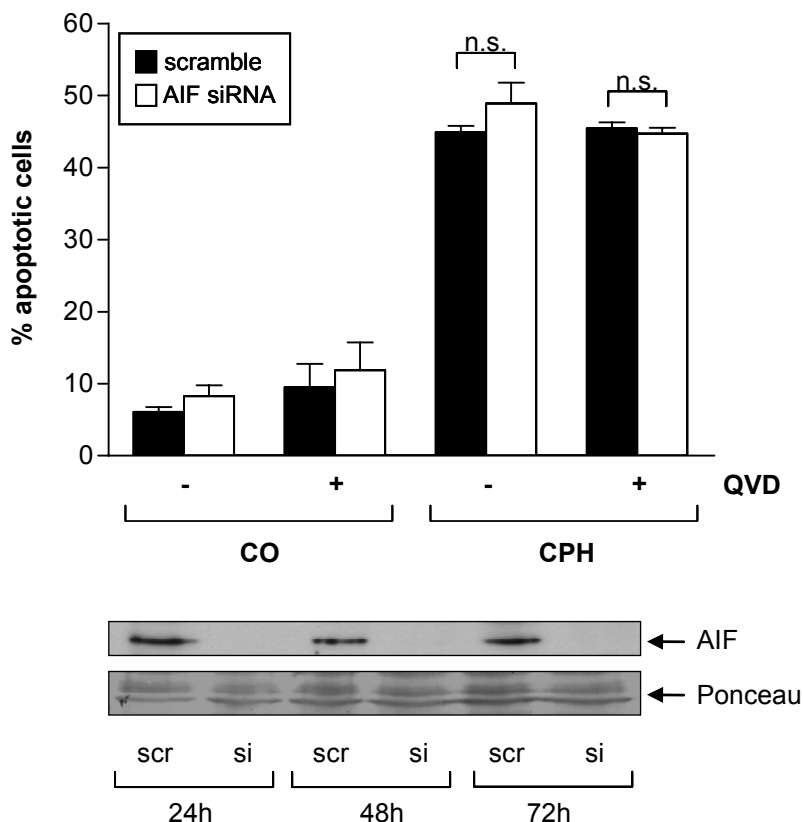


**Figure III.16 AIF is not responsible for cephalostatin induced apoptosis in SK-Mel-5 cells**

Upper panel: SK-Mel-5 cells were transfected with siRNA targeting AIF or a scramble siRNA as described in “Materials and Methods”. Cells were preincubated with 500 nM Q-VD-OPh (right panel) for 1 h. Cells were left untreated (CO) or treated with cephalostatin 2 (CPH; 1  $\mu$ M) for the indicated times. Apoptotic cells were quantified by flow cytometry as described in “Materials and Methods”. Downregulation of AIF was verified by Western Blot. Equal protein loading was controlled by staining membranes with Ponceau S (a representative section of the stained membrane is shown). All experiments were carried out two times. Bars, the mean  $\pm$  SE of two independent experiments performed in triplicates (n.s. not significant  $P < 0.05$ ; unpaired two-tailed t test).

## 5 CEPHALOSTATIN INDUCES PREFERENTIAL SMAC RELEASE

### 5.1 SMAC BUT NOT CYTOCHROME C IS PREDOMINATELY RELEASED IN VARIOUS TUMOR CELLS UPON CEPHALOSTATIN TREATMENT.

A characteristic event in cephalostatin-induced apoptosis is the selective mitochondrial release of Smac but not cytochrome c in Jurkat leukemia T cells (15). Figure III.17 shows that upon cephalostatin (CPH)-treatment only Smac is released into cytosol, whereas staurosporine (ST) strongly induces the release of Smac and cytochrome c.

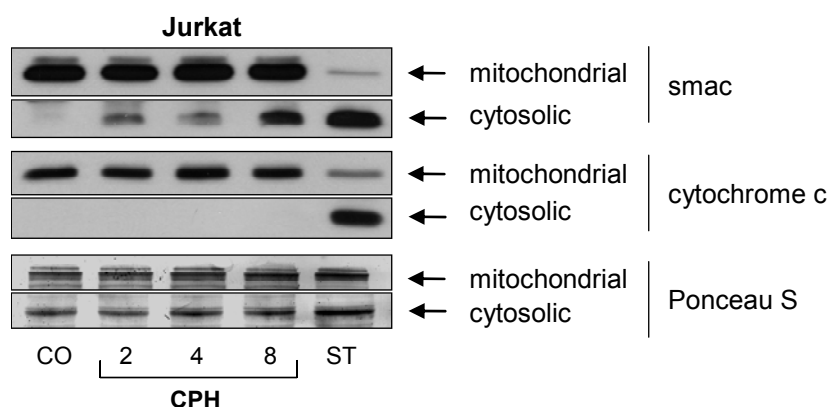


**Figure III.17 Smac is selectively released in Jurkat T cells**

Jurkat T cells were either left untreated (CO) or treated with cephalostatin 2 (CPH; 50 nM) or staurosporine (ST; 1  $\mu$ M, 8 h) for the indicated times. Smac and cytochrome c release was analyzed by Western blot. Equal protein loading was controlled by staining membranes with Ponceau S (a representative section of the stained membrane is shown). All experiments were carried out three times.

To further confirm that this unusual finding is not a cell type-specific phenomenon, but a characteristic event for cephalostatin-induced apoptosis, we investigated the release of Smac and cytochrome c in two further cell lines, SK-Mel-5 and MCF-7 cells. As seen in Figure III.18 A and Figure III.18 B (right panel), Smac - in contrast to cytochrome c - is rapidly and markedly released from mitochondria upon cephalostatin treatment in SK-Mel-5 and MCF-7 cells, whereas staurosporine and etoposide induce the translocation of both proteins into cytosol. These results

were further supported by confocal microscopy studies (Figure III.18 B left panel) using MCF-7 cells either expressing cytochrome c-GFP or Smac-YFP. Untreated control cells show the co-localization of cytochrome c-GFP and Smac-YFP with a mitochondrial dye, proofing the mitochondrial localization of the fusion proteins.

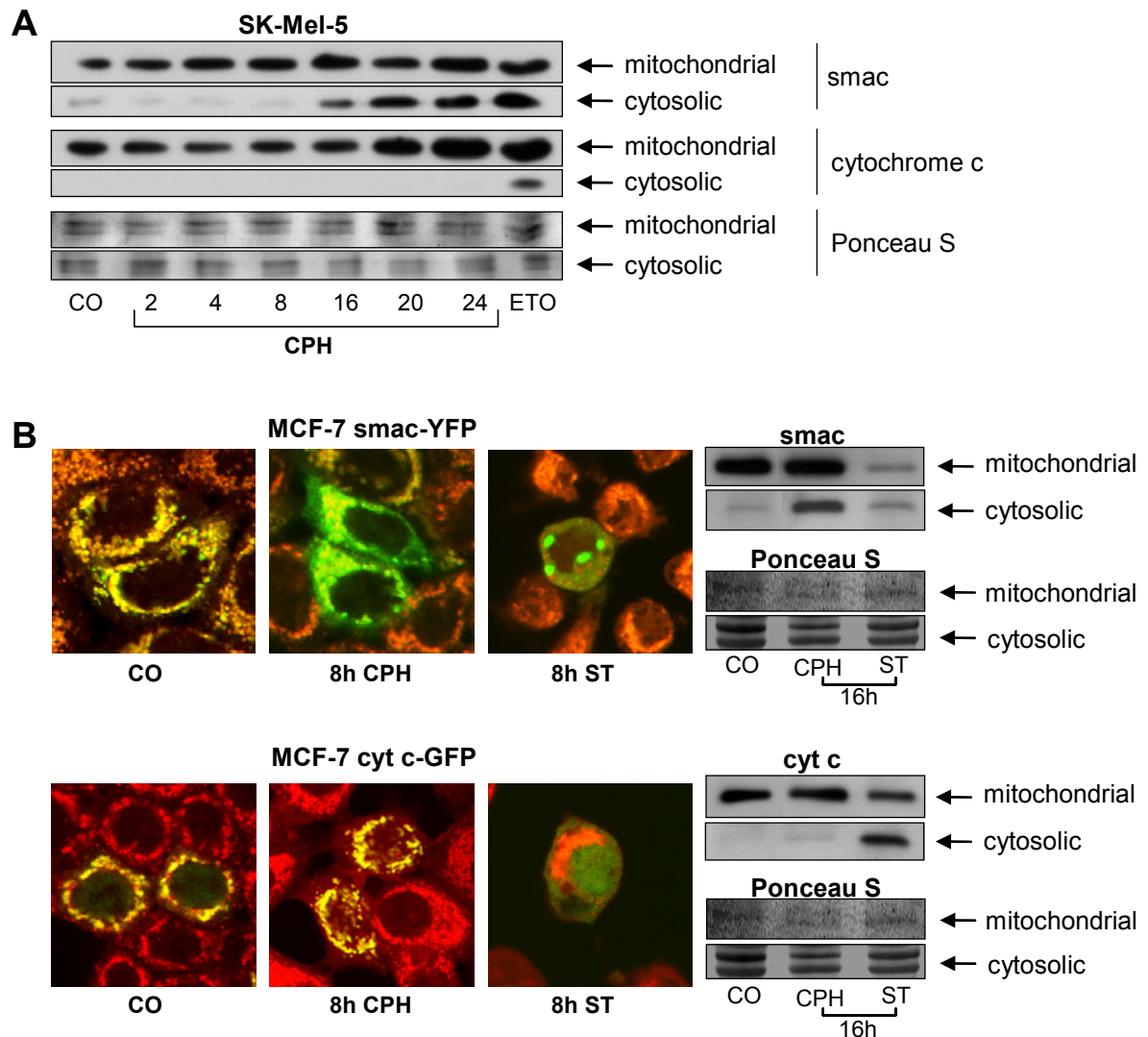


**Figure III.18 Smac is selectively released upon cephalostatin treatment regardless of cell type**

A) SK-Mel-5 cells were either left untreated (CO) or treated with cephalostatin 2 (CPH; 1  $\mu$ M) or etoposide (ETO; 10  $\mu$ M, 24 h) for the indicated times. Smac and cytochrome c release was analyzed by Western blot. Equal protein loading was controlled by staining membranes with Ponceau S (a representative section of the stained membrane is shown). B) MCF-7 cells stably expressing either cytochrome c-GFP or Smac-YFP were left untreated (CO) or treated with cephalostatin 2 (CPH; 50 nM) or staurosporine (ST; 1  $\mu$ M) for the indicated times. Smac and cytochrome c release were analyzed by confocal microscopy as well as Western blot as described in "Materials and Methods". Mitochondria are shown in red; merge of mitochondria with cytochrome c-GFP or Smac-YFP is shown yellow. Smac and cytochrome c released into cytosol is displayed green.

After stimulation with cephalostatin Smac-YFP is found in cytosol whereas cytochrome *c*-GFP is still mitochondria-localized. In contrast, staurosporine induces the release of both proteins.

## 6 MECHANISM OF CEPHALOSTATIN-INDUCED SMAC RELEASE

### 6.1 SMAC RELEASE IS NOT MEDIATED BY JNK OR CASPASE-2

Smac can be released from mitochondria in several ways. A few reports (78, 79) show that JNK is involved in the release of Smac from mitochondria. Since cephalostatin activates JNK (16), we investigated the impact of JNK and its upstream regulatory kinase ASK1 on cephalostatin-induced Smac release. As shown in Figure III.19, neither the inhibition of JNK by the inhibitor SP600125 nor the use of Jurkat cells that express an inactive form of ASK1, an upstream regulatory kinase of JNK, could prevent cephalostatin-induced Smac release.

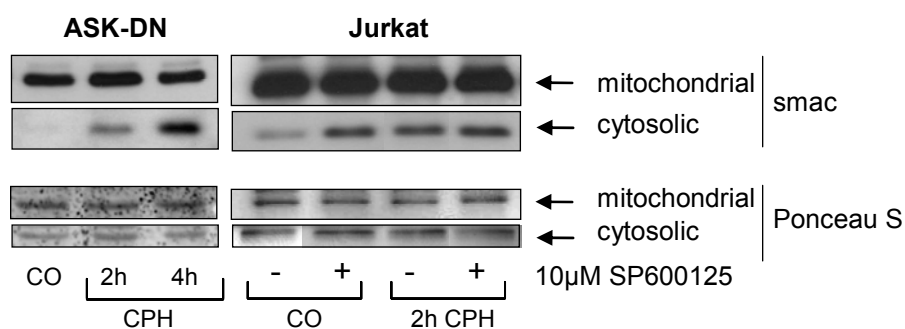


**Figure III.19 Cephalostatin induced Smac release is not dependent on JNK**

Left panel: ASK1-DN Jurkat cells were left untreated (CO) or treated with cephalostatin 2 (CPH; 50 nM) for the indicated times and Smac release was analyzed by Western blot. Right panel: Jurkat cells were left untreated (CO) or treated with cephalostatin 2 (CPH; 50 nM) for the indicated times. 30 min prior to stimulation cells were incubated with 10  $\mu$ M JNK inhibitor SP600125. Smac release was analyzed by Western blot. Equal protein loading was controlled by staining membranes with Ponceau S (a representative section of the stained membrane is shown). All experiments were carried out three times.

As previously shown by our group, the PANcaspase inhibitor zVADfmk does not inhibit cephalostatin-induced Smac release (15). Due to the fact that caspase-2 is supposed to be insensitive against zVADfmk (80) and can directly influence mitochondria (81, 82, 83), the specific inhibitor of caspase-2 benzyloxycarbonyl-Val-Asp-Val-Ala-Asp-fluoromethylketone (zVDVADfmk) was used, but again no inhibition of Smac release could be observed (Figure III.20).

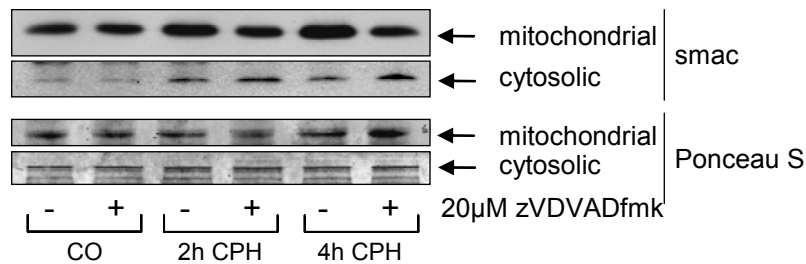


**Figure III.20 Cephalostatin induced Smac release is not dependent on caspase-2**

Jurkat cells were left untreated (CO) or treated with cephalostatin 2 (CPH; 50 nM) for the indicated times. Prior to stimulation cells were incubated for 1 hour with 20  $\mu$ M zVDVADfmk, a specific caspase-2 inhibitor. Smac release was analyzed by Western blot. Equal protein loading was controlled by staining membranes with Ponceau S (a representative section of the stained membrane is shown). All experiments were carried out three times.

## 6.2 BAK DEFICIENCY DELAYS BUT CAN NOT PREVENT SMAC RELEASE

The onset of Smac release and induction of apoptosis induced by cephalostatin is known to be inhibited by overexpression of the antiapoptotic protein Bcl- $x_L$  (15). Since Jurkat cells do not express Bax (84) we used Jurkat cells additionally deficient for Bak to investigate the impact of these proapoptotic proteins on Smac release. As shown in Figure III.21A, Bak deficiency delayed, but did not prevent the onset of Smac release in cephalostatin-treated Jurkat cells (experiment performed by Dr. Nancy López-Antón). The cells are resistant to apoptotic stimuli like staurosporine and taxol, but cephalostatin-induced cell death (Figure III.21B) was not influenced. Staurosporine and taxol use the intrinsic pathway, characterized by cytochrome c release, further pointing to a cytochrome c independent signaling pathway for cephalostatin, in which Smac could play an important role.

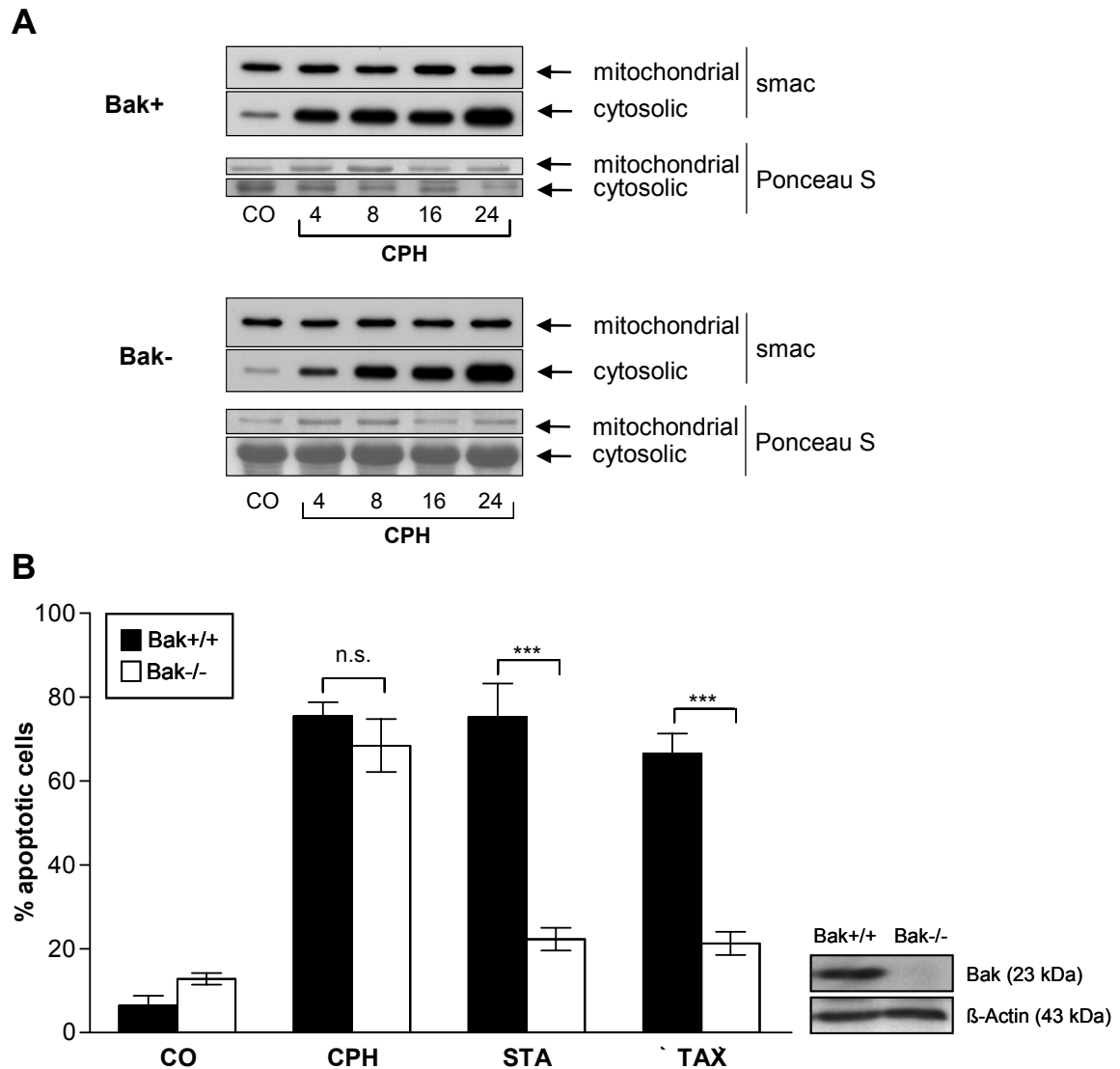


**Figure III.21 Bak deficiency can not prevent Smac release and apoptosis induced by cephalostatin**

A) Bak reconstituted (Bak<sup>+/+</sup>) and Bak deficient (Bak<sup>-/-</sup>) Jurkat cells were left untreated (CO) or treated with cephalostatin 2 (CPH; 50 nM) for the indicated times. Smac release was analyzed by Western blot. Equal protein loading was controlled by staining membranes with Ponceau S (a representative section of the stained membrane is shown). All experiments were carried out three times. B) Bak-reconstituted (Bak<sup>+/+</sup>) and Bak-deficient (Bak<sup>-/-</sup>) Jurkat cells were left untreated (CO) or treated with 50 nM cephalostatin 2 (CPH), 250 nM staurosporine (STA) or 1  $\mu$ M taxol (TAX) for 24 hours. Apoptotic cells were quantified by flow cytometry as described in "Materials and Methods". Protein extracts from Bak<sup>+/+</sup> and Bak<sup>-/-</sup> cells were prepared and Bak levels analyzed by Western blot.  $\beta$ -Actin was used as loading control (right panel).

### 6.3 SMAC RELEASE IS PARTIALLY DEPENDENT ON CALPAIN

The  $\text{Ca}^{2+}$ -dependent calpain family of cysteine proteases is known to mediate apoptosis upon several conditions, amongst others by cleaving Bcl-2 family proteins and inducing release of mitochondrial factors. Calpain is activated upon  $\text{Ca}^{2+}$  binding and further autolytic processing to its 76 kDa subunit (85, 86). In fact, cephalostatin leads to calpain activation already after one hour of treatment (Figure III.22, upper panel; experiment was performed by Dr. Irina Müller). Due to this fast activation we investigated a possible influence of calpain on the selective Smac release by employing the inhibitor calpastatin, which was coupled to penetratin. Interestingly, cephalostatin-induced Smac release into cytosol was diminished by calpain inhibition (Figure III.22, lower panel).

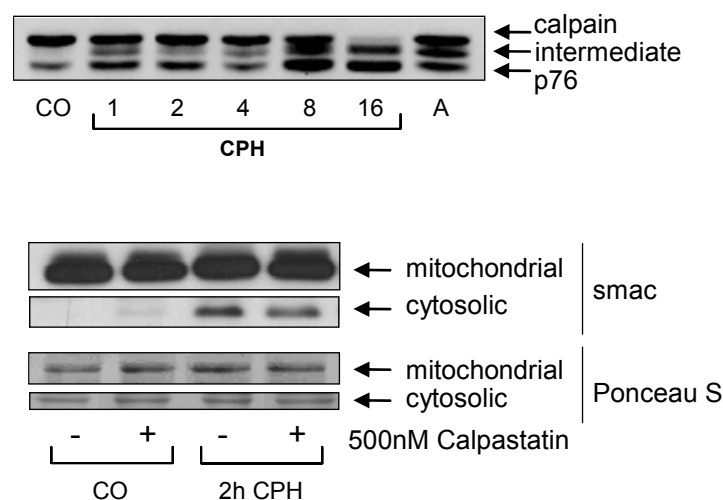


**Figure III.22 Cephalostatin induced Smac release is partially mediated by calpain**

Upper panel: Jurkat cells were left untreated (CO) or treated with cephalostatin for the indicated times. The calcium ionophore A23187 (A; 1  $\mu\text{M}$  16 h) was used as positive control. Calpain activation was analyzed by Western blot. Lower panel: Jurkat cells were left untreated (CO) or treated with cephalostatin (CPH, 50 nM) for 2 hours. 1 hour prior to stimulation cells were incubated with 500 nM calpastatin-penetratin. Smac release was analyzed by Western blot. Equal protein loading was controlled by staining membranes with Ponceau S (a representative section of the stained membrane is shown). All experiments were carried out three times.

## 7 IMPACT OF SMAC ON CEPHALOSTATIN-INDUCED APOPTOSIS

### 7.1 XIAP OVEREXPRESSION CAN NOT PREVENT APOPTOSIS

Inhibitor of apoptosis proteins (IAPs) are shown to be expressed to a higher extent in cancer than in normal tissue and are connected to chemoresistance. Smac/DIABLO binds to various IAPs thus neutralizing their inhibitory effect on caspases. The BIR3 domain of X-linked IAP (XIAP), the most potent member of the IAP family, is recognized by mature Smac/DIABLO. Thus, Smac is able to compete with caspase-9 for binding to the BIR3 domain of IAPs and thereby favors its activation. Smac/DIABLO also binds to the BIR2 motif of XIAP, thereby counteracting the XIAP-dependent inhibition of caspase-3 and -7 (34). If Smac is functional and important in cephalostatin induced cell death it thus should counteract XIAP overexpression. Therefore, apoptosis was measured in XIAP overexpressing in comparison to wildtype Jurkat cells. Figure III.23 strikingly shows that cephalostatin induced cell death is not influenced by XIAP overexpression, whereas etoposide mediated cell death is almost completely inhibited.

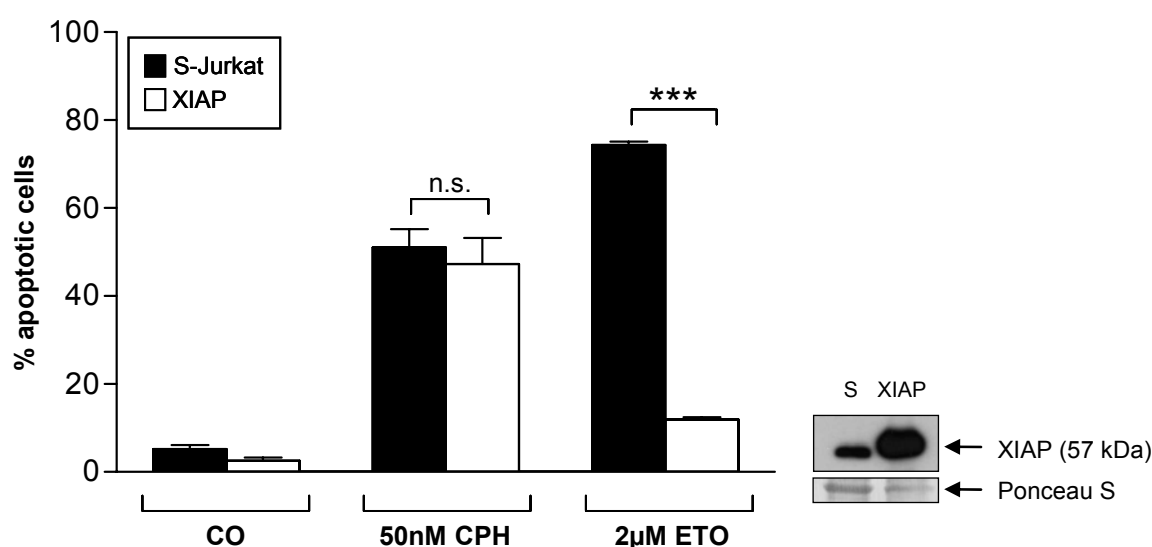


**Figure III.23 XIAP overexpression does not prevent cephalostatin-induced cell death**

XIAP overexpressing (XIAP) and wildtype Jurkat (S-Jurkat) cells were left untreated (CO) or treated with 50 nM cephalostatin 2 (CPH) or 2 µM etoposide (ETO) for 24 hours. Apoptotic cells were quantified by flow cytometry as described in “Materials and Methods”. Protein extracts from XIAP and S-Jurkat cells were prepared and XIAP levels analyzed by Western Blot. Equal protein loading was controlled by staining membranes with Ponceau S (a representative section of the stained membrane is shown). All experiments were carried out three times (n.s. not significant; \*\*\*,  $P < 0.001$  (unpaired two-tailed t test)).

## 7.2 SMAC SILENCING INHIBITS CEPHALOSTATIN-INDUCED APOPTOSIS

Due to the unique characteristic of cephalostatin to induce a selective Smac release, we investigated the role of Smac in cephalostatin-induced cell death by silencing the Smac gene *via* siRNA. As shown in Figure III.24, silencing of Smac significantly inhibited cephalostatin-induced apoptosis.

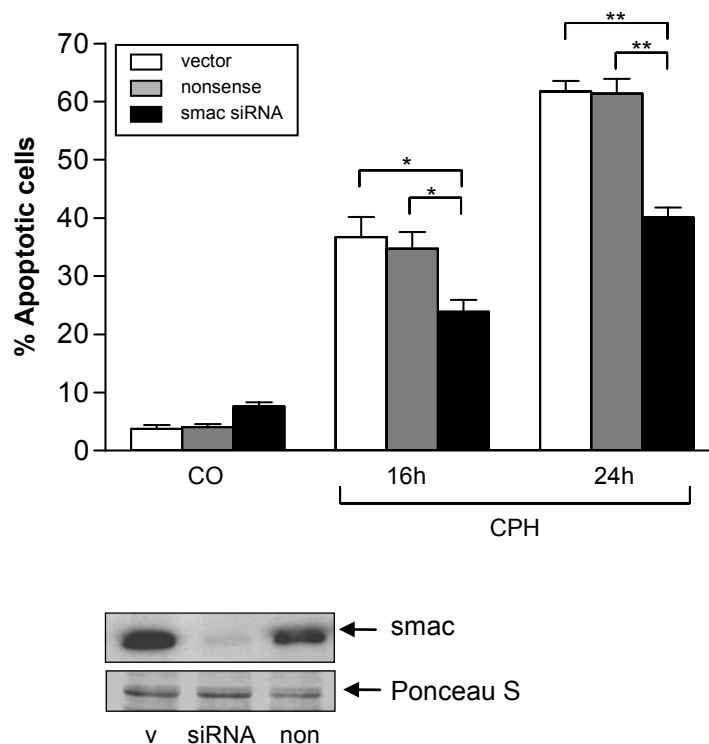


**Figure III.24 Smac siRNA inhibits cephalostatin-induced apoptosis**

Jurkat cells were transfected with plasmids encoding for either Smac siRNA or nonsense sequence or vector without insert as described in "Material and Methods". Cells were left untreated (CO) or treated with cephalostatin 2 (CPH; 50 nM) for the indicated times. Apoptotic cells were quantified by flow cytometry as described in "Materials and Methods". Downregulation was verified by Western blot. Equal protein loading was controlled by staining membranes with Ponceau S (a representative section of the stained membrane is shown). All experiments were carried out three times. Bars, the mean  $\pm$  SE of three independent experiments performed in triplicate. (\*,  $P < 0.05$ ; \*\*,  $P < 0.01$  unpaired two-tailed t test)

Caspase-9 is known to be an important initiator caspase in cephalostatin mediated cell death (17). As shown in Figure III.25 cephalostatin activates caspase-9. The importance of caspase-9 was investigated in caspase-9 deficient and caspase-9 reconstituted Jurkat cells. Apoptosis was almost completely prevented in caspase-

9 deficient cells. Since Smac is known to abolish the inhibitory effect of XIAP on caspase-9 and -3, we investigated the effect of Smac downregulation on cephalostatin-mediated caspase activation.

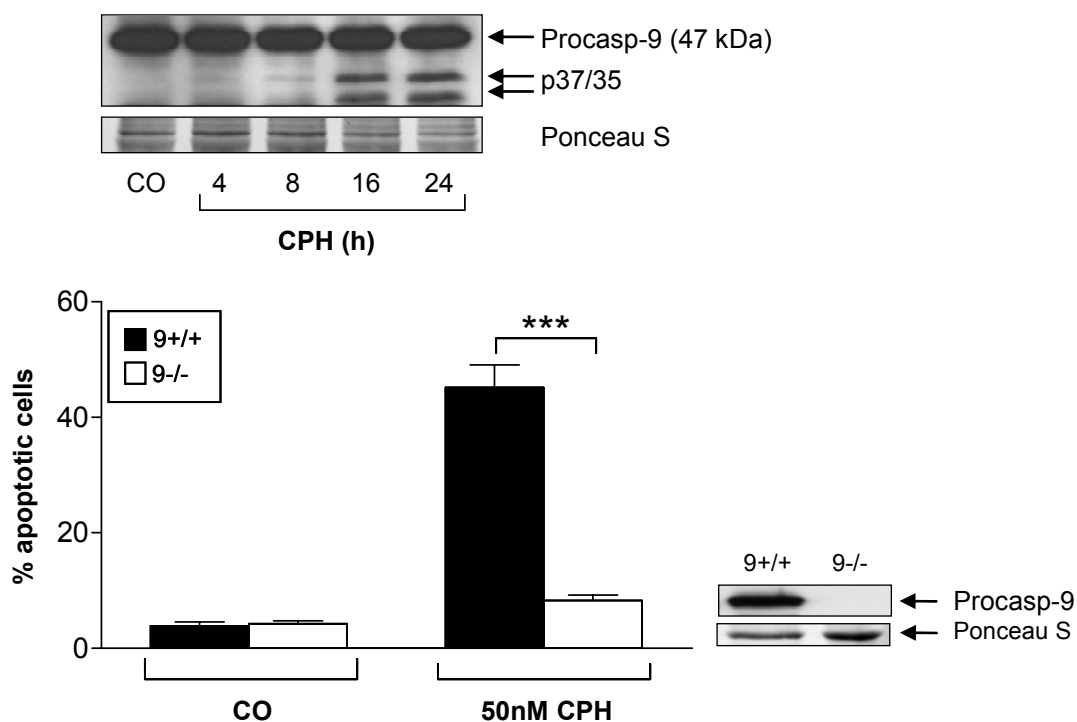


**Figure III.25 Caspase-9 is essential for cephalostatin-induced cell death**

Upper panel: Jurkat cells were left untreated (CO) or treated with cephalostatin 2 (CPH; 50 nM) for the indicated times. Activation of caspase-9 was examined by Western blot. Equal protein loading was controlled by staining membranes with Ponceau S (a representative section of the stained membrane is shown). All experiments were carried out three times. Lower panel: Caspase-9 deficient (9<sup>-/-</sup>) and caspase-9 reconstituted Jurkat (9<sup>+/+</sup>) cells were left untreated (CO) or treated with 50 nM cephalostatin 2 (CPH) for 24 hours. Apoptotic cells were quantified by flow cytometry as described in “Materials and Methods”. Bars, the mean  $\pm$  SE of three independent experiments performed in triplicate. (\*\*\*,  $P < 0.001$  unpaired two-tailed t test). Protein extracts from 9<sup>-/-</sup> and 9<sup>+/+</sup> cells were prepared and caspase-9 level analyzed by Western Blot. Equal protein loading was controlled by staining membranes with Ponceau S (a representative section of the stained membrane is shown).

### 7.3 SMAC ENHANCES THE APOPTOTIC SIGNALING CASCADE

Silencing of Smac clearly suppressed the appearance of caspase-9 cleavage products indicating a reduced activation of the initiator caspase-9 in Smac-depleted cells, whereas the activation of the initiator caspase-4 remained unaffected (Figure III.26 A). Smac siRNA had also influence on caspase-3 activation and consequently PARP cleavage as shown in Figure III.26 B by

reduced caspase-3 cleavage products and strongly diminished appearance of the 85 kDa PARP cleavage product. Caspase-2 has characteristics of initiator caspase due to its long CARD-containing prodomain. The prodomain and the linker region between the large and the small subunit are removed during generation of the active enzyme resulting in different cleavage products (27, 87).

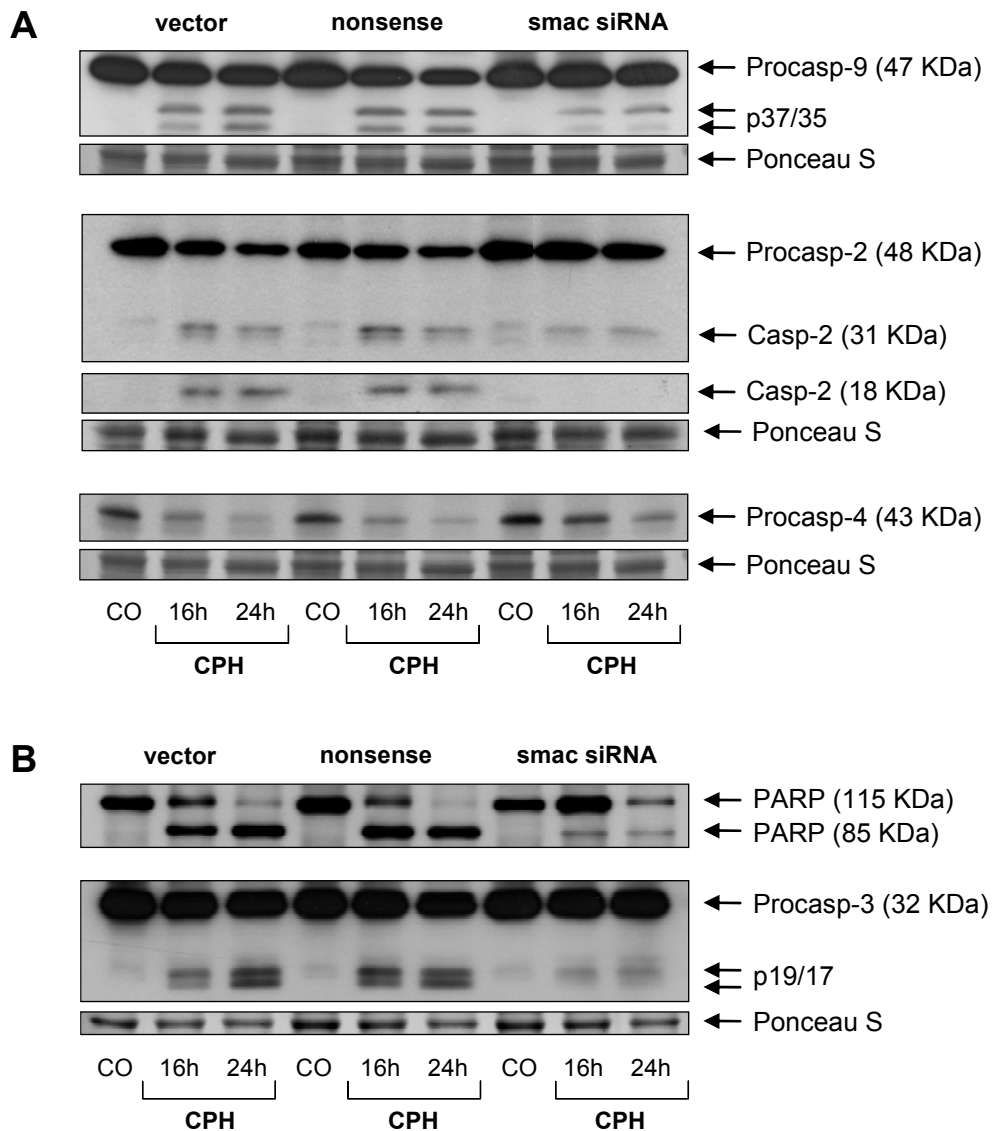


**Figure III.26 Smac silencing reduces activation of caspase-9, caspase-3 and caspase-2 but not caspase-4.**

Jurkat cells were transfected with plasmids encoding for either Smac siRNA, nonsense sequence or with vector alone as described in "Materials and Methods". Cells were left untreated (CO) or treated with cephalostatin 2 (CPH; 50 nM) for the indicated times. Activation of caspase-9, caspase-2, caspase-3 and caspase-4 as well as PARP cleavage was examined by Western blot. Equal protein loading was controlled by staining membranes with Ponceau S (a representative section of the stained membrane is shown). All experiments were carried out three times.

Interestingly, cephalostatin-induced processing of caspase-2 to its 18 kDa fragment was prevented upon Smac silencing (Figure III.26 A), pointing to a participation of caspase-2 in cephalostatin-induced cell death.

## **8 INVOLVEMENT OF CASPASE-2 IN CEPHALOSTATIN-INDUCED APOPTOSIS**

### **8.1 CASPASE-2 PARTICIPATES IN APOPTOSIS INDUCTION**

In fact, treatment of cells with cephalostatin leads to an early activation of caspase-2 as demonstrated in Figure III.27 A by the appearance of the caspase-2 cleavage product p31 already after 8 h of incubation.

For investigating the impact of caspase-2 in cephalostatin-induced apoptosis, caspase-2 was inhibited by use of the selective inhibitor zVDVADfmk and by siRNA. Use of zVDVADfmk (Figure III.27 B left panel; experiment performed by Dr. Nancy López-Antón) significantly inhibits cephalostatin-mediated apoptosis.

Cells transiently transfected with a siRNA targeting caspase-2 showed a significantly reduced amount of annexin V positive cells compared to cells transfected with a nonsense siRNA sequence (Figure III.27 B right panel). These results indicate that caspase-2 contributes to cephalostatin-mediated apoptosis.

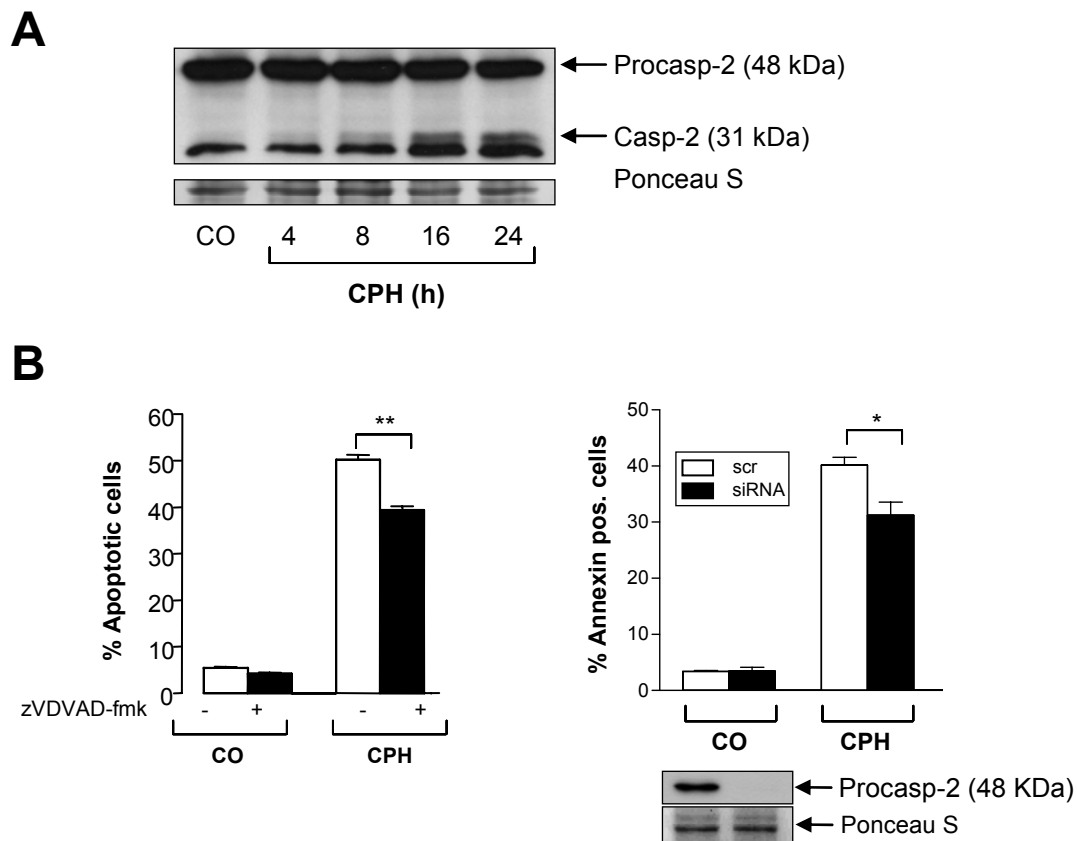


**Figure III.27 Cephalostatin activates caspase-2**

A) Jurkat cells were either left untreated (CO) or treated with 50 nM cephalostatin (CPH) for the indicated times. Caspase-2 activation was examined by Western blot. B) Left panel: Jurkat cells were left untreated (CO) or treated with cephalostatin 2 (CPH; 50 nM). Cells were preincubated with 25  $\mu$ M PANcaspase inhibitor zVADfmk for 1 h. Apoptotic cells were analyzed by flow cytometry as described in "Materials and Methods". Right panel: Cells were transfected with either caspase-2 siRNA or scramble siRNA and left untreated (CO) or treated with cephalostatin 2 (CPH; 50 nM). Apoptotic cells were analyzed by Annexin staining as described in "Materials and Methods". Downregulation of caspase-2 was verified by Western blot analysis. Equal protein loading was controlled by staining membranes with Ponceau S (a representative section of the stained membrane is shown). All experiments were carried out three times. Bars, the mean  $\pm$  SE of three independent experiments performed in triplicate. (\*,  $P < 0.05$ ; \*\*,  $P < 0.01$  unpaired two-tailed t test).

## 8.2 CASPASE-2 IS ACTIVATED INDEPENDENT OF CASPASE-9 UPON CEPHALOSTATIN TREATMENT.

Caspase-2 can be activated upstream (88, 89) or downstream (90) of caspase-9. We hypothesized that, in addition to caspase-4, caspase-2 could act as an apical caspase in cephalostatin-induced apoptosis.

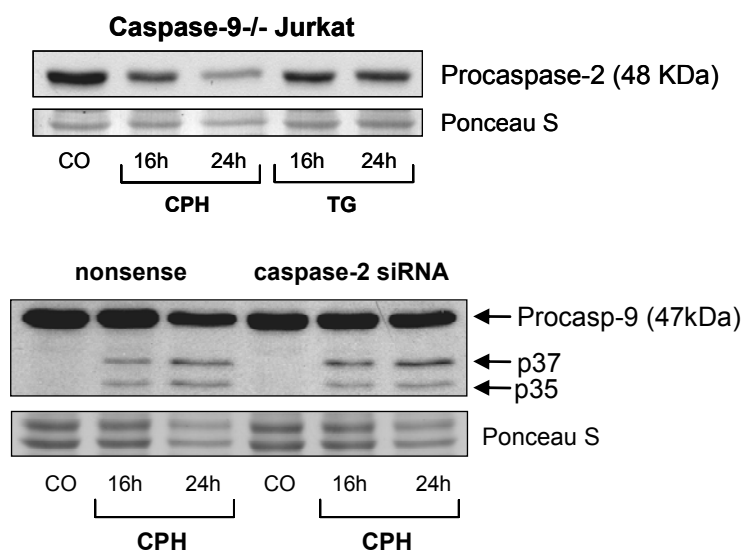


**Figure III.28 Caspase-2 is activated independent of caspase-9**

Upper panel: Jurkat cells lacking caspase-9 (Caspase-9<sup>-/-</sup>) were either left untreated (CO) or treated with cephalostatin 2 (CPH; 50 nM) or thapsigargin (TG; 3  $\mu$ M) for the indicated times. Processing of procaspase-2 was examined by Western blot. Lower panel: Jurkat cells were transfected with caspase-2 siRNA or scramble siRNA and left either untreated (CO) or treated with cephalostatin 2 (CPH, 50 nM) for the indicated times. Caspase-9 processing was examined by Western blot. Equal protein loading was controlled by staining membranes with Ponceau S (a representative section of the stained membrane is shown).

To this end, activation of caspase-2 was examined in caspase-9-deficient cells and activation of caspase-9 was investigated in caspase-2-silenced cells. Caspase-2 activation upon cephalostatin treatment as well as by thapsigargin is independent of an activated caspase-9, as shown using caspase-9-deficient Jurkat cells (Caspase 9<sup>-/-</sup>, Figure III.28 upper panel). On the other hand, caspase-9 is activated to the same extent in caspase-2 silenced cells as in cells transfected with scramble siRNA (Figure III.28 lower panel). Thus, cephalostatin-induced

caspase-2 does not affect caspase-9 activation which differs from the role of cephalostatin-induced caspase-4.

Caspase-2 acts as initiator caspase and independently from caspase-9. In a next step we were interested in the mechanism of this initial caspase-2 activation induced by cephalostatin.

## **9 CEPHALOSTATIN INDUCES THE FORMATION OF THE PIDDOSOME COMPLEX.**

Although processing of caspase-2 to its active fragments was observed after 8 hours of treatment with cephalostatin, similarly to caspase-9, recruitment to a large protein complex (independent of the Apaf-1 apoptosome) is sufficient to mediate its activation (91).

Later on, appearance of cleavage fragments is mediated by self-processing and further enhances its catalytic activity (27, 87). This newly identified caspase-2 activating protein complex is referred to as the PIDDosome (56), composed of the proteins PIDD, RAIDD and procaspase-2. To investigate the participation of the PIDDosome in our system we studied the protein interaction by immunoprecipitation of caspase-2, RAIDD and PIDD. Western blot analysis of the precipitation complex of each antibody reveals the basal interaction of RAIDD and PIDD in untreated cells (Figure III.29).

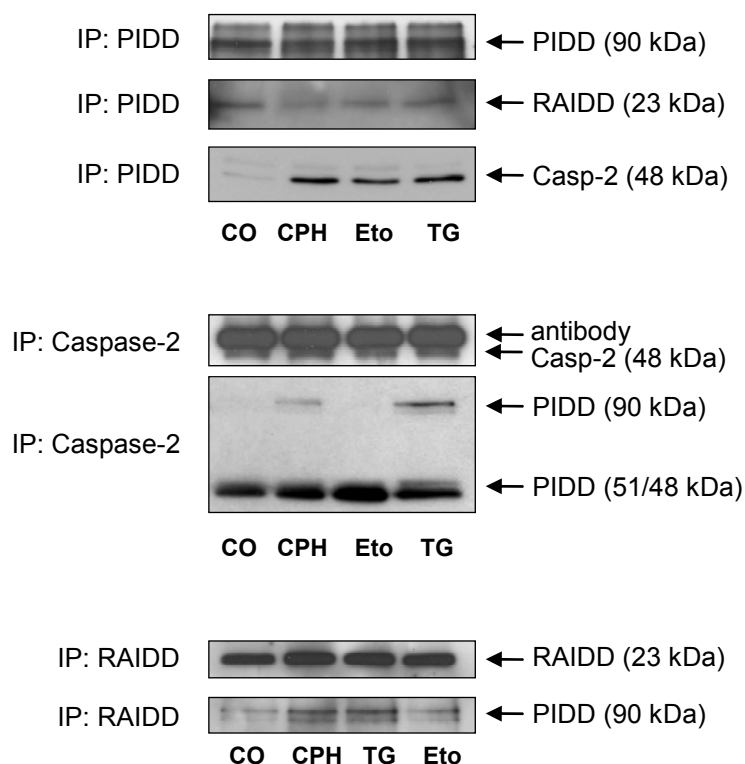


**Figure III.29 The PIDDosome is formed upon cephalostatin treatment**

Jurkat cells were either left untreated (CO) or treated with cephalostatin 2 (CPH; 50 nM), thapsigargin (TG; 3  $\mu$ M) or etoposide (Eto, 2  $\mu$ M) for 1h. Caspase-2, PIDD or RAIDD were immunoprecipitated as described in “Materials and Methods” and caspase-2, PIDD and RAIDD levels were detected by Western blot.

Importantly, upon 1 h of incubation with cephalostatin procaspase-2 is recruited to the PIDD and RAIDD complex (Figure III.29), suggesting the assembly of the PIDDosome as the possible mechanism of caspase-2 activation.

## IV DISCUSSION

Many chemotherapeutic drugs used in cancer therapy induce apoptosis via the extrinsic or the intrinsic pathway. Since accumulation of chemoresistance is often connected to defects in these apoptotic signaling pathways, it is of high interest to find novel mechanisms for tumor cell death induction. The cephalostatins are promising substances in this context, particularly because cephalostatin mediates cell death apoptosome- and CD95/caspase-8-independent (15). Therefore, cephalostatin-induced cell death mechanisms were further investigated to find potentially new targets for cancer therapy.

### 1 COMPARISON OF CEPHALOSTATIN 2, 10 AND 12

Structure-activity studies have been performed on different cephalostatins. The results indicate that the Northern part is the most shared unit among the cephalostatins and is also strongly associated with antitumor activity (18). This is in line with cephalostatin 10 showing dose dependencies comparable to cephalostatin 1 and 2 (6, 7, 10), whereas an increased level of hydroxylation in the Southern part results in a decrease in antitumor activity, as in the case of cephalostatin 12 (18). In the present work, cytotoxicity of CPH 2, 10 and 12 was tested on Jurkat leukemia T cells and the results obtained from MTT-test ( $IC_{50}$  for CPH 2: 1 nM, CPH 10: 9.7 nM and CPH 12: 560 nM) and from measurement of DNA-fragmentation showed that CPH 2 is more potent than CPH 10 and CPH 12. This corresponds to the expected pattern that their potency varies depending on the chemical composition (Figure I.2).

## 2 CELL TYPE INDEPENDENT APOPTOSIS INDUCTION

To investigate whether cephalostatin is able to induce apoptosis independent of cell type, various cell lines were tested: the cervix carcinoma cell line HeLa, the breast adenocarcinoma cell line MCF-7, the malignant melanoma cell line SK-Mel-5 and the ovarian cancer cell line SK-OV-3. In the entire listed cell lines cephalostatin is able to induce apoptosis, manifesting cell type independence, even though except for HeLa a higher cephalostatin concentration is needed for cell death induction in MCF-7, SK-OV-3 and SK-Mel-5 cells. Since SK-OV-3 has dysfunctional apoptosome activity (92) and SK-Mel-5 cells are shown to have very low Apaf 1 levels (93, 94), there is further evidence that apoptosome formation is not necessary for cephalostatin induced cell death. Melanoma is a very aggressive form of cancer being highly resistant to most therapies (95) due to inactivation of the apoptotic machinery (96). For that reason a long term assay was employed. Cephalostatin induced almost complete inhibition of clonal tumor growth contrary to taxol, although taxol is able to induce DNA-fragmentation in the short-time Nicoletti assay. This result highlights the potential of cephalostatin to fight on chemoresistance, since a very short treatment time (2 h) is sufficient to induce complete tumor cell growth inhibition.

## 3 INVOLVEMENT OF CASPASES

Caspases are the main executioners of classical apoptotic cell death. Cephalostatin mediated apoptosis is almost completely caspase-dependent in Jurkat (15) and HeLa cells, but the apoptosis in MCF-7 cells lacking caspase-3 is not diminished compared to caspase-3 reconstituted cells. Since this cell line still expresses other effector caspases, caspase-7 (97) maybe compensating for caspase-3. Surprisingly, cephalostatin induces caspase-independent cell death in the more resistant SK-OV-3 and SK-Mel-5 cell lines, as shown by the use of the broad spectrum caspase inhibitor zVADfmk. To control these results another caspase inhibitor, Q-VD-OPh (98), was tested in SK-Mel-5. Again, DNA-fragmentation could not be blocked. One could presume, that these inhibitors can not operate because of inactivation or increased efflux, but several studies show an inhibitory influence of zIETDfmk (caspase-8 inhibitor) (99) or zVADfmk (100),

on DNA-fragmentation or PARP cleavage (101) in SK-Mel-5 cells, clearly demonstrating its activity. Upon this interesting finding cell death induction in SK-Mel-5 cells was further investigated.

## **4 CELL DEATH INDUCTION IN SK-MEL-5 CELLS**

The normally transiently activated and strictly controlled transcription factor STAT3 is constitutively activated at 50 – 90% frequency in human cancers, including melanoma and is amongst other factors critically involved in tumor cell growth by regulating the expression of genes that contribute to survival and proliferation. Interestingly, a permanent STAT3 activation was observed in a majority of tested melanoma cell lines and primary melanoma but not in normal skin from the same patients, making STAT3 a highly interesting therapeutic target (61, 102).

Studies have shown that overexpression of STAT3 results in elevated levels of the antiapoptotic proteins survivin, Bcl-x<sub>L</sub> and Mcl-1 and of the cell cycle regulators cyclin D1 and c-Myc, which regulate the G1 to S transition. Inhibition of STAT3 by dominant negative mutants leads to the downregulation of the above named STAT3 targets and to cell cycle arrest in G1 phase (37, 103).

First experiments show that cephalostatin induces not only the degradation of the Ser 727 and Tyr 705 phosphorylated STAT3 proteins but also degradation of the total STAT3 protein. This is in contrast to other studies with apoptosis inducing compounds (103), where total protein levels are not affected. Therefore, it has to be further explored whether STAT3 protein (e.g. by proteasome or lysosome) or mRNA level is affected.

Cell cycle analysis revealed that upon cephalostatin treatment cells are significantly arrested in G1 phase. If this arrest is a consequence of STAT3 inhibition has to be further investigated by studying the STAT3 regulated cell cycle related proteins cyclin D1 and c-Myc. As a second downstream target of STAT3 survivin protein was examined and was observed to be completely degraded by cephalostatin. Following survivin downregulation the release of proapoptotic factors from mitochondria such as cytochrome c and AIF is described (62). Since cephalostatin induces caspase-independent DNA-fragmentation in SK-Mel-5 the impact of AIF was investigated, but contrary to other studies (101, 104) AIF is not

involved in cephalostatin-mediated DNA-fragmentation, suggesting that other caspase-independent factors like EndoG or Omi/HtrA2 could be responsible for DNA-fragmentation.

The late DNA-fragmentation, independence of caspases and the remarkable protein degradation of STAT3 and survivin in SK-Mel-5 leads to the suggestion that an alternative apoptosis pathway like autophagy could be induced. Autophagy (25, 105) is a non-apoptotic form of programmed cell death characterized by caspase-independence, very late (if at all) DNA-fragmentation and increased lysosomal activity, leading to degradation of cytosolic content in large autophagic vesicles. If cephalostatin induces autophagy and the related formation of autophagosomes is under current investigation by transmission electron microscopy.

## **5 MECHANISM OF SMAC RELEASE**

The release of mitochondrial intermembrane space proteins to the cytosol is a key event during apoptosis. For instance cytochrome *c* is required for the initiation of the apoptosome and activation of caspases whereas Smac/DIABLO is believed to enhance caspase activation through the neutralization of the inhibitor of apoptosis proteins (106). Upon apoptotic stimuli these mitochondrial factors are usually released together in a manner that is coordinately initiated (107). Thus, the fact that cephalostatin leads to a marked and early Smac release without detectable amounts of cytochrome *c* deserves attention and asks for the mechanism of release as well as for the impact of Smac in cephalostatin-induced cell death.

Similar to our data, the group of Anderson (78, 108) reported about an Apaf-1/cytochrome *c*-independent and Smac-dependent induction of apoptosis in multiple myeloma cells by dexamethasone. The authors identified activated JNK to be responsible for Smac release using the JNK inhibitor SP600125. Cephalostatin is also able to rapidly induce JNK activation (16). However, blocking JNK activity via SP600125 or overexpression of a dominant-negative form of its upstream kinase ASK1 in our hands did not affect Smac release. Furthermore, inhibition of caspase-2, which has been reported to directly induce release of mitochondrial proteins, did neither influence Smac release. First experiments show that overexpression of the antiapoptotic Bcl-2 family member Bcl-x<sub>L</sub> (15) as well as the

absence of the proapoptotic Bcl-2 protein Bak delays, but can not inhibit Smac release, suggesting that cephalostatin may trigger a signal directly influencing the mitochondrial pore formation. Furthermore, cell death by cephalostatin was not inhibited by Bak deficiency. Contrary, staurosporine- and etoposide-induced apoptosis was inhibited, further pointing to a cytochrome c independent and Smac dependent mechanism for cephalostatin.

The calpain family of proteases seems to be an important factor in the induction of apoptosis via mitochondria, since Bax has been identified as a target of calpain (109) and calpain inhibition has been shown to inhibit the release of Smac and cytochrome c from mitochondria (86). Calpain is rapidly activated upon cephalostatin treatment and is partially involved in the selective Smac release, further supporting the crosstalk between calpain and mitochondria. Further studies will focus on details regarding the selective release of Smac and its underlying mechanism.

## **6 IMPACT OF SMAC ON APOPTOSIS**

Smac has been discovered in the search for proteins which are able to interact with mammalian and baculoviral IAPs (110). IAPs, which are characterized by one or more baculovirus IAP repeat (BIR) domains antagonize caspases by binding to and inhibiting mainly caspase-9, -3 and -7 (111). Smac has been reported to promote apoptosis in response to various apoptosis inducers by antagonizing IAP-mediated inhibition of caspases (35). If Smac is important in cephalostatin induced cell death it thus should counteract XIAP overexpression. This could clearly be shown in XIAP overexpressing Jurkat cells in comparison to wildtype Jurkat cells, whereas etoposide mediated cell death is almost completely inhibited. To this end Smac agonists sensitized various tumor cells for cell death (112, 113). We used siRNA technique to silence the Smac gene and subsequently examined the impact of endogenous Smac released upon cephalostatin treatment. As expected, we observed a strong reduction in caspase-9 as well as caspase-3 activation. No effect of caspase-4 activation in Smac-depleted cells was seen. Taken together, our results demonstrate an essential role of Smac in cephalostatin-induced caspase cascade most likely by promoting caspase activity. In this respect, the fact that caspase-2 activity triggered by cephalostatin is markedly reduced in cells

depleted by Smac draws attention to caspase-2 as a further caspase involved in the apoptosome-independent cell death induced by cephalostatin.

## 7 INVOLVEMENT OF CASPASE-2

Even though caspase-2 was the second mammalian caspase identified, its exact role in the regulation of cell death is controversial and relatively unknown, in part due to its different function dependent on cell type and stimulus. Caspase-2 contains a CARD domain and can act as initiator caspase (72, 88, 89) but has characteristics of effector caspases (114, 115). It is localized predominantly to the Golgi complex and the nucleus, but also in mitochondria and cytosol (116).

Many reports, including studies employing caspase-2-deficient mice, exclude an essential role of caspase-2 in apoptosis presumably due to the compensation by other caspases (90, 117, 118). However, caspase-2 is activated in response to DNA damage, where it acts as the only initiator caspase (116), and appears necessary for apoptosis triggered by UV (ultraviolet) irradiation (72), trophic factor withdrawal (119), serum deprivation (120) or administration of TRAIL (121, 122). Caspase-2 has been also implicated in neuronal death induced by  $\beta$ -amyloid (123) and recently in ER stress (124, 125, 126).

We depleted caspase-2 via siRNA transfection and observed a minor but significant effect on the extent of apoptotic cell death induced by cephalostatin. Use of the rather selective inhibitor of caspase-2 zVDVAD-fmk results in a similar reduction of cell death indicating that caspase-2 is involved in the unusual apoptotic pathway induced by cephalostatin. The question arises as to whether caspase-2 is functioning as an initiator or as an effector caspase. Both roles have been described (72, 89, 90). The fact that caspase-2 is activated in caspase-9-deficient cells similarly to parental Jurkat cells clearly votes for caspase-2 activation to be an upstream event.

Caspase-2 has been reported to engage directly the mitochondrial apoptotic pathway by inducing release of mitochondrial factors (81, 82, 83, 122, 127). We show that caspase-2 induced by cephalostatin is not involved in Smac release. Importantly, caspase-2 activation is not involved in apoptosome-independent activation of caspase-9 as reported previously for cephalostatin-induced caspase-4.

Our next step was to understand how caspase-2 is activated upon cephalostatin treatment. In this respect, most interestingly caspase-2 was reported to be activated by recruitment into a large multiprotein complex independently of Apaf-1 and cytochrome c (91). This putative complex has been proposed to be the PIDDosome (56), formed by association of the protein PIDD (p53-induced protein with a DD), RAIDD (RIP associated ICH-1/CED-3-homologous protein with DD) and procaspase-2. The PIDDosome was proposed to regulate caspase-2 activation and apoptosis induced by genotoxic agents. Upon recruitment to the complex, caspase-2 was activated and autoprocessed, but it was not clear whether activated caspase-2 was involved in cell death (56). RAIDD together with caspase-2 has been recently demonstrated to participate in the induction of apoptosis under conditions of trophic factor withdrawal but not DNA damage (119), arguing against the exclusive formation of the caspase-2 activation complexes by genotoxic stress (56). Along this line cephalostatin does not induce DNA damage (16) and is to our best knowledge one of the few drugs (128, 129) which has clearly shown to induce recruitment of caspase-2 to PIDD and RAIDD leading to formation of the PIDDosome.

## V SUMMARY

The presented work reports unusual apoptotic signaling pathways induced by the experimental chemotherapeutic drug cephalostatin with the following new findings:

### **Cephalostatin induces apoptosis independent of cell type.**

Apoptosis induction was investigated in leukemia (Jurkat), breast adenocarcinoma (MCF-7), cervix carcinoma (HeLa), ovarian cancer (SK-OV-3) and melanoma (SK-Mel-5) cell lines. In all cell lines cell death could be induced, proving the usability of cephalostatin for cancer treatment. Interestingly, cephalostatin induces caspase-dependent cell death in Jurkat and HeLa cells, but caspase-independent apoptosis in SK-OV-3 and SK-Mel-5 cells. Thus, the mechanism of apoptosis induction seems to be cell dependent.

### **Cephalostatin-induced cell death in SK-Mel-5 cells.**

Due to the surprising fact that caspases are not involved in apoptosis induction in SK-Mel-5 cells, the cell death induction by cephalostatin was further investigated in this cell line. AIF, a classical caspase-independent apoptosis mediator, is not involved in DNA-fragmentation. Interestingly, cephalostatin induces cell cycle arrest in G1 phase and the transcription factor STAT3 and the IAP survivin were identified as targets.

### **Mechanism of selective Smac – release from mitochondria.**

Smac – not cytochrome c – is predominately released from mitochondria of cephalostatin treated cells. Neither JNK nor caspase-2 is responsible for the selective release. First experiments show that calpain, which is rapidly activated upon cephalostatin treatment, is partially involved in Smac release.

### **Smac enhances the apoptotic signaling cascade in Jurkat leukemia T cells.**

Smac was demonstrated to have significant impact on cephalostatin-induced apoptosis. This was due to increased caspase activity. Caspase-4 which is known to be activated by cephalostatin (17) was not influenced. Interestingly, apart from caspase-9, caspase-3 and PARP mainly caspase-2 activity was affected by Smac.

### Caspase-2 is involved in apoptosis induction in Jurkat T cells.

Cephalostatin has been reported previously to activate caspase-9 apoptosome-independent and partially *via* ER stress (17). Caspase-2 acts as a further initiator caspase and contributes independent of caspase-9 to cephalostatin-induced cell death.

### Cephalostatin induces the formation of the PIDDosome.

The PIDDosome is large protein complex, implicated in the activation of caspase-2. Cephalostatin is one of the few drugs, known so far, able to induce the formation of this complex consisting of caspase-2, RAIDD and PIDD.

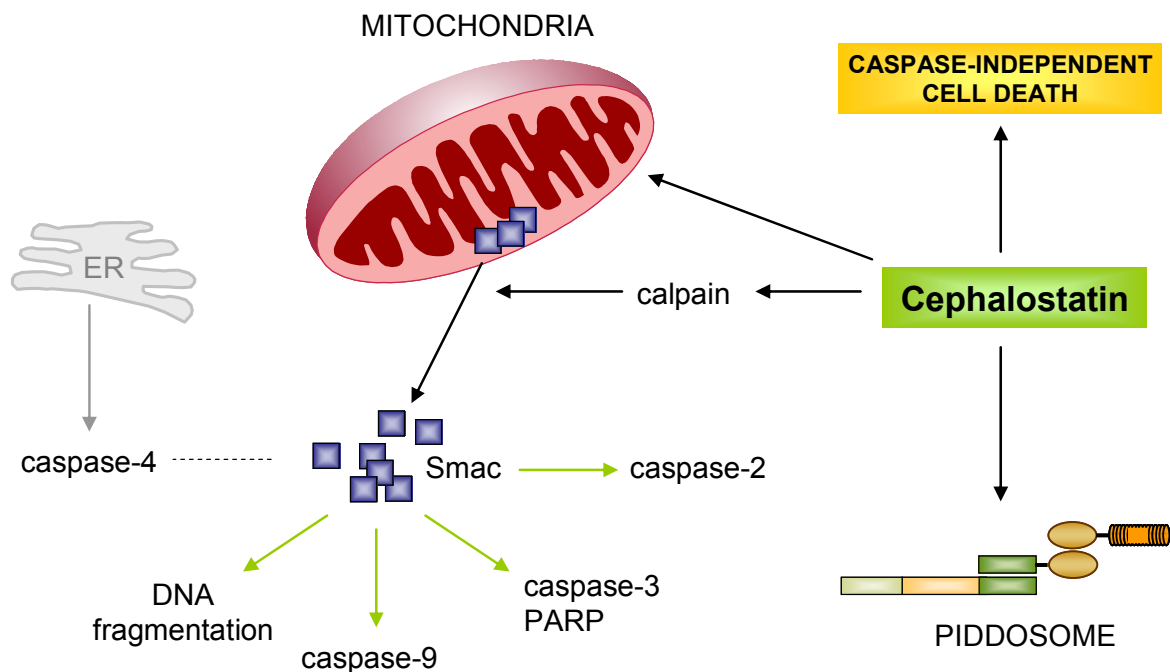


**Figure V.1 Summary of cephalostatin-induced cell death mechanisms**

**In summary**, the experimental drug cephalostatin 2, which was isolated from a marine organism, proved to be both a very valuable tool to discover novel aspects in apoptotic signaling such as recruitment of a PIDDosome responsible for caspase-2 activation as well a promising therapeutic agent promoting caspase-independent apoptosis in chemoresistant melanoma cells.

---

## VI REFERENCES

1. Mann J. Natural products in cancer chemotherapy: past, present and future. *Nat Rev Cancer* 2002;2:143-148.
2. da Rocha AB, Lopes RM, Schwartzmann G. Natural products in anticancer therapy. *Curr Opin Pharmacol* 2001;1:364-369.
3. Nagle DG, Zhou YD, Mora FD, Mohammed KA, Kim YP. Mechanism targeted discovery of antitumor marine natural products. *Curr Med Chem* 2004;11:1725-1756.
4. Newman DJ, Cragg GM. Marine natural products and related compounds in clinical and advanced preclinical trials. *J Nat Prod* 2004;67:1216-1238.
5. Simmons TL, Andrianasolo E, McPhail K, Flatt P, Gerwick WH. Marine natural products as anticancer drugs. *Mol Cancer Ther* 2005;4:333-342.
6. Pettit GR, Inoue M, Kamano Y et al. Isolation and Structure of the Hemichordate Cell-Growth Inhibitors Cephalostatin-2, Cephalostatin-3, and Cephalostatin-4. *Journal of the Chemical Society-Chemical Communications* 1988:865-867.
7. Pettit GR, Inoue M, Kamano Y et al. Isolation and Structure of the Powerful Cell-Growth Inhibitor Cephalostatin-1. *Journal of the American Chemical Society* 1988;110:2006-2007.
8. Pettit GR, Kamano Y, Dufresne C et al. Isolation and Structure of the Unusual Indian-Ocean Cephalodiscus-Gilchristi Components, Cephalostatins 5 and 6. *Canadian Journal of Chemistry-Revue Canadienne de Chimie* 89 A.D.;67:1509-1513.
9. Pettit GR, Kamano Y, Inoue M et al. Antineoplastic Agents .214. Isolation and Structure of Cephalostatins 7-9. *Journal of Organic Chemistry* 1992;57:429-431.
10. Pettit GR, Xu JP, Williams MD et al. Isolation and Structure of Cephalostatin-10 and Cephalostatin-11. *Journal of Natural Products* 1994;57:52-63.
11. Pettit GR, Ichihara Y, Xu JP, Boyd MR, Williams MD. Isolation and Structure of the Symmetrical Diteroidal Alkaloids Cephalostatin-12 and Cephalostatin-13. *Bioorganic & Medicinal Chemistry Letters* 1994;4:1507-1512.
12. Pettit GR, Xu JP, Ichihara Y, Williams MD, Boyd MR. Antineoplastic Agents .285. Isolation and Structures of Cephalostatin-14 and Cephalostatin-15. *Canadian Journal of Chemistry-Revue Canadienne de Chimie* 1994;72:2260-2267.

13. Pettit GR, Xu JP, Schmidt JM, Boyd MR. Isolation and Structure of the Exceptional Pterobranchia Human Cancer Inhibitors Cephalostatin-16 and Cephalostatin-17. *Bioorganic & Medicinal Chemistry Letters* 1995;5:2027-2032.
14. Pettit GR, Tan R, Xu JP et al. Antineoplastic agents. 398. Isolation and structure elucidation of cephalostatins 18 and 19. *Journal of Natural Products* 1998;61:955-958.
15. Dirsch VM, Muller IM, Eichhorst ST et al. Cephalostatin 1 selectively triggers the release of Smac/DIABLO and subsequent apoptosis that is characterized by an increased density of the mitochondrial matrix. *Cancer Res* 2003;63:8869-8876.
16. Muller IM, Dirsch VM, Rudy A et al. Cephalostatin 1 inactivates Bcl-2 by hyperphosphorylation independent of M-phase arrest and DNA damage. *Mol Pharmacol* 2005;67:1684-1689.
17. Lopez-Anton N, Rudy A, Barth N et al. The marine product cephalostatin 1 activates an ER stress-specific and apoptosome-independent apoptotic signaling pathway. *J Biol Chem* 2006.
18. Urban S, Hickford SJH, Blunt JW, Munro MHG. Bioactive Marine Alkaloids. *Current Organic Chemistry* 2000;4:765-807.
19. Fulda S, Debatin KM. Extrinsic versus intrinsic apoptosis pathways in anticancer chemotherapy. *Oncogene* 2006;25:4798-4811.
20. Assuncao GC, Linden R. Programmed cell deaths. Apoptosis and alternative deathstyles. *Eur J Biochem* 2004;271:1638-1650.
21. Kerr JF, Wyllie AH, Currie AR. Apoptosis: a basic biological phenomenon with wide-ranging implications in tissue kinetics. *Br J Cancer* 1972;26:239-257.
22. Jaattela M, Tschopp J. Caspase-independent cell death in T lymphocytes. *Nat Immunol* 2003;4:416-423.
23. Okada H, Mak TW. Pathways of apoptotic and non-apoptotic death in tumour cells. *Nat Rev Cancer* 2004;4:592-603.
24. Broker LE, Kruyt FA, Giaccone G. Cell death independent of caspases: a review. *Clin Cancer Res* 2005;11:3155-3162.
25. Lockshin RA, Zakeri Z. Apoptosis, autophagy, and more. *Int J Biochem Cell Biol* 2004;36:2405-2419.
26. Castedo M, Perfettini JL, Roumier T et al. Cell death by mitotic catastrophe: a molecular definition. *Oncogene* 2004;23:2825-2837.

27. Ho PK, Hawkins CJ. Mammalian initiator apoptotic caspases. *FEBS J* 2005;272:5436-5453.
28. Riedl SJ, Shi Y. Molecular mechanisms of caspase regulation during apoptosis. *Nat Rev Mol Cell Biol* 2004;5:897-907.
29. Siegel RM. Caspases at the crossroads of immune-cell life and death. *Nat Rev Immunol* 2006;6:308-317.
30. Shiozaki EN, Shi Y. Caspases, IAPs and Smac/DIABLO: mechanisms from structural biology. *Trends Biochem Sci* 2004;29:486-494.
31. Donepudi M, Grutter MG. Structure and zymogen activation of caspases. *Biophys Chem* 2002;101-102:145-153.
32. Shi Y. Mechanisms of caspase activation and inhibition during apoptosis. *Mol Cell* 2002;9:459-470.
33. Fischer U, Janicke RU, Schulze-Osthoff K. Many cuts to ruin: a comprehensive update of caspase substrates. *Cell Death Differ* 2003;10:76-100.
34. Wrzesien-Kus A, Smolewski P, Sobczak-Pluta A, Wierzbowska A, Robak T. The inhibitor of apoptosis protein family and its antagonists in acute leukemias. *Apoptosis* 2004;9:705-715.
35. Vaux DL, Silke J. IAPs, RINGs and ubiquitylation. *Nat Rev Mol Cell Biol* 2005;6:287-297.
36. Eckelman BP, Salvesen GS, Scott FL. Human inhibitor of apoptosis proteins: why XIAP is the black sheep of the family. *EMBO Rep* 2006;7:988-994.
37. Jing N, Tweardy DJ. Targeting Stat3 in cancer therapy. *Anticancer Drugs* 2005;16:601-607.
38. McNeish IA, Lopes R, Bell SJ et al. Survivin interacts with Smac/DIABLO in ovarian carcinoma cells but is redundant in Smac-mediated apoptosis. *Exp Cell Res* 2005;302:69-82.
39. Johnson ME, Howerth EW. Survivin: a bifunctional inhibitor of apoptosis protein. *Vet Pathol* 2004;41:599-607.
40. Kaufmann SH, Hengartner MO. Programmed cell death: alive and well in the new millennium. *Trends Cell Biol* 2001;11:526-534.
41. Arnold R, Brenner D, Becker M, Frey CR, Krammer PH. How T lymphocytes switch between life and death. *Eur J Immunol* 2006;36:1654-1658.

42. MacFarlane M, Williams AC. Apoptosis and disease: a life or death decision. *EMBO Rep* 2004;5:674-678.
43. Vermeulen K, Van Bockstaele DR, Berneman ZN. Apoptosis: mechanisms and relevance in cancer. *Ann Hematol* 2005;84:627-639.
44. Samejima K, Earnshaw WC. Trashing the genome: the role of nucleases during apoptosis. *Nat Rev Mol Cell Biol* 2005;6:677-688.
45. Jin Z, El-Deiry WS. Overview of cell death signaling pathways. *Cancer Biol Ther* 2005;4:139-163.
46. Ashe PC, Berry MD. Apoptotic signaling cascades. *Prog Neuropsychopharmacol Biol Psychiatry* 2003;27:199-214.
47. Robertson JD, Orrenius S. Role of mitochondria in toxic cell death. *Toxicology* 2002;181-182:491-496.
48. van Gurp M, Festjens N, van Loo G, Saelens X, Vandenabeele P. Mitochondrial intermembrane proteins in cell death. *Biochem Biophys Res Commun* 2003;304:487-497.
49. Wilkinson JC, Wilkinson AS, Scott FL et al. Neutralization of Smac/Diablo by inhibitors of apoptosis (IAPs). A caspase-independent mechanism for apoptotic inhibition. *J Biol Chem* 2004;279:51082-51090.
50. Burlacu A. Regulation of apoptosis by Bcl-2 family proteins. *J Cell Mol Med* 2003;7:249-257.
51. Cory S, Adams JM. The Bcl2 family: regulators of the cellular life-or-death switch. *nature* 2002;2:647-656.
52. Festjens N, van Gurp M, van Loo G, Saelens X, Vandenabeele P. Bcl-2 family members as sentinels of cellular integrity and role of mitochondrial intermembrane space proteins in apoptotic cell death. *Acta Haematol* 2004;111:7-27.
53. Festjens N, Cornelis S, Lamkanfi M, Vandenabeele P. Caspase-containing complexes in the regulation of cell death and inflammation. *Biol Chem* 2006;387:1005-1016.
54. Bao Q, Shi Y. Apoptosome: a platform for the activation of initiator caspases. *Cell Death Differ* 2007;14:56-65.
55. Lamkanfi M, Declercq W, Vanden BT, Vandenabeele P. Caspases leave the beaten track: caspase-mediated activation of NF-kappaB. *J Cell Biol* 2006;173:165-171.

56. Tinel A, Tschopp J. The PIDDosome, a protein complex implicated in activation of caspase-2 in response to genotoxic stress. *Science* 2004;304:843-846.
57. Wu ZH, Mabb A, Miyamoto S. PIDD: a switch hitter. *Cell* 2005;123:980-982.
58. Queirolo P, Acquati M. Targeted therapies in melanoma. *Cancer Treat Rev* 2006;32:524-531.
59. Smalley KS, Herlyn M. Targeting intracellular signaling pathways as a novel strategy in melanoma therapeutics. *Ann N Y Acad Sci* 2005;1059:16-25.
60. Fesik SW. Promoting apoptosis as a strategy for cancer drug discovery. *Nat Rev Cancer* 2005;5:876-885.
61. Kortylewski M, Jove R, Yu H. Targeting STAT3 affects melanoma on multiple fronts. *Cancer Metastasis Rev* 2005;24:315-327.
62. Liu T, Brouha B, Grossman D. Rapid induction of mitochondrial events and caspase-independent apoptosis in Survivin-targeted melanoma cells. *Oncogene* 2004;23:39-48.
63. Shankar SL, Mani S, O'Guin KN et al. Survivin inhibition induces human neural tumor cell death through caspase-independent and -dependent pathways. *J Neurochem* 2001;79:426-436.
64. Sah NK, Khan Z, Khan GJ, Bisen PS. Structural, functional and therapeutic biology of survivin. *Cancer Lett* 2006;244:164-171.
65. Samraj AK, Keil E, Ueffing N, Schulze-Osthoff K, Schmitz I. Loss of caspase-9 provides genetic evidence for the type I/ II concept of CD95-mediated apoptosis. *J Biol Chem* 2006.
66. Rehm M, Dussmann H, Prehn JH. Real-time single cell analysis of Smac/DIABLO release during apoptosis. *J Cell Biol* 2003;162:1031-1043.
67. [http://biology.berkeley.edu/crl/flow\\_images/fig1.gif](http://biology.berkeley.edu/crl/flow_images/fig1.gif) 2007.
68. Nicoletti I, Migliorati G, Pagliacci MC, Grignani F, Riccardi C. A rapid and simple method for measuring thymocyte apoptosis by propidium iodide staining and flow cytometry. *J Immunol Methods* 1991;139:271-279.
69. Bradford MM. A rapid and sensitive method for the quantitation of microgram quantities of protein utilizing the principle of protein-dye binding. *Anal Biochem* 1976;72:248-254.
70. Laemmli UK. Cleavage of structural proteins during the assembly of the head of bacteriophage T4. *nature* 1970;227:680-685.

71. McManus MT, Sharp PA. Gene silencing in mammals by small interfering RNAs. *Nat Rev Genet* 2002;3:737-747.
72. Lassus P, Opitz-Araya X, Lazebnik Y. Requirement for caspase-2 in stress-induced apoptosis before mitochondrial permeabilization. *Science* 2002;297:1352-1354.
73. Park MT, Kim MJ, Kang YH et al. Phytosphingosine in combination with ionizing radiation enhances apoptotic cell death in radiation-resistant cancer cells through ROS-dependent and -independent AIF release. *Blood* 2005;105:1724-1733.
74. Kurokawa H, Nishio K, Fukumoto H et al. Alteration of caspase-3 (CPP32/Yama/apopain) in wild-type MCF-7, breast cancer cells. *Oncol Rep* 1999;6:33-37.
75. Vandenabeele P, Orrenius S, Zhivotovsky B. Serine proteases and calpains fulfill important supporting roles in the apoptotic tragedy of the cellular opera. *Cell Death Differ* 2005;12:1219-1224.
76. Galluzzi L, Larochette N, Zamzami N, Kroemer G. Mitochondria as therapeutic targets for cancer chemotherapy. *Oncogene* 2006;25:4812-4830.
77. Cregan SP, Dawson VL, Slack RS. Role of AIF in caspase-dependent and caspase-independent cell death. *Oncogene* 2004;23:2785-2796.
78. Chauhan D, Li GL, Hideshima T et al. JNK-dependent release of mitochondrial protein, Smac, during apoptosis in multiple myeloma (MM) cells. *Journal of Biological Chemistry* 2003;278:17593-17596.
79. Deng Y, Ren X, Yang L, Lin Y, Wu X. A JNK-dependent pathway is required for TNFalpha-induced apoptosis. *Cell* 2003;115:61-70.
80. Garcia-Calvo M, Peterson EP, Leiting B et al. Inhibition of human caspases by peptide-based and macromolecular inhibitors. *J Biol Chem* 1998;273:32608-32613.
81. Robertson JD, Gogvadze V, Kropotov A et al. Processed caspase-2 can induce mitochondria-mediated apoptosis independently of its enzymatic activity. *EMBO Rep* 2004;5:643-648.
82. Enoksson M, Robertson JD, Gogvadze V et al. Caspase-2 permeabilizes the outer mitochondrial membrane and disrupts the binding of cytochrome c to anionic phospholipids. *J Biol Chem* 2004;279:49575-49578.
83. Robertson JD, Enoksson M, Suomela M, Zhivotovsky B, Orrenius S. Caspase-2 acts upstream of mitochondria to promote cytochrome c release during etoposide-induced apoptosis. *J Biol Chem* 2002;277:29803-29809.

84. Brimmell M, Mendiola R, Mangion J, Packham G. BAX frameshift mutations in cell lines derived from human haemopoietic malignancies are associated with resistance to apoptosis and microsatellite instability. *Oncogene* 1998;16:1803-1812.
85. Wang KK. Calpain and caspase: can you tell the difference? *Trends Neurosci* 2000;23:20-26.
86. Altnauer F, Conus S, Cavalli A, Folkers G, Simon HU. Calpain-1 regulates Bax and subsequent Smac-dependent caspase-3 activation in neutrophil apoptosis. *J Biol Chem* 2004;279:5947-5957.
87. Baliga BC, Read SH, Kumar S. The biochemical mechanism of caspase-2 activation. *Cell Death Differ* 2004;11:1234-1241.
88. Lin CF, Chen CL, Chang WT et al. Sequential caspase-2 and caspase-8 activation upstream of mitochondria during ceramide and etoposide-induced apoptosis. *J Biol Chem* 2004;279:40755-40761.
89. Dirsch VM, Kirschke SO, Estermeier M, Steffan B, Vollmar AM. Apoptosis signaling triggered by the marine alkaloid ascididemin is routed via caspase-2 and JNK to mitochondria. *Oncogene* 2004;23:1586-1593.
90. O'Reilly LA, Ekert P, Harvey N et al. Caspase-2 is not required for thymocyte or neuronal apoptosis even though cleavage of caspase-2 is dependent on both Apaf-1 and caspase-9. *Cell Death Differ* 2002;9:832-841.
91. Read SH, Baliga BC, Ekert PG, Vaux DL, Kumar S. A novel Apaf-1-independent putative caspase-2 activation complex. *J Cell Biol* 2002;159:739-745.
92. Liu JR, Pipari AW, Tan L et al. Dysfunctional apoptosome activation in ovarian cancer: implications for chemoresistance. *Cancer Res* 2002;62:924-931.
93. Furukawa Y, Nishimura N, Furukawa Y et al. Apaf-1 is a mediator of E2F-1-induced apoptosis. *J Biol Chem* 2002;277:39760-39768.
94. Soengas MS, Capodici P, Polsky D et al. Inactivation of the apoptosis effector Apaf-1 in malignant melanoma. *nature* 2001;409:207-211.
95. Anichini A, Mortarini R, Sensi M, Zanon M. APAF-1 signaling in human melanoma. *Cancer Lett* 2006;238:168-179.
96. Soengas MS, Lowe SW. Apoptosis and melanoma chemoresistance. *Oncogene* 2003;22:3138-3151.
97. Semenov DV, Aronov PA, Kuligina EV, Potapenko MO, Richter VA. Oligonucleosomal DNA fragmentation in MCF-7 cells undergoing palmitate-induced apoptosis. *Biochemistry (Mosc)* 2003;68:1335-1341.

98. Caserta TM, Smith AN, Gultice AD, Reedy MA, Brown TL. Q-VD-OPh, a broad spectrum caspase inhibitor with potent antiapoptotic properties. *Apoptosis* 2003;8:345-352.
99. Ahonen M, Poukkula M, Baker AH et al. Tissue inhibitor of metalloproteinases-3 induces apoptosis in melanoma cells by stabilization of death receptors. *Oncogene* 2003;22:2121-2134.
100. Yang J, Amiri KI, Burke JR, Schmid JA, Richmond A. BMS-345541 targets inhibitor of kappaB kinase and induces apoptosis in melanoma: involvement of nuclear factor kappaB and mitochondria pathways. *Clin Cancer Res* 2006;12:950-960.
101. Panka DJ, Wang W, Atkins MB, Mier JW. The Raf inhibitor BAY 43-9006 (Sorafenib) induces caspase-independent apoptosis in melanoma cells. *Cancer Res* 2006;66:1611-1619.
102. Yu H, Kortylewski M, Pardoll D. Crosstalk between cancer and immune cells: role of STAT3 in the tumour microenvironment. *Nat Rev Immunol* 2007;7:41-51.
103. Selvendiran K, Koga H, Ueno T et al. Luteolin promotes degradation in signal transducer and activator of transcription 3 in human hepatoma cells: an implication for the antitumor potential of flavonoids. *Cancer Res* 2006;66:4826-4834.
104. Liu T, Biddle D, Hanks AN et al. Activation of dual apoptotic pathways in human melanocytes and protection by survivin. *J Invest Dermatol* 2006;126:2247-2256.
105. Kroemer G, Jaattela M. Lysosomes and autophagy in cell death control. *Nat Rev Cancer* 2005;5:886-897.
106. Green DR. Apoptotic pathways: paper wraps stone blunts scissors. *Cell* 2000;102:1-4.
107. Munoz-Pinedo C, Guio-Carrion A, Goldstein JC et al. Different mitochondrial intermembrane space proteins are released during apoptosis in a manner that is coordinately initiated but can vary in duration. *Proc Natl Acad Sci U S A* 2006;103:11573-11578.
108. Chauhan D, Hideshima T, Rosen S et al. Apaf-1/cytochrome c-independent and Smac-dependent induction of apoptosis in multiple myeloma (MM) cells. *J Biol Chem* 2001;276:24453-24456.
109. Wood DE, Thomas A, Devi LA et al. Bax cleavage is mediated by calpain during drug-induced apoptosis. *Oncogene* 1998;17:1069-1078.
110. Verhagen AM, Ekert PG, Pakusch M et al. Identification of DIABLO, a mammalian protein that promotes apoptosis by binding to and antagonizing IAP proteins. *Cell* 2000;102:43-53.

111. Salvesen GS, Duckett CS. IAP proteins: blocking the road to death's door. *Nat Rev Mol Cell Biol* 2002;3:401-410.
112. Giagkousiklidis S, Vogler M, Westhoff MA et al. Sensitization for gamma-irradiation-induced apoptosis by second mitochondria-derived activator of caspase. *Cancer Res* 2005;65:10502-10513.
113. Vogler M, Giagkousiklidis S, Genze F et al. Inhibition of clonogenic tumor growth: a novel function of Smac contributing to its antitumor activity. *Oncogene* 2005;24:7190-7202.
114. Mancini M, Machamer CE, Roy S et al. Caspase-2 is localized at the Golgi complex and cleaves golgin-160 during apoptosis. *J Cell Biol* 2000;149:603-612.
115. Talanian RV, Quinlan C, Trautz S et al. Substrate specificities of caspase family proteases. *J Biol Chem* 1997;272:9677-9682.
116. Zhivotovsky B, Orrenius S. Caspase-2 function in response to DNA damage. *Biochem Biophys Res Commun* 2005;331:859-867.
117. Bergeron L, Perez GI, Macdonald G et al. Defects in regulation of apoptosis in caspase-2-deficient mice. *Genes Dev* 1998;12:1304-1314.
118. Troy CM, Rabacchi SA, Hohl JB et al. Death in the balance: alternative participation of the caspase-2 and -9 pathways in neuronal death induced by nerve growth factor deprivation. *J Neurosci* 2001;21:5007-5016.
119. Wang Q, Maniati M, Jabado O et al. RAIDD is required for apoptosis of PC12 cells and sympathetic neurons induced by trophic factor withdrawal. *Cell Death Differ* 2006;13:75-83.
120. Chauvier D, Lecoer H, Langonne A et al. Upstream control of apoptosis by caspase-2 in serum-deprived primary neurons. *Apoptosis* 2005;10:1243-1259.
121. Shin S, Lee Y, Kim W et al. Caspase-2 primes cancer cells for TRAIL-mediated apoptosis by processing procaspase-8. *EMBO J* 2005;24:3532-3542.
122. Wagner KW, Engels IH, Deveraux QL. Caspase-2 can function upstream of bid cleavage in the TRAIL apoptosis pathway. *J Biol Chem* 2004;279:35047-35052.
123. Troy CM, Rabacchi SA, Friedman WJ et al. Caspase-2 mediates neuronal cell death induced by beta-amyloid. *J Neurosci* 2000;20:1386-1392.
124. Cheung HH, Lynn KN, Liston P, Korneluk RG. Involvement of caspase-2 and caspase-9 in endoplasmic reticulum stress-induced apoptosis: a role for the IAPs. *Exp Cell Res* 2006;312:2347-2357.

## VI REFERENCES

---

125. Dahmer MK. Caspases-2, -3, and -7 are involved in thapsigargin-induced apoptosis of SH-SY5Y neuroblastoma cells. *J Neurosci Res* 2005;80:576-583.
126. Bando Y, Katayama T, Taniguchi M et al. RA410/Sly1 suppresses MPP+ and 6-hydroxydopamine-induced cell death in SH-SY5Y cells. *Neurobiol Dis* 2005;18:143-151.
127. Gao Z, Shao Y, Jiang X. Essential roles of the Bcl-2 family of proteins in caspase-2-induced apoptosis. *J Biol Chem* 2005;280:38271-38275.
128. Vakifahmetoglu H, Olsson M, Orrenius S, Zhivotovsky B. Functional connection between p53 and caspase-2 is essential for apoptosis induced by DNA damage. *Oncogene* 2006.
129. Taghiyev AF, Guseva NV, Glover RA, Rokhlin OW, Cohen MB. TSA-induced cell death in prostate cancer cell lines is caspase-2 dependent and involves the PIDDosome. *Cancer Biol Ther* 2006;5:1199-1205.

## VII APPENDIX

### 1 PUBLICATIONS

#### 1.1 ABSTRACTS

Rudy A., López-Antón N., Barth N., Pettit G.R., Vollmar A.M.

Cephalostatin 2 potentiates apoptosis induced by paclitaxel in the melanoma cell line SK-Mel-5.

47<sup>th</sup> Spring Meeting of the Deutsche Gesellschaft für experimentelle klinische Pharmakologie und Toxikologie, April 4.-6., 2006, Mainz, Germany.

Naunyn-Schmiedeberg's Archive of Pharmacology, Vol 372, Supplement 1

#### 1.2 ORIGINAL PUBLICATIONS

Rudy A.\*, López-Antón N.\*, Barth N., Pettit G.R., Dirsch V.M., Schulze-Osthoff K., Rehm M., Prehn J. H.M., Vogler M., Fulda S., Vollmar A.M.

Cephalostatin-mediated apoptosis is Smac-dependent and involves assembly of the PIDDosome

*Submitted*

\* These authors contributed equally to this work.

López-Antón N., Rudy A., Barth N., Schmitz M.L., Pettit G.R., Schulze-Osthoff K., Dirsch V.M., Vollmar A.M.

The marine product cephalostatin 1 activates an endoplasmic reticulum stress-specific and apoptosome-independent apoptotic signaling pathway.

J. Biol. Chem. 2006 Nov. 3; 281(44): 33078-86

Müller I.M., Dirsch V.M., Rudy A., López-Antón N., Pettit G.R., Vollmar A.M.

Cephalostatin 1 inactivates Bcl-2 by hyperphosphorylation independent of M-phase arrest and DNA-damage.

Mol.Pharmacol., 2005 May; 67(5): 1684-9

## 2 CURRICULUM VITAE

### Persönliche Daten:

Name: Anita Rudy  
Geburtsdatum: 18.06.1977  
Geburtsort: Altötting  
Staatsangehörigkeit: deutsch

### Promotion:

05/2003 – 03/2007      Dissertation am Lehrstuhl für Pharmazeutische Biologie  
Prof. Dr. A.M. Vollmar  
Department Pharmazie, LMU München

### Studium:

1996 – 2002:      Studium der Gartenbauwissenschaften,  
TU München / Weihenstephan  
1999:              Vordiplom  
2002:              Abschluss: Dipl. Ing. agr. univ.

### Schulbildung:

1983 – 1987:      Grundschule Stammham  
1987 – 1996:      König-Karlmann-Gymnasium Altötting  
Abschluss: Allgemeine Hochschulreife

### 3 ACKNOWLEDGEMENTS

First of all, I am deeply grateful to Prof. Dr. Angelika M. Vollmar for giving me the opportunity to perform this work in her laboratories. Her constant scientific guidance, encouragement and enthusiasm for this project were of particular importance to me.

Special thanks go to my thesis committee, especially PD Dr. Carsten Culmsee for acting as second examiner.

I am very grateful to PD Dr. S. Zahler for his support and patience in introducing me to confocal microscopy. Furthermore I would like to thank Prof. Dr. Verena M. Dirsch for her guidance in the beginning of this work and Dr. Nicole Barth for her support.

Many thanks go to ALL members of the working group for this really enjoyable working atmosphere and the helpfulness, especially to my first “Boxenluder” Thommaß for this great time in our box, for always helping me and for all that non-scientific stuff like “Salzkrebschen züchten”. Kathi, Anja, Hanna, kleiner Thomas, Irina, Lila, Nancy and second “Boxenluder” Andrea: Thank you for your friendship, the good team work and the great time in- and outside the lab. Lots of thank go also to our technical staff Conny, Jana, Rita and Frau Schnegg for their cooperativeness.

Last but not least I want to thank my family for their encouragement and Jochen for his unlimited comprehension and for just being there whenever I needed him.